Electronic Supplementary Material (ESI) for New Journal of Chemistry.
This journal is © The Royal Society of Chemistry and the Centre National de la Recherche Scientifique 2024

Electronic Supplementary Information:

Triphenyl Borates used to Avoid the Bay-Position Halogenation of Boron Subnaphthalocyanines; and for the Subnaphthalocyanine, Subphthalocyanine and Hybrids Formation.

Devon P. Holst[a], Aleksa Dovijarski[a], Alan J. Lough[a], and Timothy P. Bender[a,b,c,d]*

[a] Department of Chemistry, University of Toronto, 80 St. George Street, Toronto, Ontario, Canada M5S 3H6

[b] Department of Chemical Engineering and Applied Chemistry, University of Toronto, 200 College Street, Toronto, Ontario, Canada M5S 3E5

[c] Department of Materials Science and Engineering, University of Toronto, 184 College Street, Toronto, Ontario, Canada M5S 3E4

[d] Department of Mechanical and Industrial Engineering, University of Toronto, 5 King's College Road, Toronto, Ontario, Canada M5S 3G8

* to whom correspondences should be addressed. Email: tim.bender@utoronto.ca

Lewis Acidity and Basicity Calculations

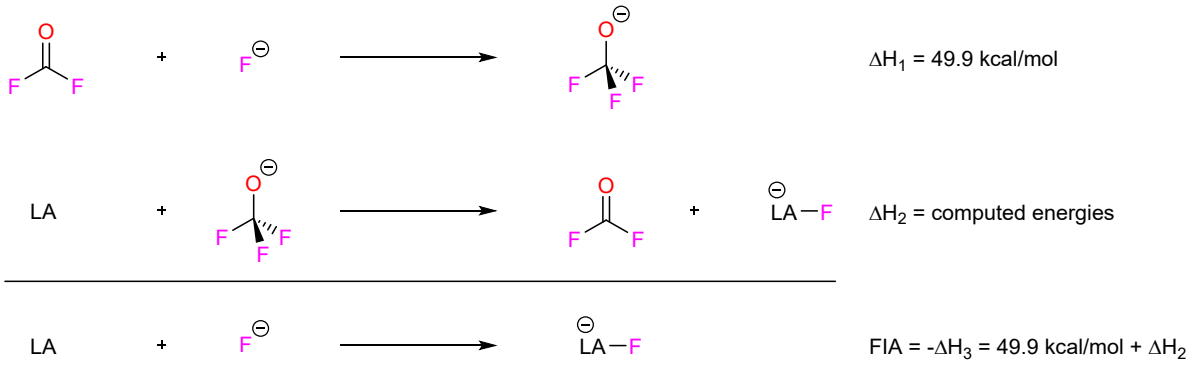

Figure S1: Depiction of the fluoride affinity method used to compute the Lewis acidity of boron sources in this study where LA is the Lewis acid of interest.[1]

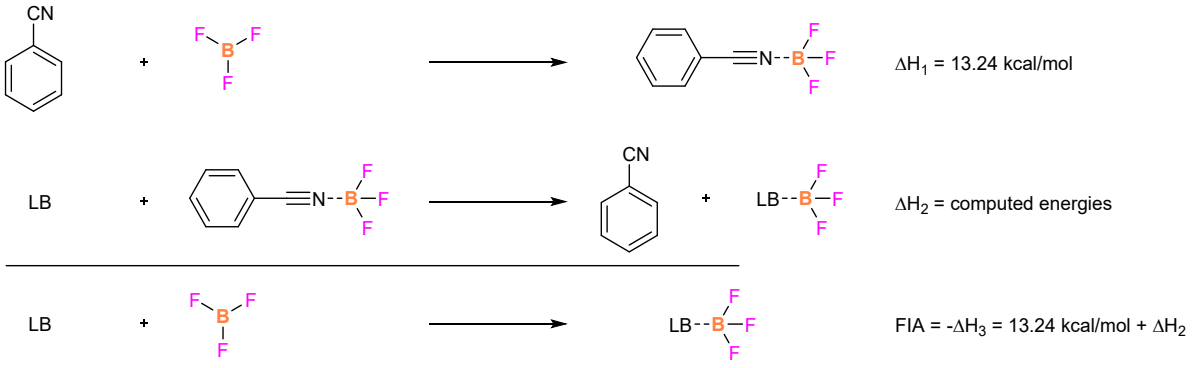

Figure S2: Depiction of the BF_3 affinity method used to compute the Lewis basicity of precursors in this study where LB is the Lewis base of interest.[2]

Characterization of $B(OC_6F_5)_3$ from the BCl_3 and BBr_3 Methods

BCl_3 Method

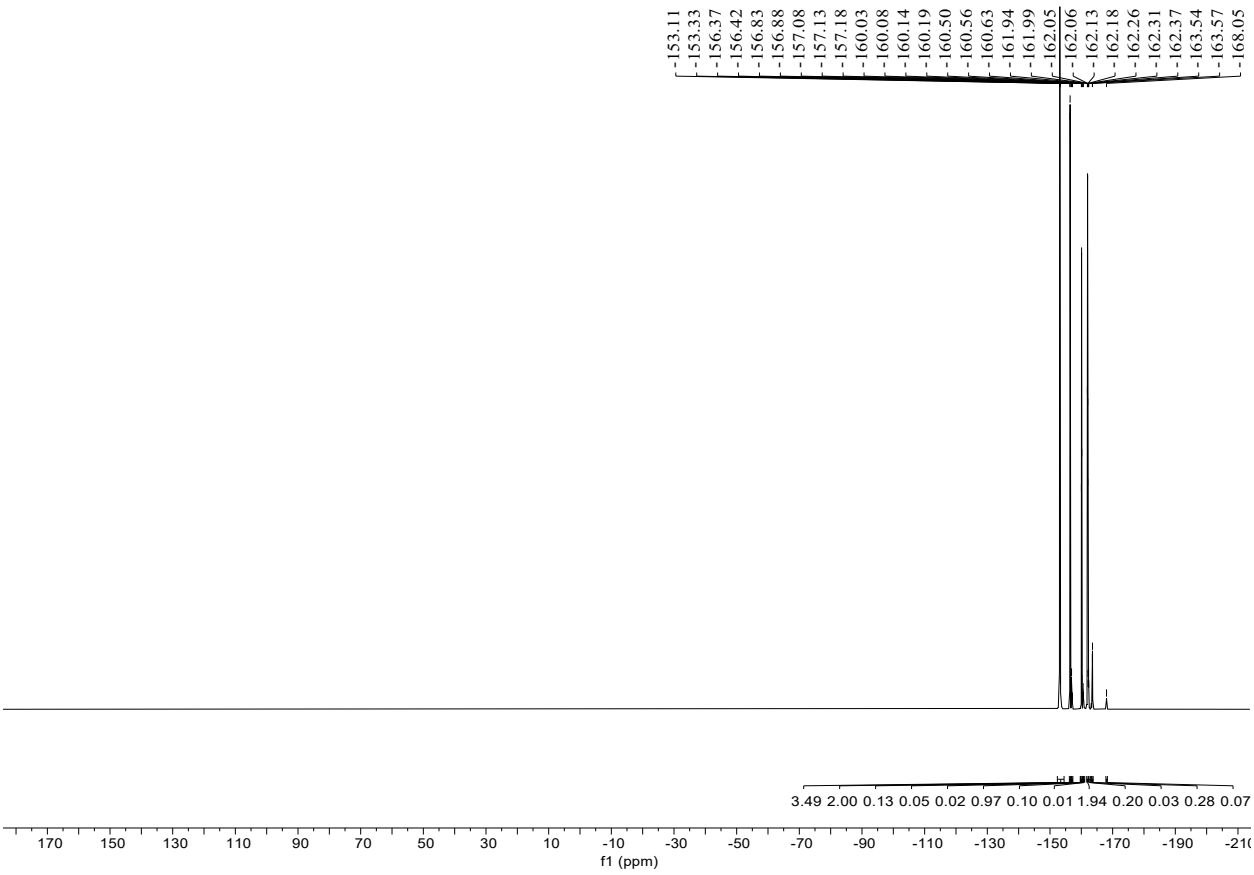

Figure S3: ^{19}F NMR spectrum (400 MHz) of $B(OC_6F_5)_3$ crude in $CDCl_3$.

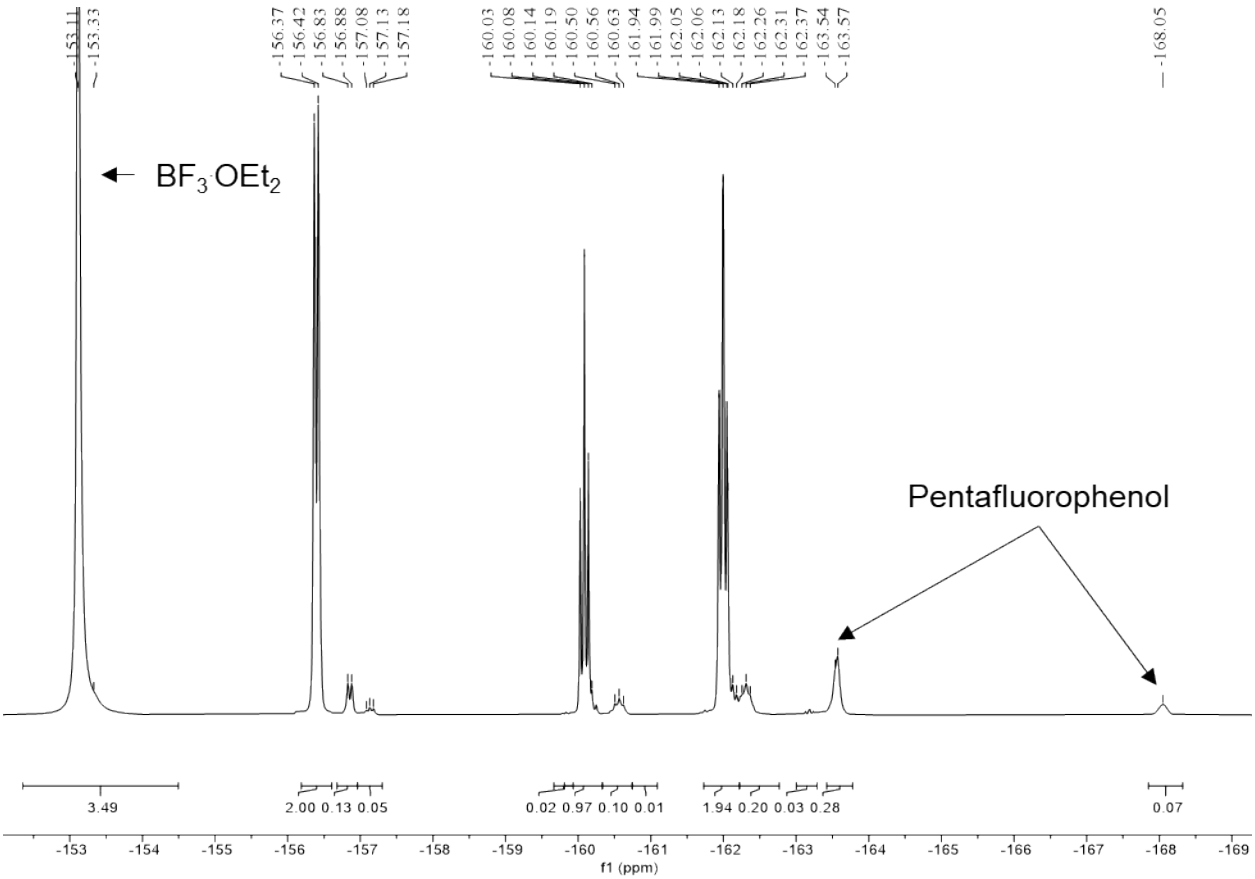

Figure S4: ^{19}F NMR spectrum (400 MHz) of $B(OC_6F_5)_3$ crude in $CDCl_3$ (zoom 1).

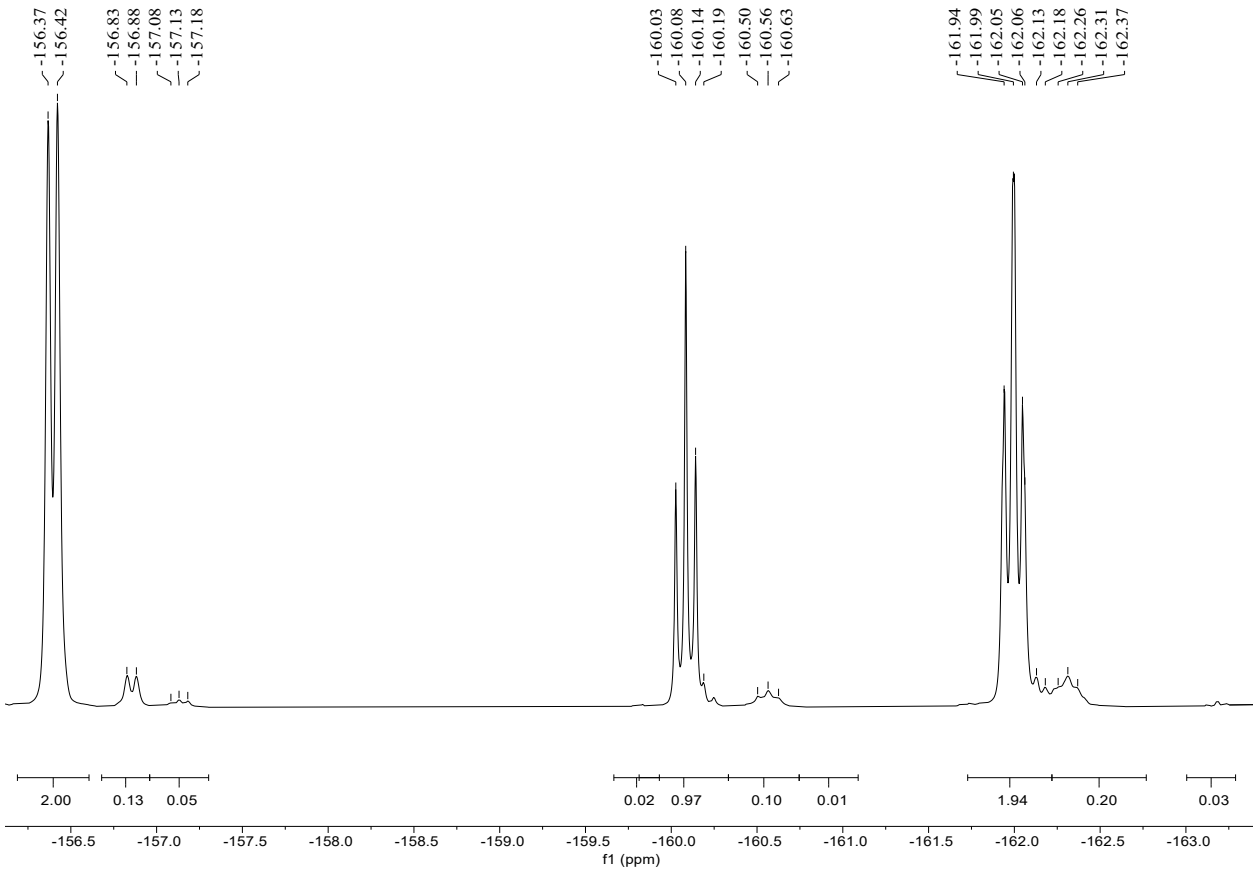

Figure S5: ^{19}F NMR spectrum (400 MHz) of $B(OC_6F_5)_3$ crude in $CDCl_3$ (zoom 2).

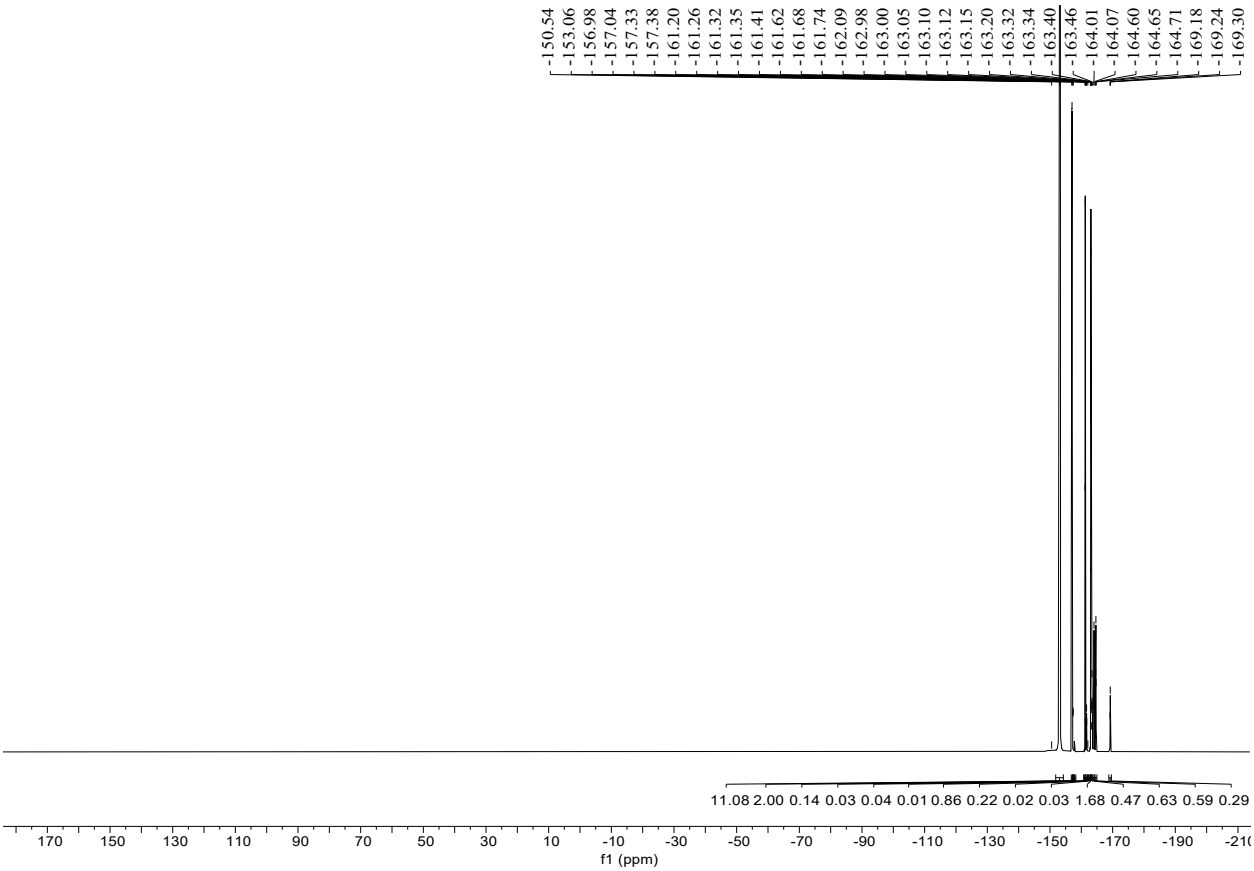

Figure S6: ^{19}F NMR spectrum (400 MHz) of $B(OC_6F_5)_3$ crude in CD_2Cl_2.

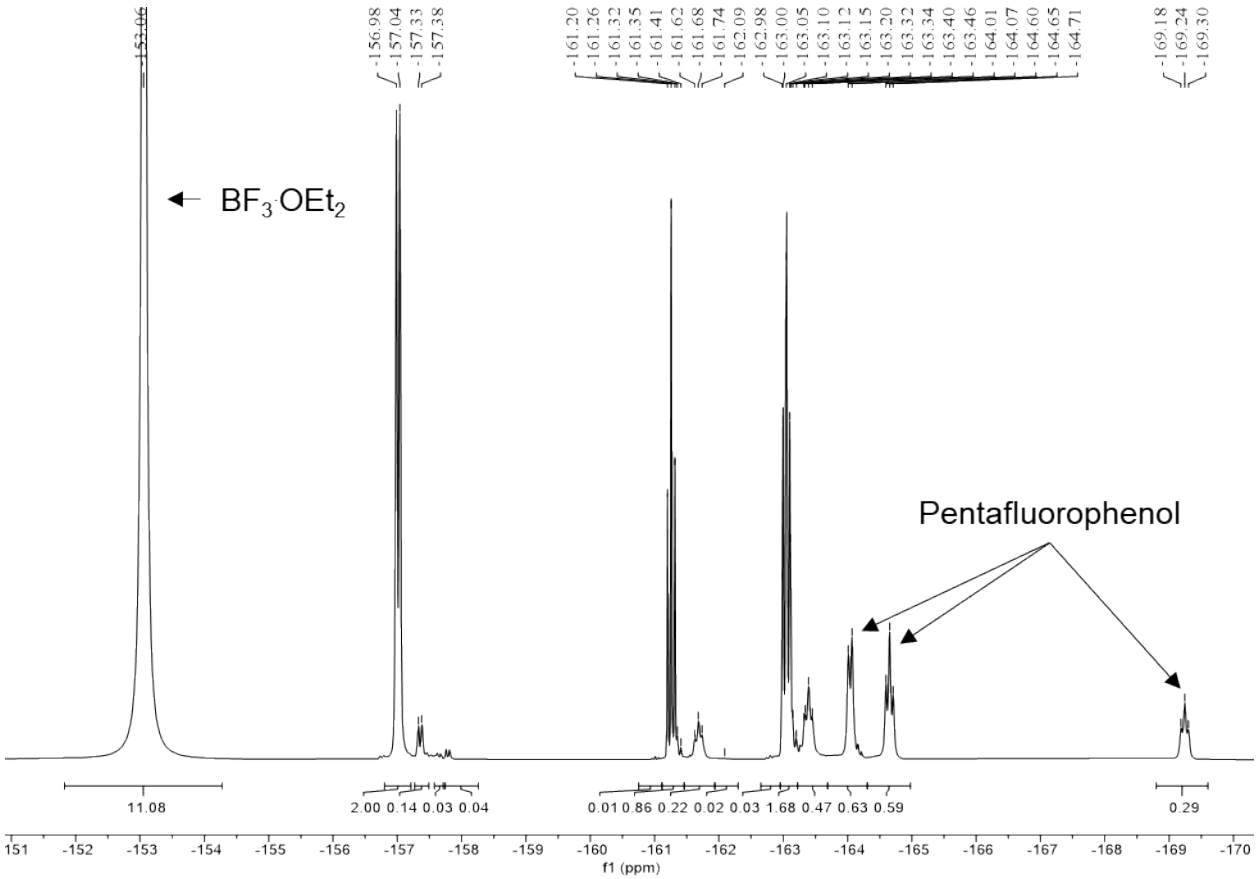

Figure S7: ^{19}F NMR spectrum (400 MHz) of $B(OC_6F_5)_3$ crude in CD_2Cl_2 (zoom 1).

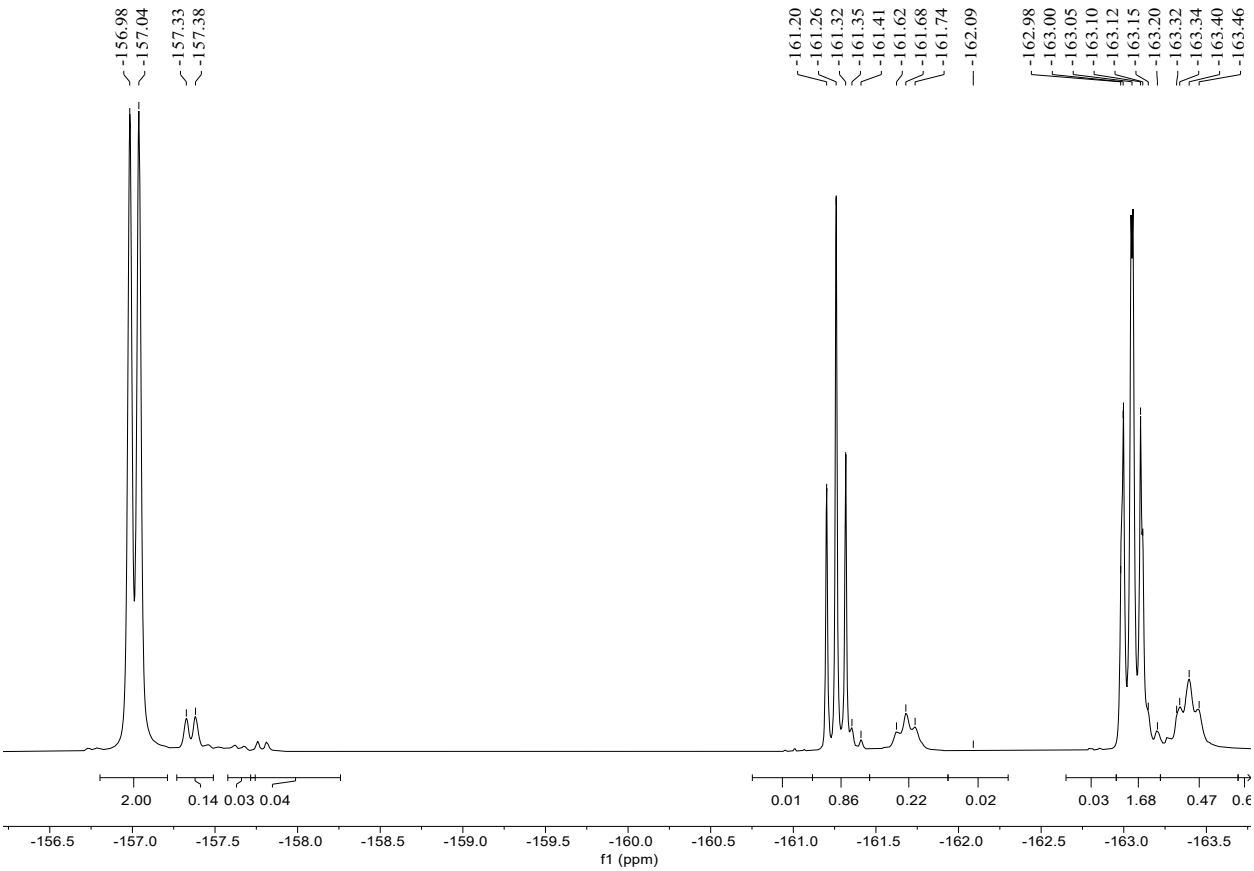

Figure S8: ^{19}F NMR spectrum (400 MHz) of $B(OC_6F_5)_3$ crude in CD_2Cl_2 (zoom 2).

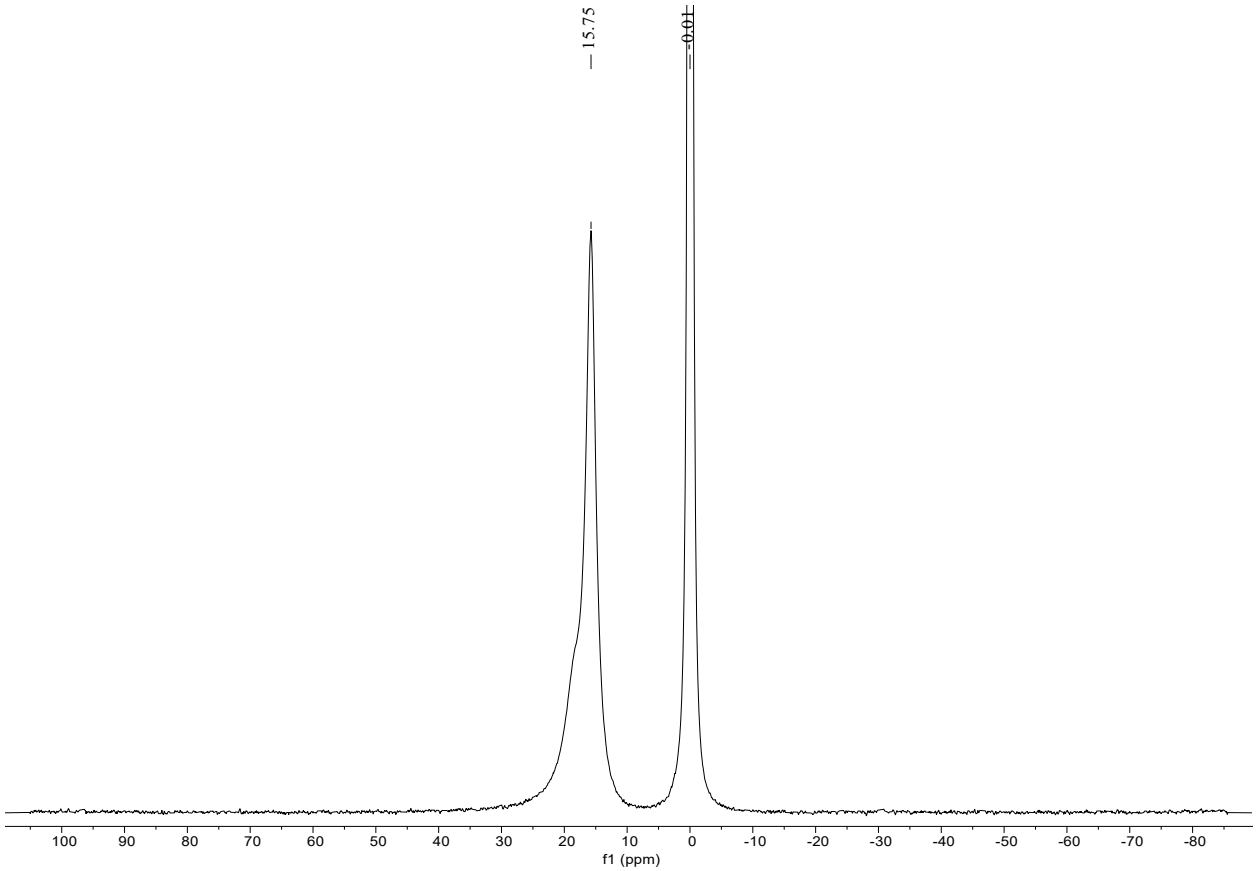

Figure S9: ^{11}B NMR spectrum (400 MHz) of $B(OC_6F_5)_3$ crude in $CDCl_3$. Referenced to $BF_3{\cdot}OEt_2$ (δ = 0.00 ppm).

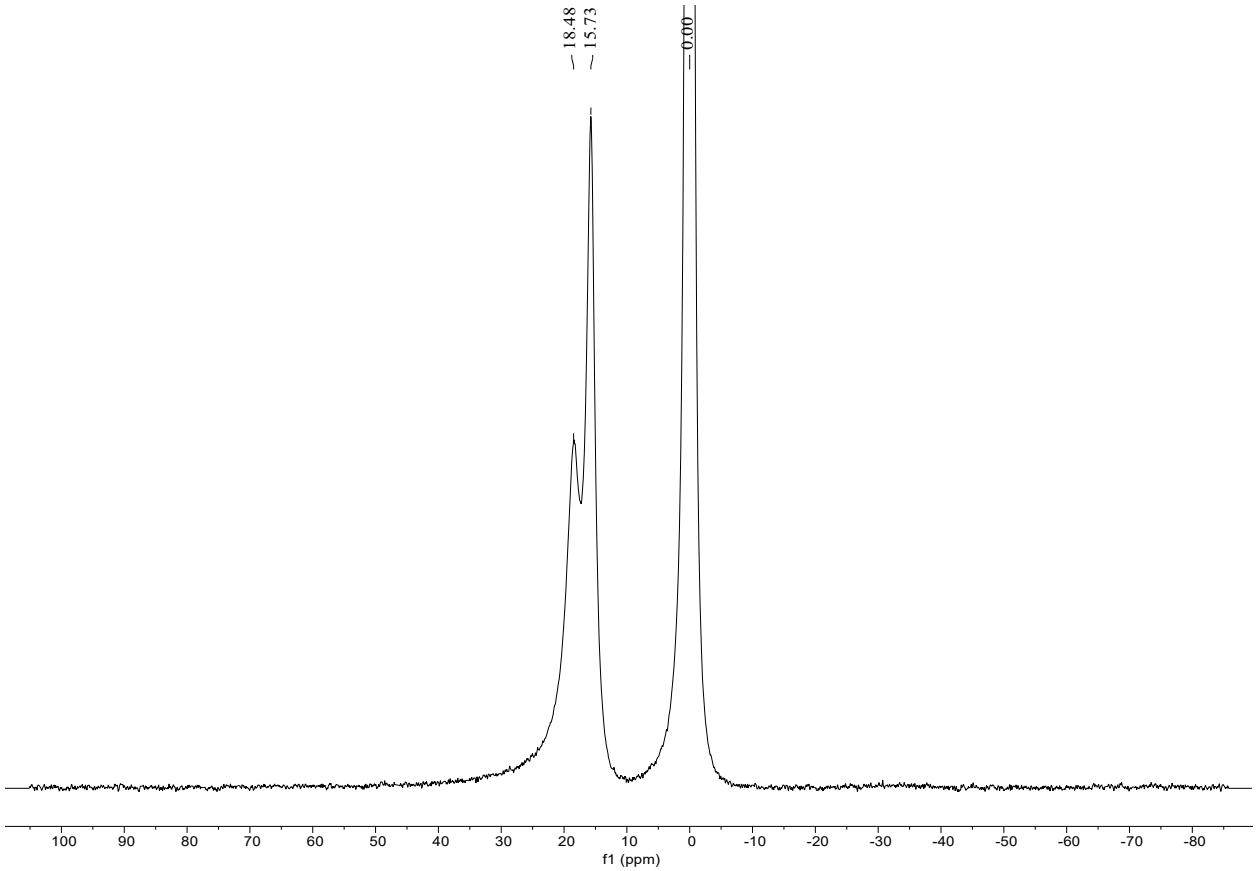

Figure S10: ^{11}B NMR spectrum (400 MHz) of $B(OC_6F_5)_3$ crude in CD_2Cl_2. Referenced to $BF_3{\cdot}OEt_2$ (δ = 0.00 ppm).

BBr_3 Method

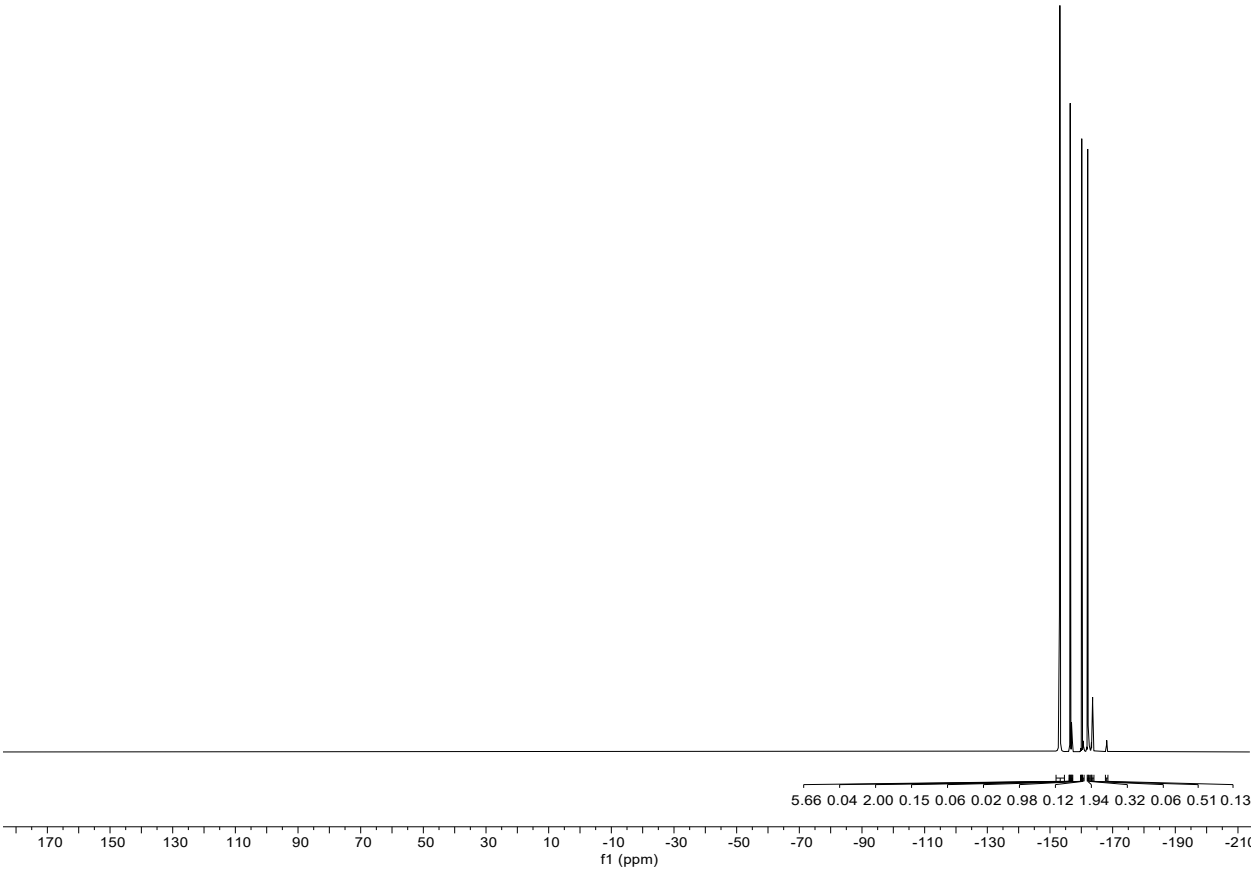

Figure S11: ^{19}F NMR spectrum (400 MHz) of $B(OC_6F_5)_3$ crude in $CDCl_3$.

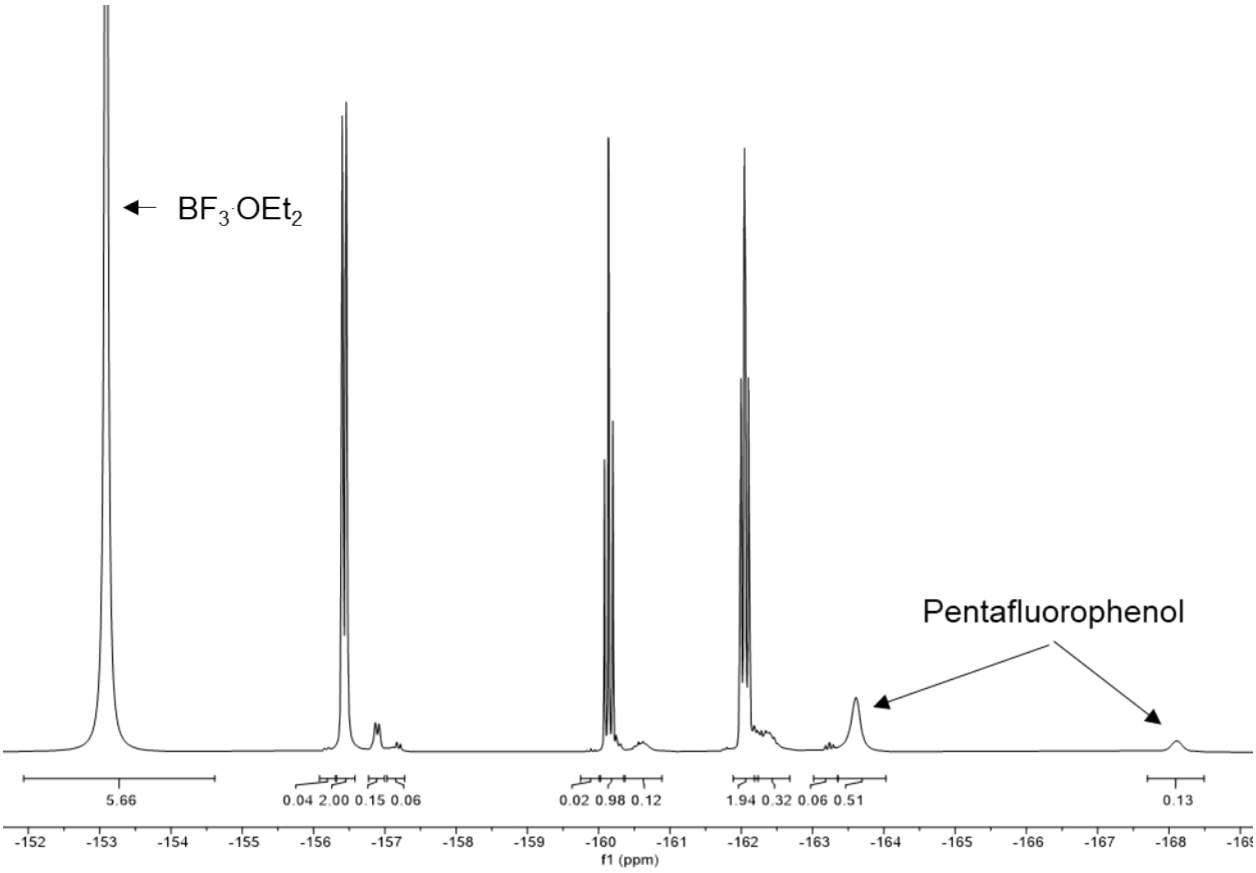

Figure S12: ^{19}F NMR spectrum (400 MHz) of $B(OC_6F_5)_3$ crude in $CDCl_3$ (zoom 1).

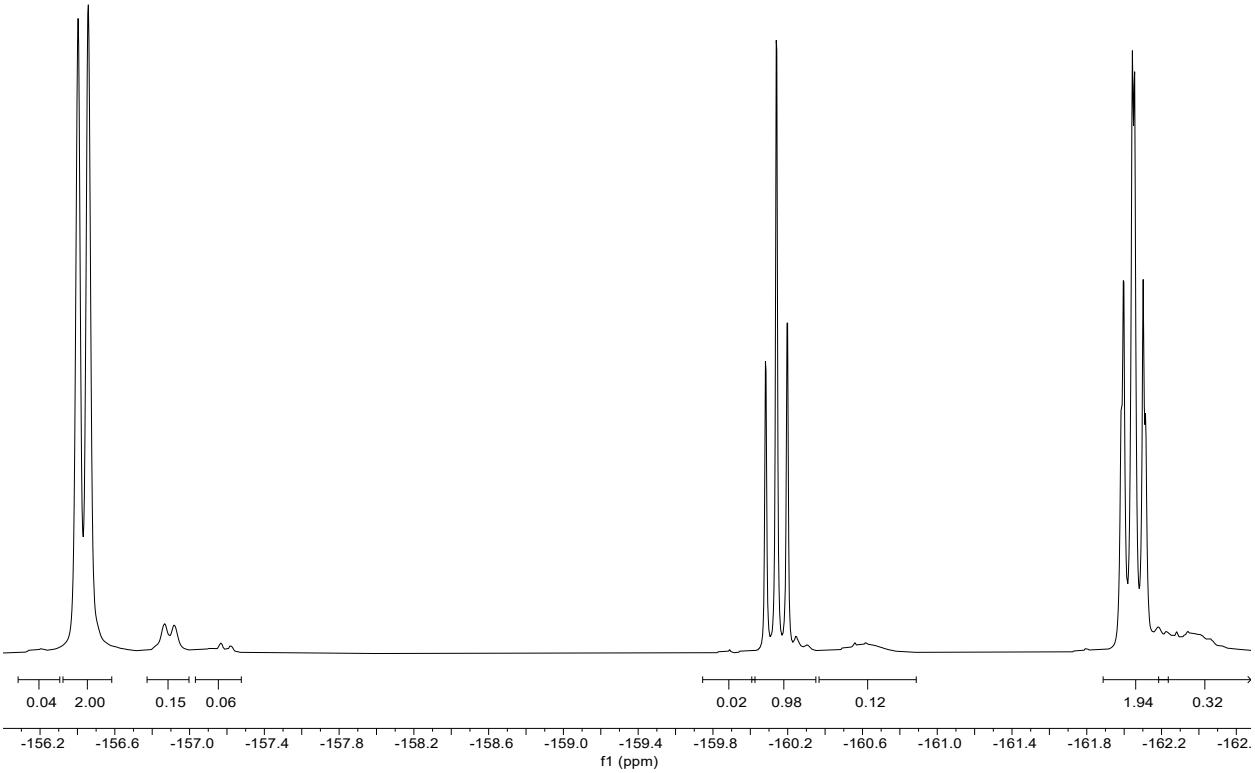

Figure S13: ^{19}F NMR spectrum (400 MHz) of $B(OC_6F_5)_3$ crude in $CDCl_3$ (zoom 2).

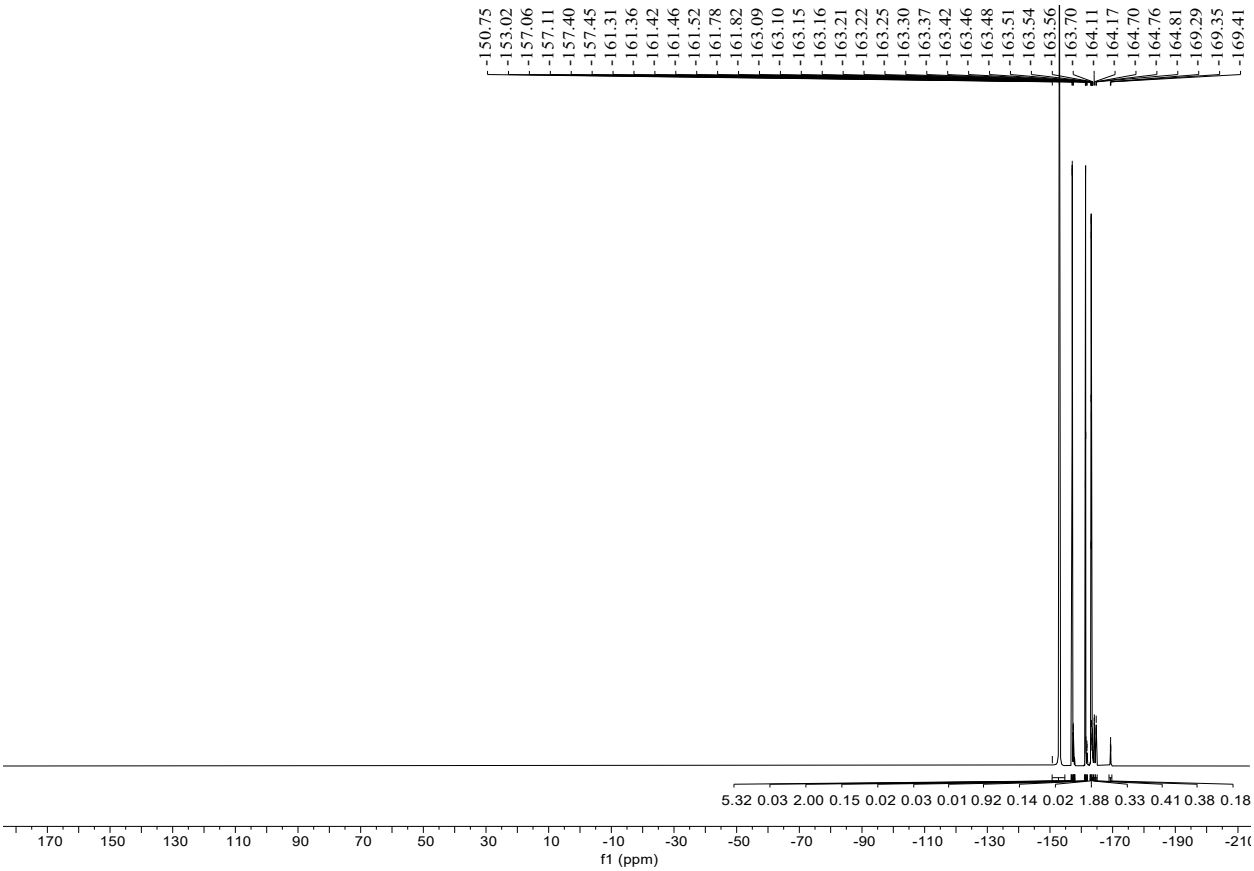

Figure S14: ^{19}F NMR spectrum (400 MHz) of $B(OC_6F_5)_3$ crude in CD_2Cl_2.

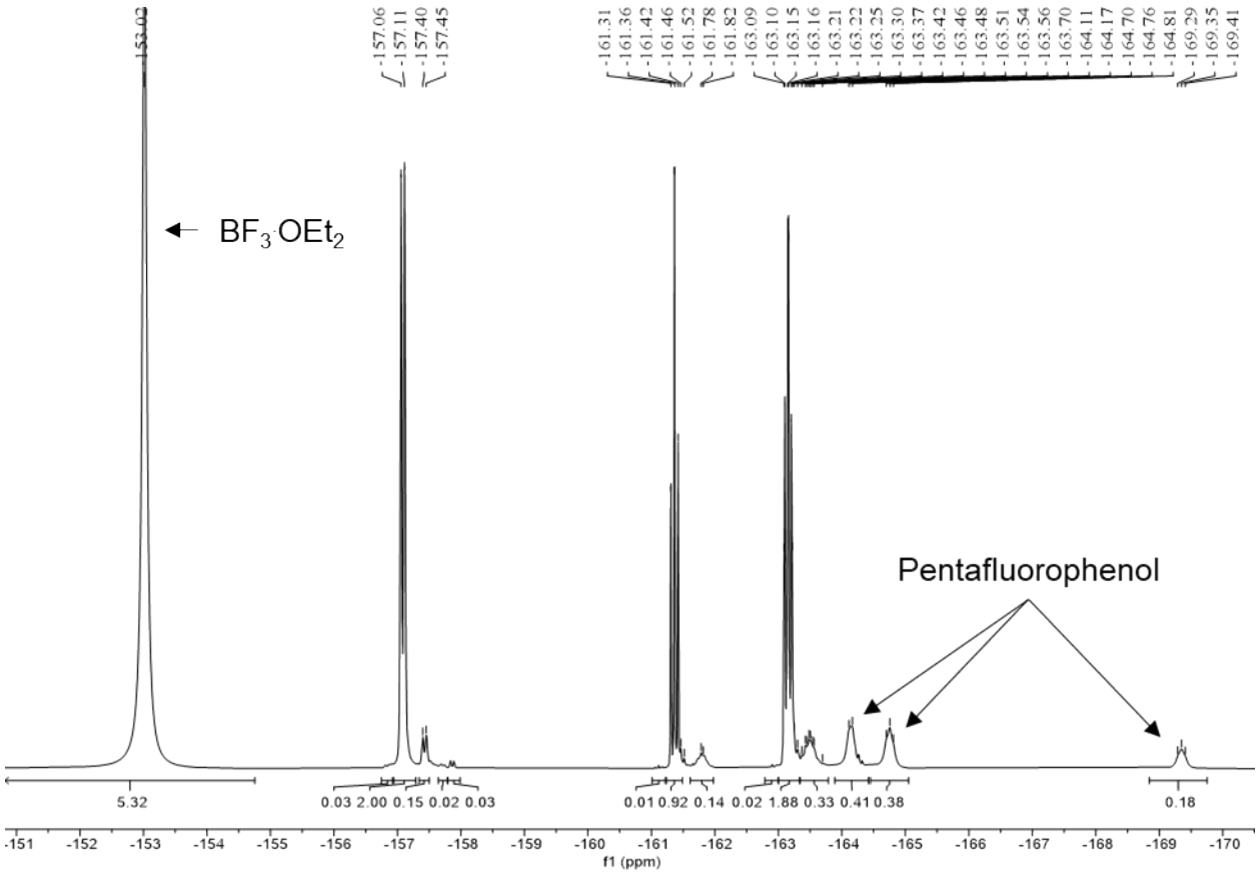

Figure S15: ^{19}F NMR spectrum (400 MHz) of $B(OC_6F_5)_3$ crude in CD_2Cl_2 (zoom 1).

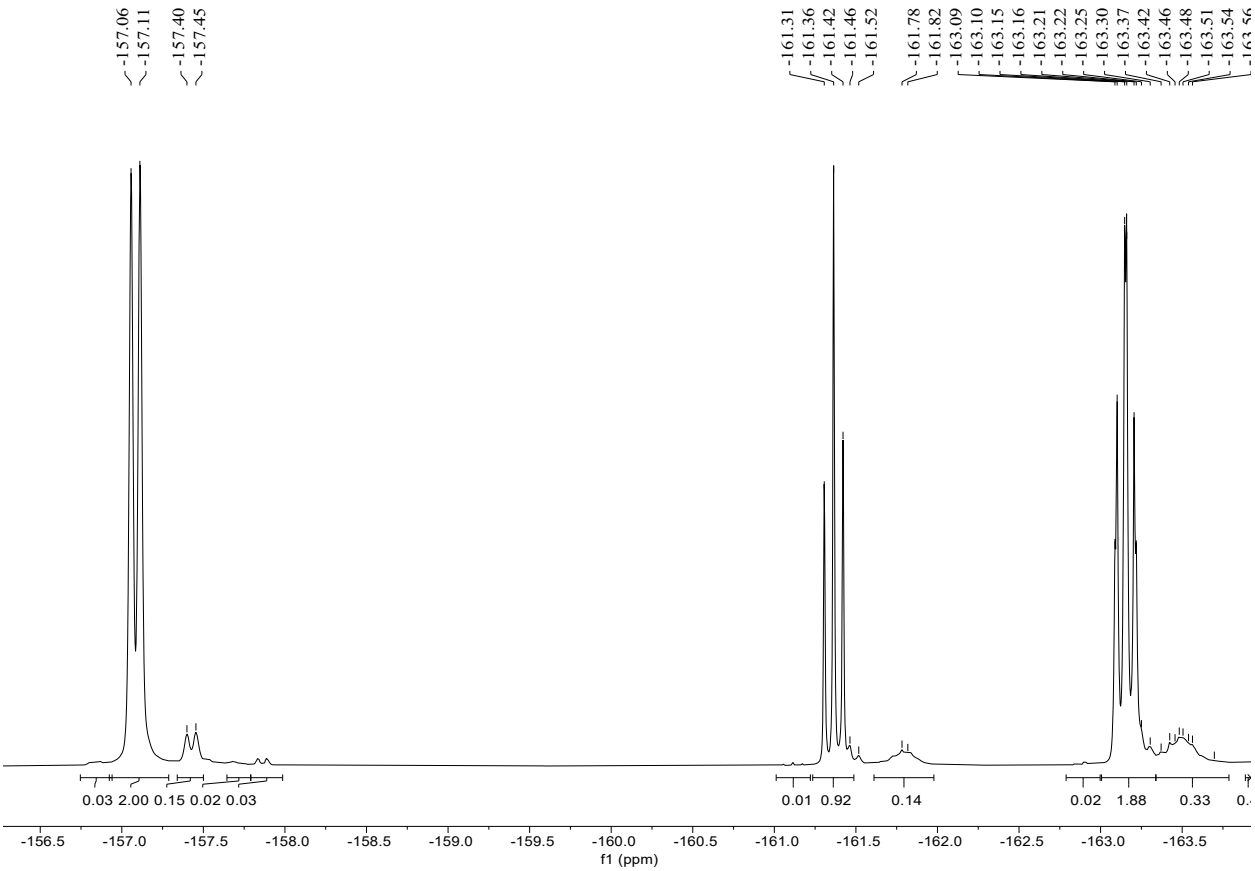

Figure S16: ^{19}F NMR spectrum (400 MHz) of $B(OC_6F_5)_3$ crude in CD_2Cl_2 (zoom 2).

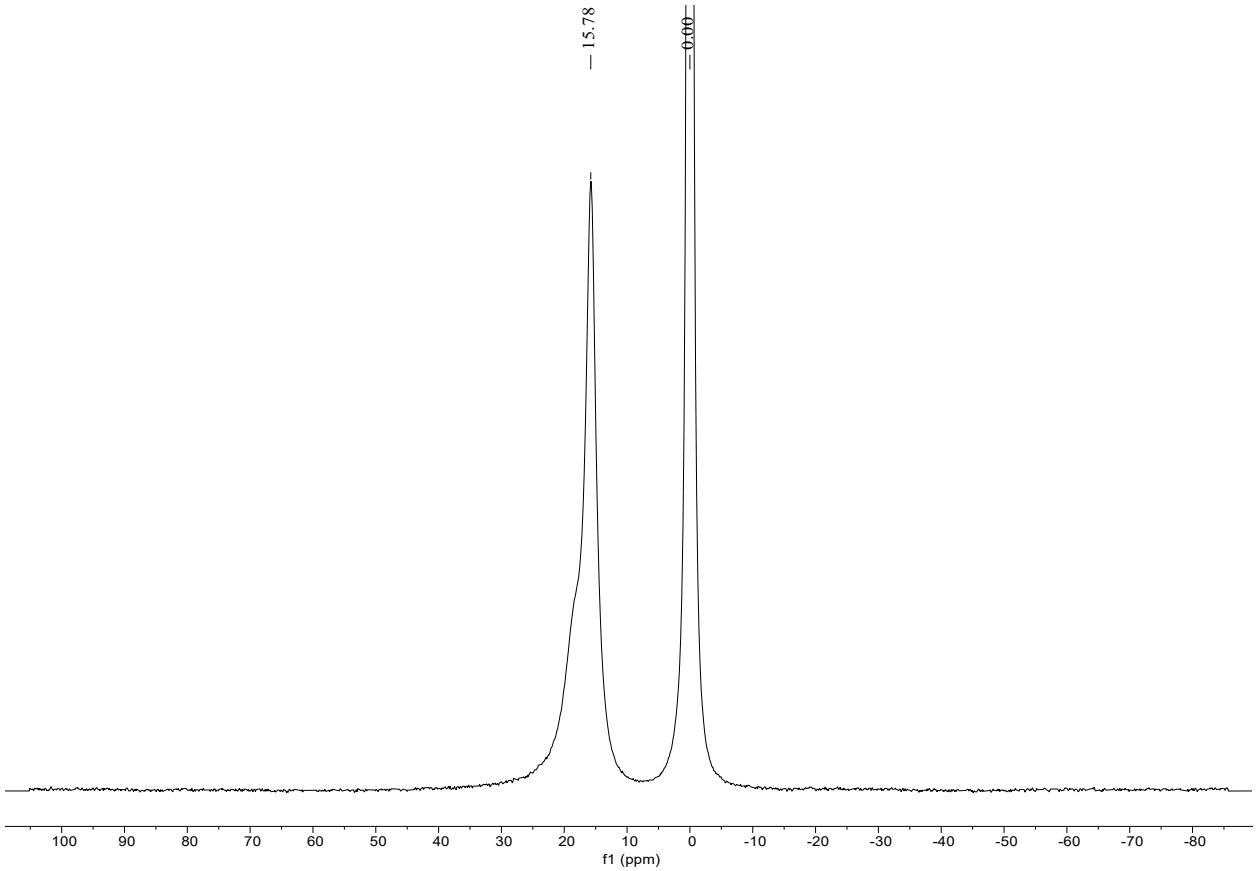

Figure S17: ^{11}B NMR spectrum (400 MHz) of $B(OC_6F_5)_3$ crude in $CDCl_3$. Referenced to $BF_3{\cdot}OEt_2$ (δ = 0.00 ppm).

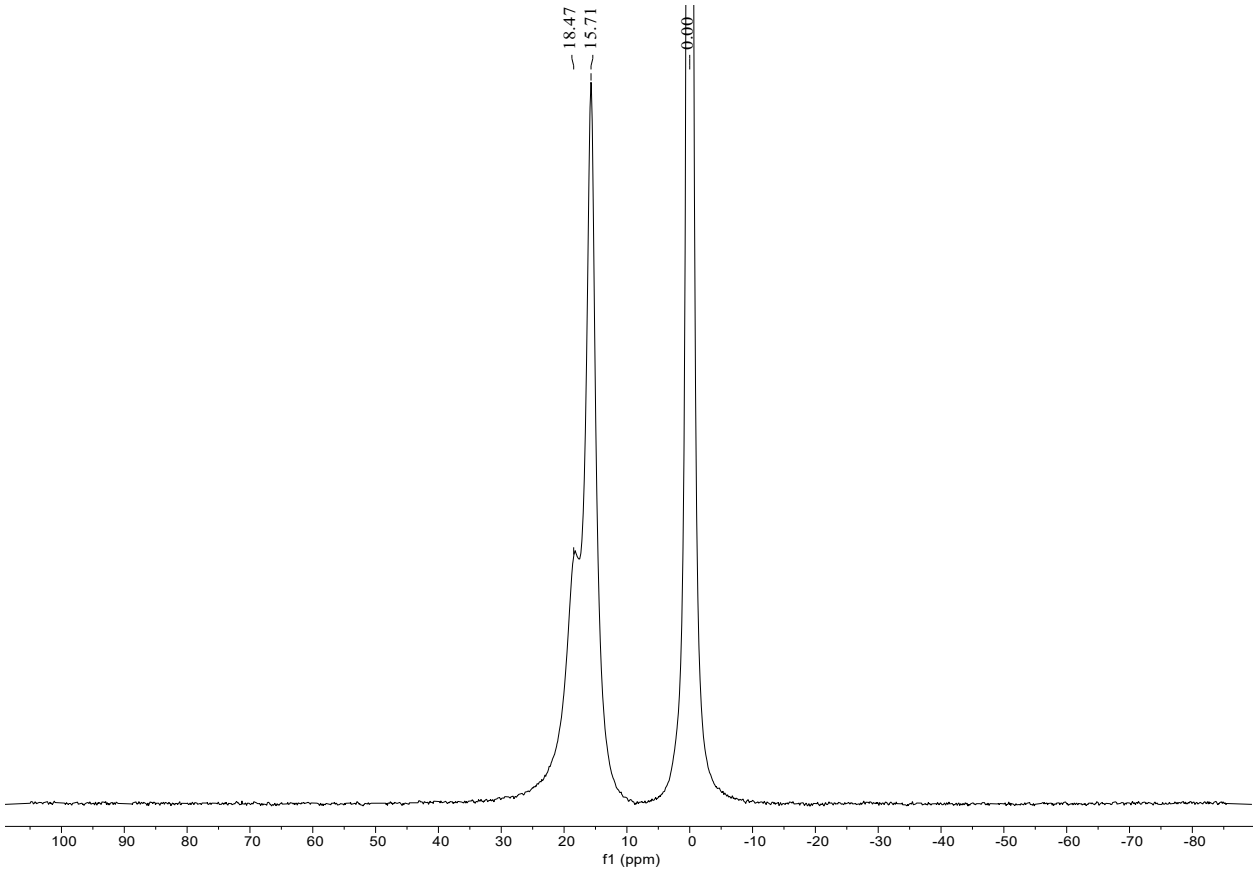

Figure S18: ^{11}B NMR spectrum (400 MHz) of $B(OC_6F_5)_3$ crude in CD_2Cl_2. Referenced to $BF_3{\cdot}OEt_2$ (δ = 0.00 ppm).

HPLC Monitoring of the $B(OC_6F_5)_3$ / Tetralin Process

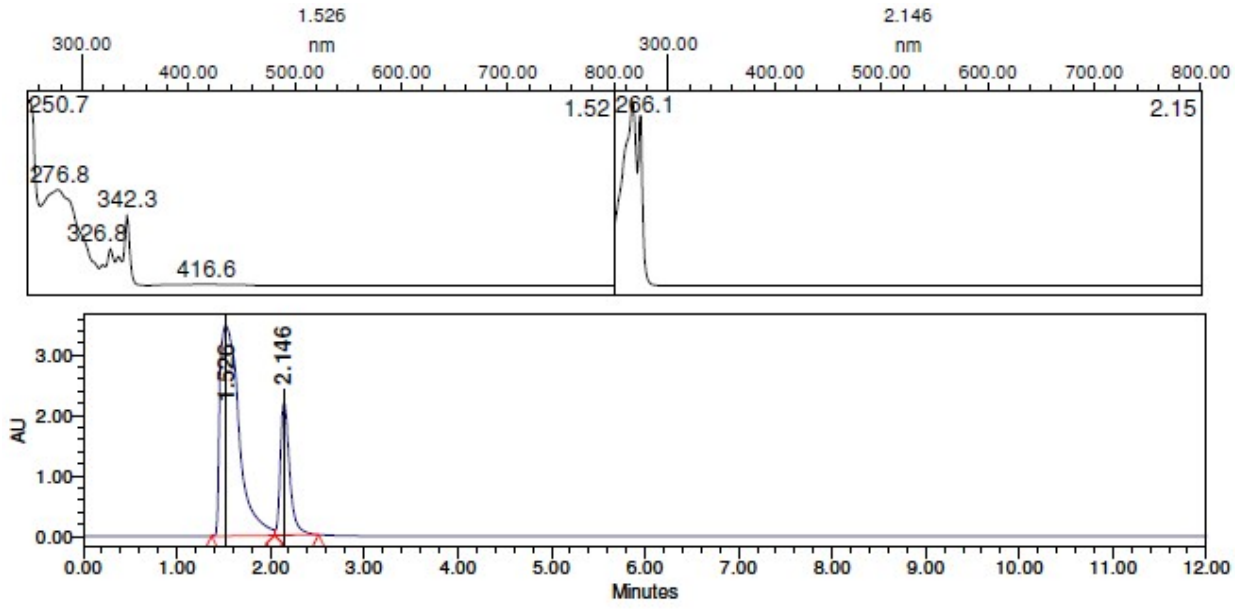

Figure S19: HPLC chromatogram of the $B(OC_6F_5)_3$/tetralin process to form F_5-BsubNc at T = 0 hours (MAX PLOT - 190 nm to 800 nm). HPLC run conducted with C18 functionalized silica as the stationary phase and 80:20 ACN:DMF (V:V) as the mobile phase.

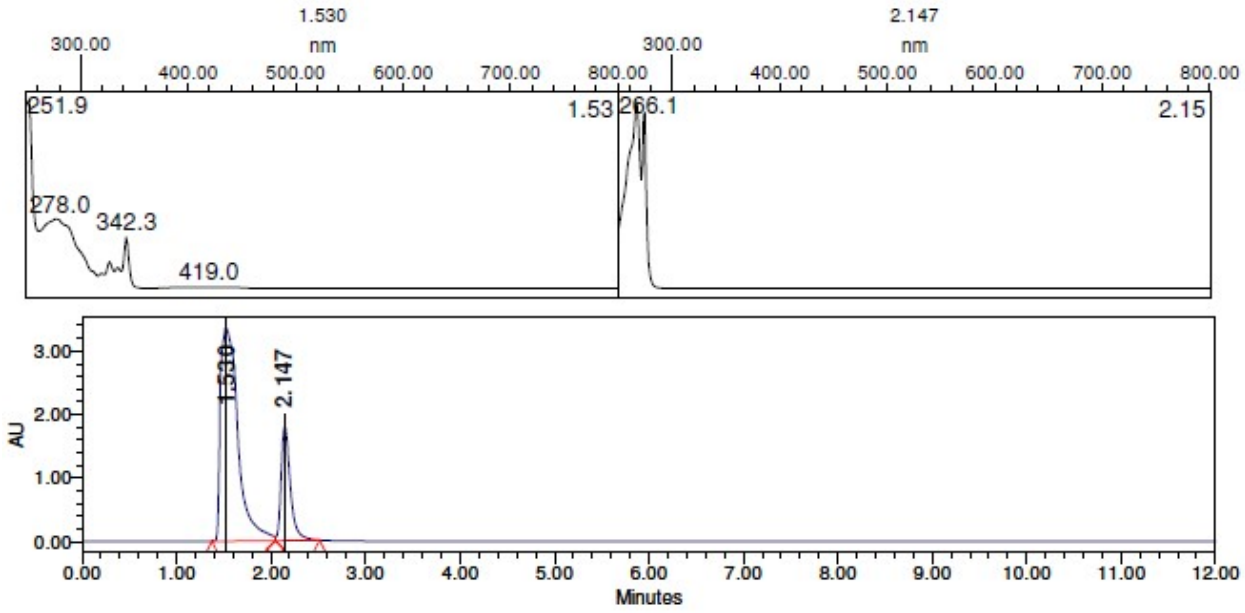

Figure S20: HPLC chromatogram of the $B(OC_6F_5)_3$/tetralin process to form F_5-BsubNc at T = 0.5 hours (MAX PLOT - 190 nm to 800 nm). HPLC run conducted with C18 functionalized silica as the stationary phase and 80:20 ACN:DMF (V:V) as the mobile phase.

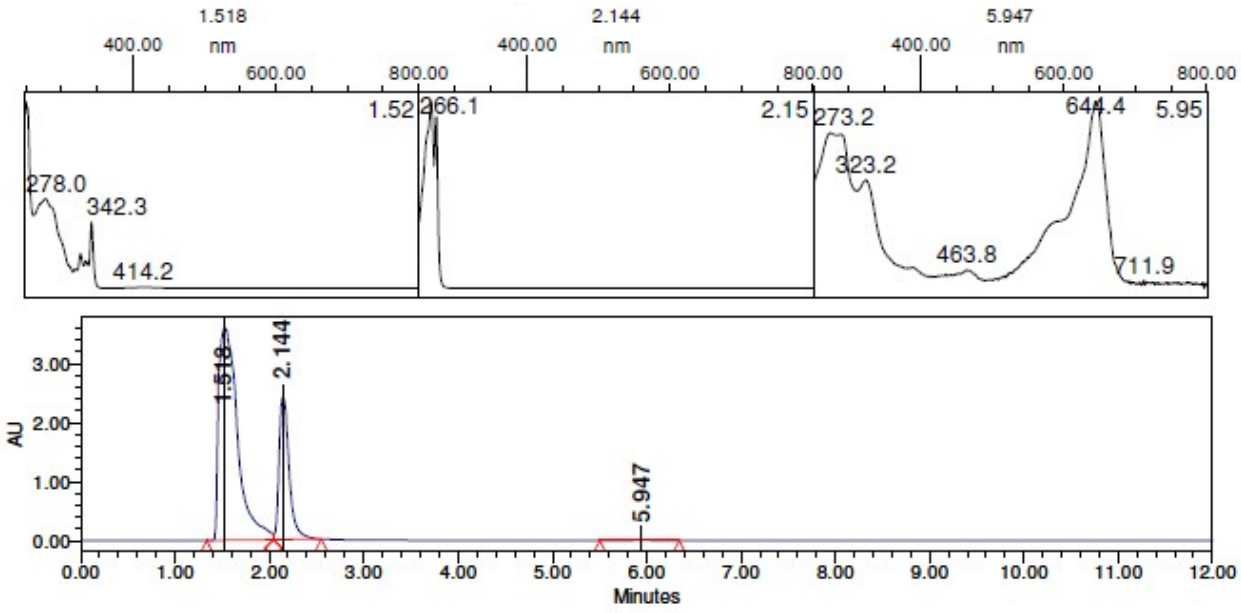

Figure S21: HPLC chromatogram of the $B(OC_6F_5)_3$/tetralin process to form F_5-BsubNc at T = 1.0 hours (MAX PLOT - 190 nm to 800 nm). HPLC run conducted with C18 functionalized silica as the stationary phase and 80:20 ACN:DMF (V:V) as the mobile phase.

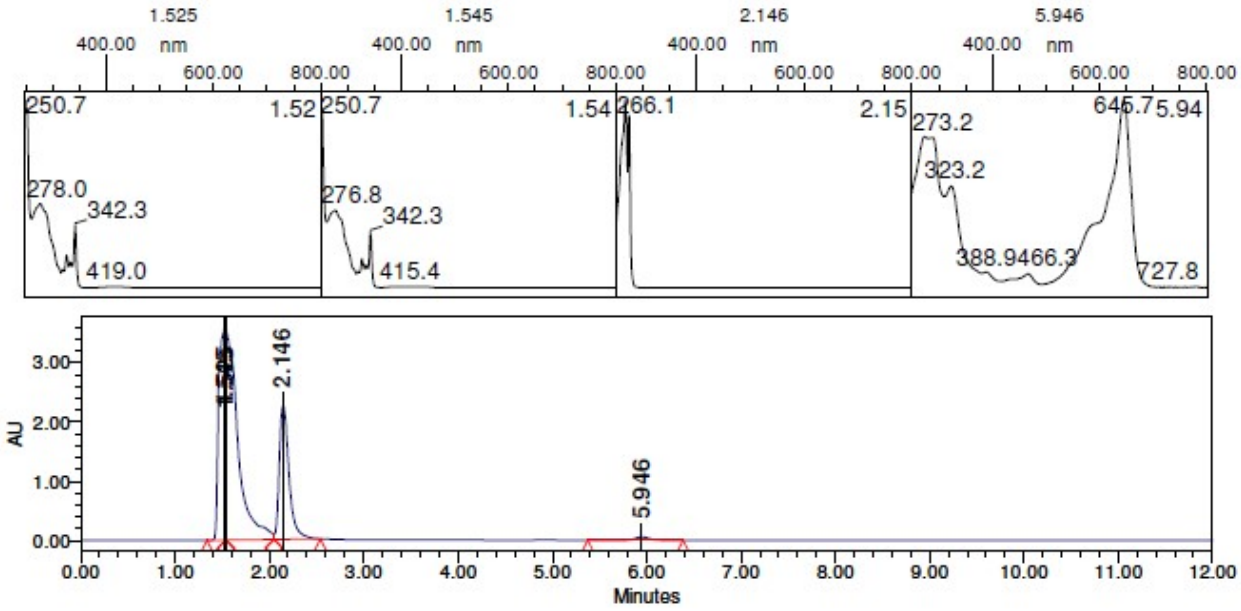

Figure S22: HPLC chromatogram of the $B(OC_6F_5)_3$/tetralin process to form F_5-BsubNc at T = 1.25 hours (MAX PLOT - 190 nm to 800 nm). HPLC run conducted with C18 functionalized silica as the stationary phase and 80:20 ACN:DMF (V:V) as the mobile phase.

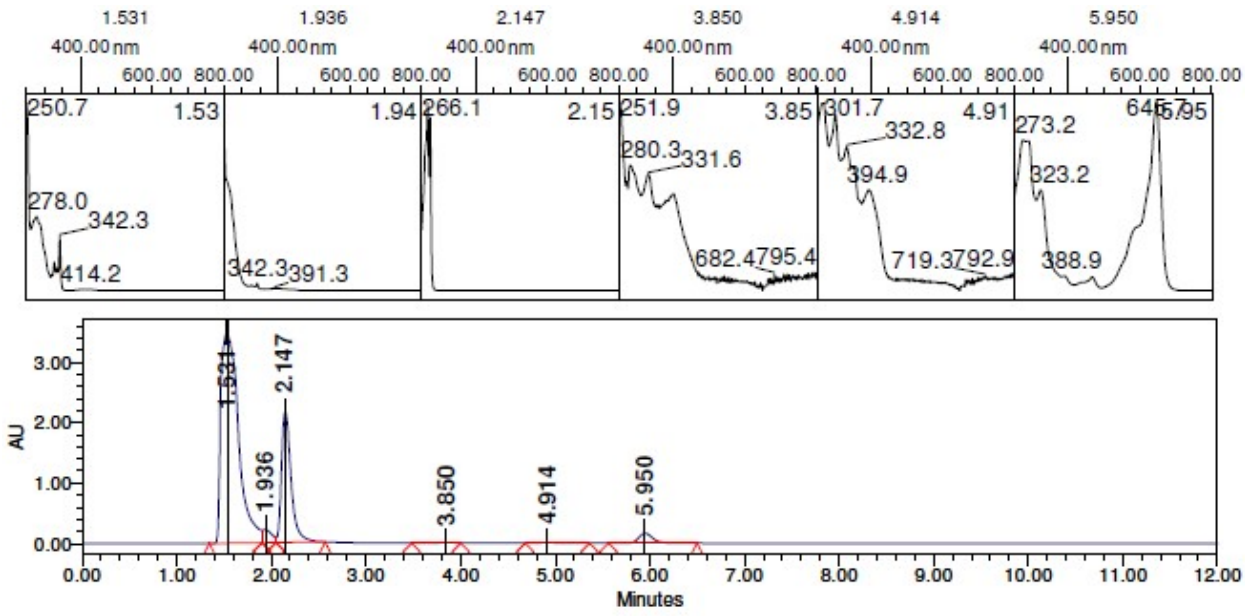

Figure S23: HPLC chromatogram of the $B(OC_6F_5)_3$/tetralin process to form F_5-BsubNc at T = 1.5 hours (MAX PLOT - 190 nm to 800 nm). HPLC run conducted with C18 functionalized silica as the stationary phase and 80:20 ACN:DMF (V:V) as the mobile phase.

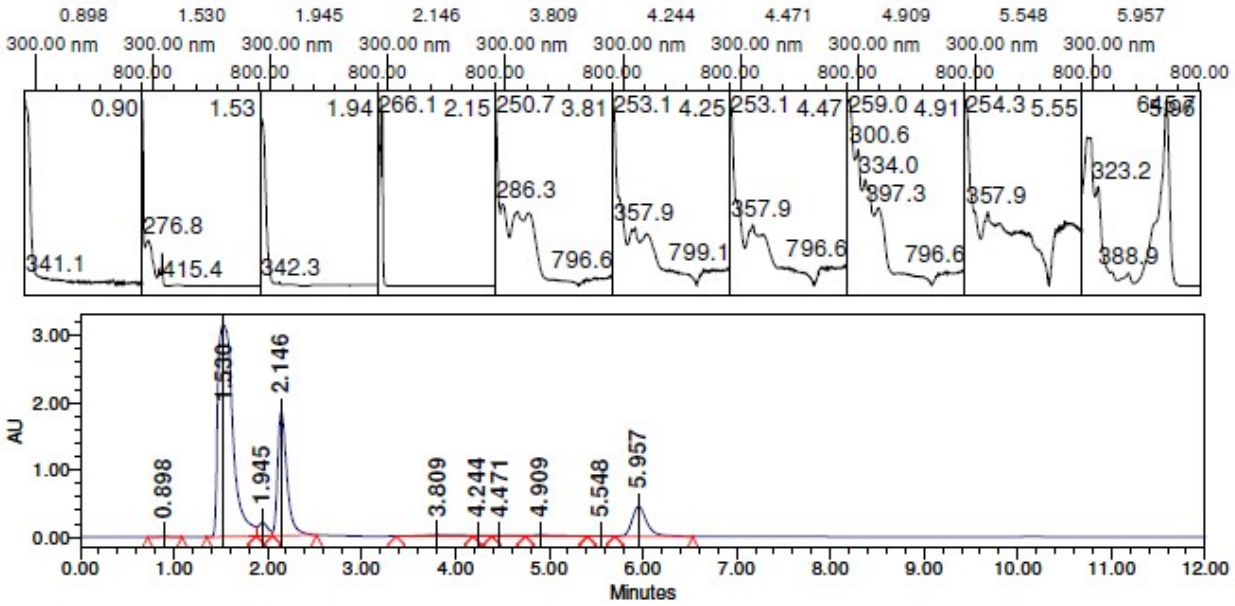

Figure S24: HPLC chromatogram of the $B(OC_6F_5)_3$/tetralin process to form F_5-BsubNc at T = 1.75 hours (MAX PLOT - 190 nm to 800 nm). HPLC run conducted with C18 functionalized silica as the stationary phase and 80:20 ACN:DMF (V:V) as the mobile phase.

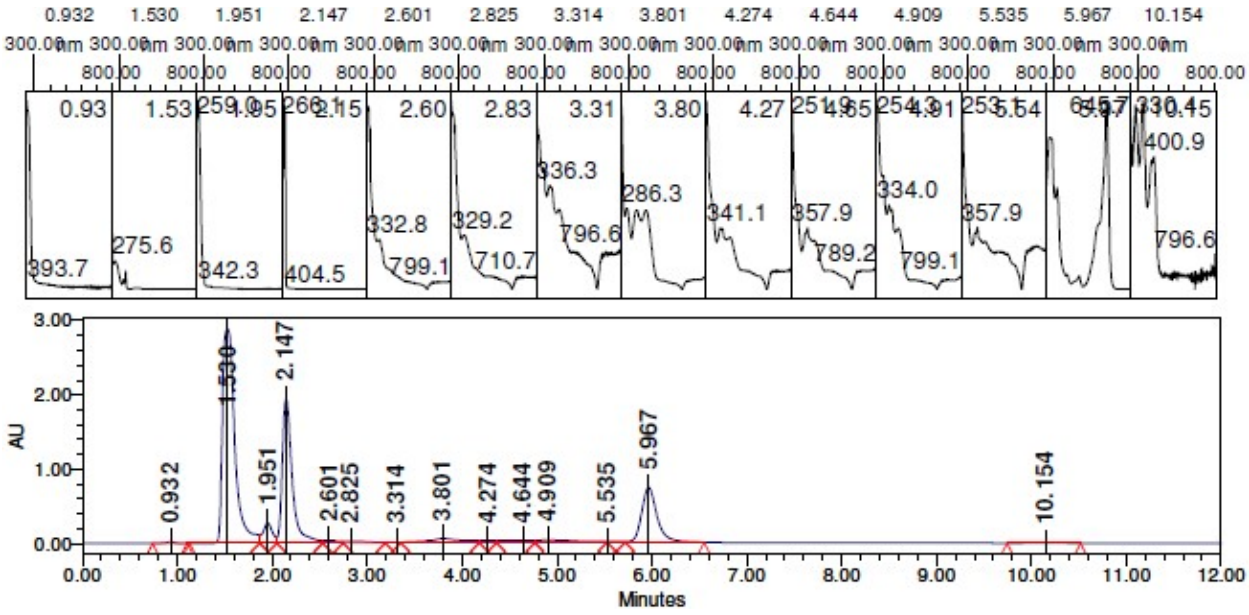

Figure S25: HPLC chromatogram of the $B(OC_6F_5)_3$/tetralin process to form F_5-BsubNc at T = 2.0 hours (MAX PLOT - 190 nm to 800 nm). HPLC run conducted with C18 functionalized silica as the stationary phase and 80:20 ACN:DMF (V:V) as the mobile phase.

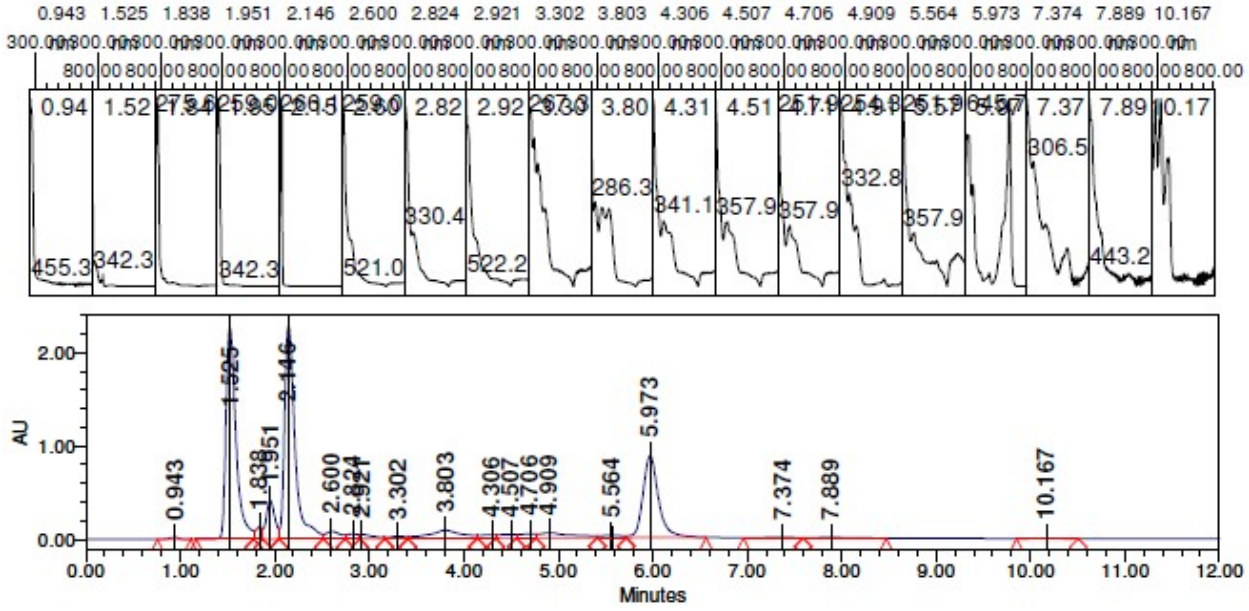

Figure S26: HPLC chromatogram of the $B(OC_6F_5)_3$/tetralin process to form F_5-BsubNc at T = 2.25 hours (MAX PLOT - 190 nm to 800 nm). HPLC run conducted with C18 functionalized silica as the stationary phase and 80:20 ACN:DMF (V:V) as the mobile phase.

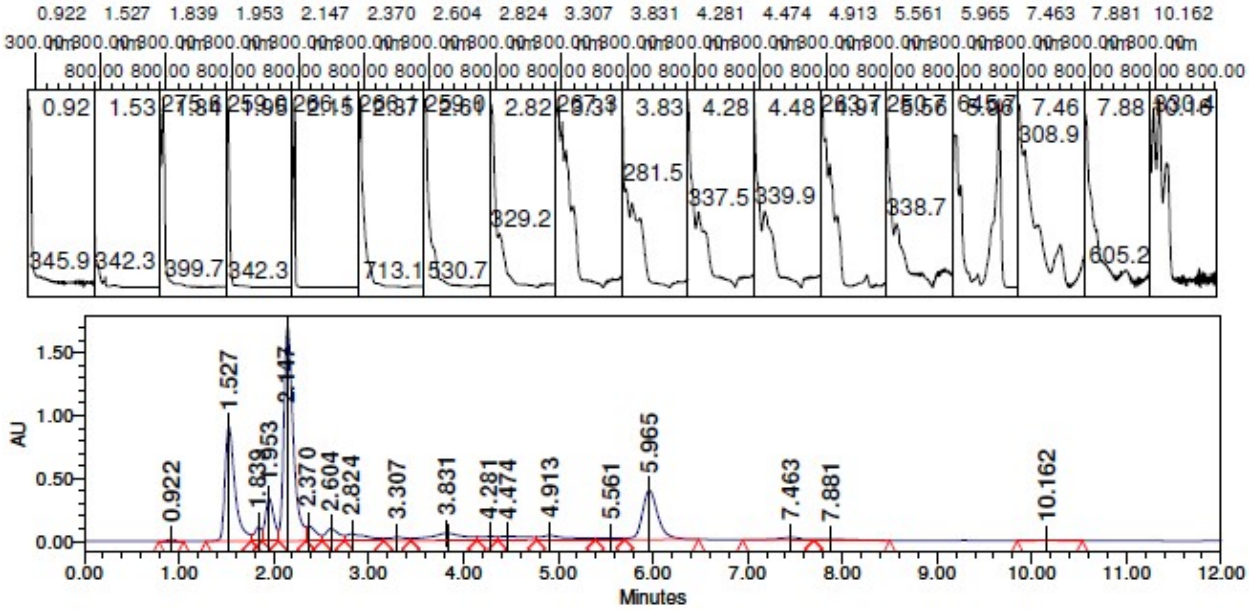

Figure S27: HPLC chromatogram of the $B(OC_6F_5)_3$/tetralin process to form F_5-BsubNc at T = 2.5 hours (MAX PLOT - 190 nm to 800 nm). HPLC run conducted with C18 functionalized silica as the stationary phase and 80:20 ACN:DMF (V:V) as the mobile phase.

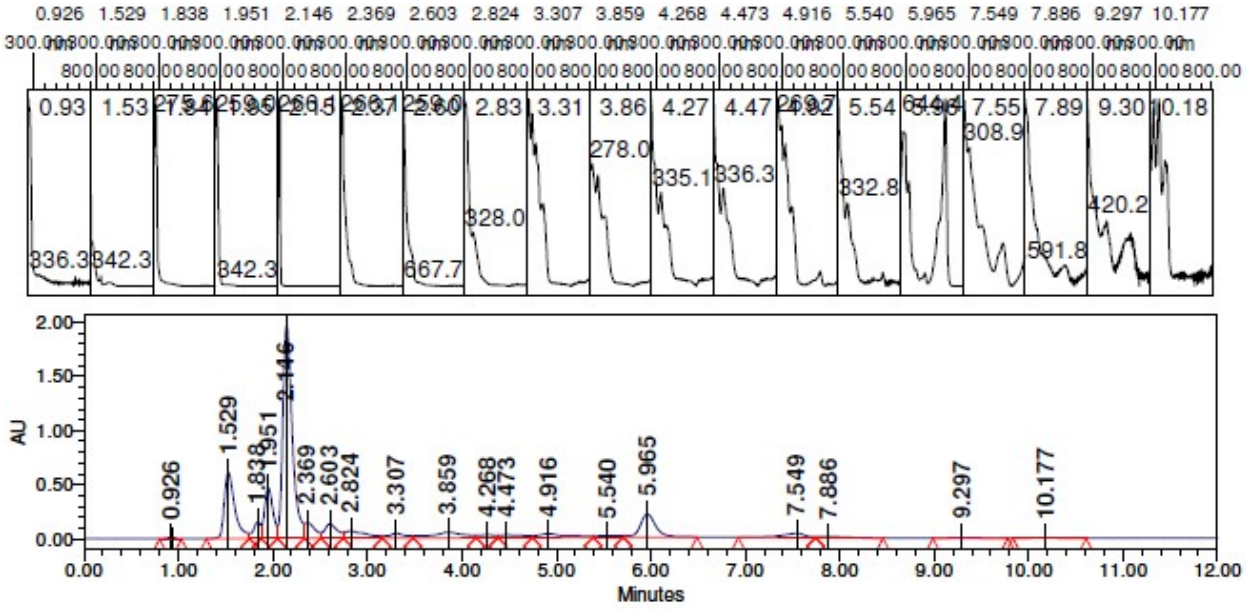

Figure S28: HPLC chromatogram of the $B(OC_6F_5)_3$/tetralin process to form F_5-BsubNc at T = 2.75 hours (MAX PLOT - 190 nm to 800 nm). HPLC run conducted with C18 functionalized silica as the stationary phase and 80:20 ACN:DMF (V:V) as the mobile phase.

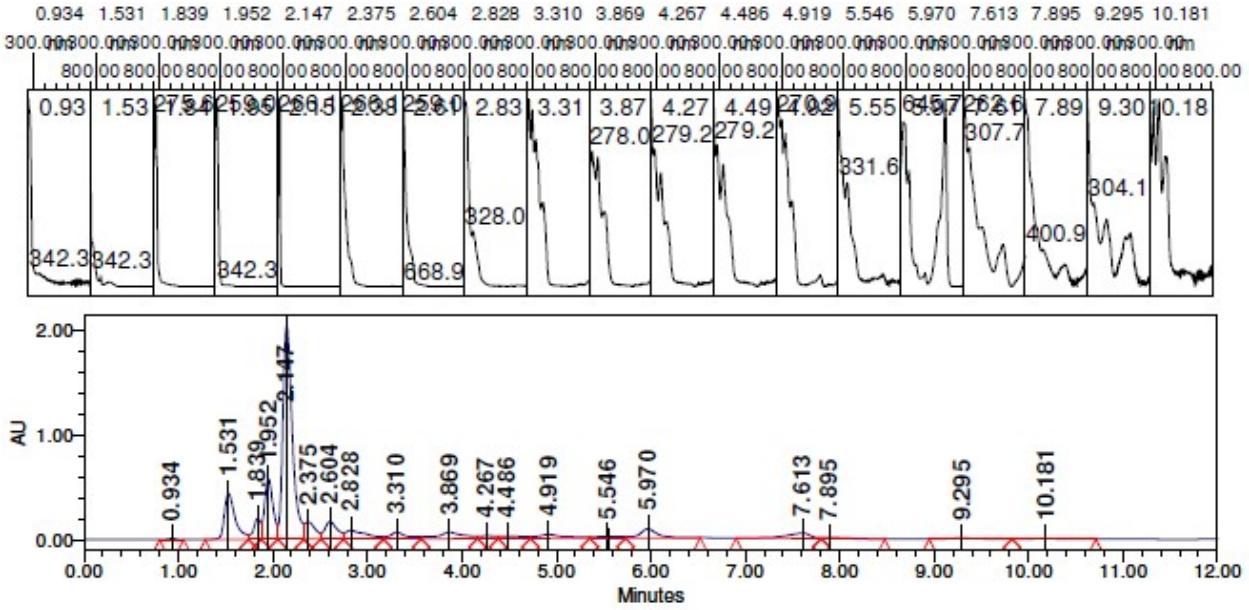

Figure S29: HPLC chromatogram of the $B(OC_6F_5)_3$/tetralin process to form F_5-BsubNc at T = 3.0 hours (MAX PLOT - 190 nm to 800 nm). HPLC run conducted with C18 functionalized silica as the stationary phase and 80:20 ACN:DMF (V:V) as the mobile phase.

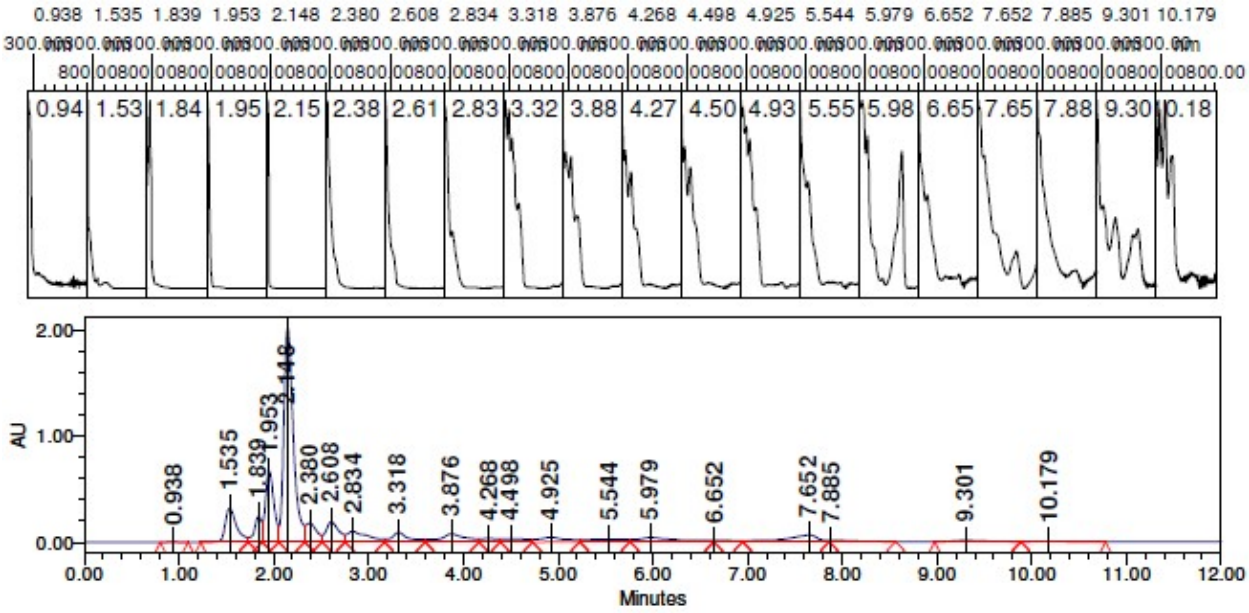

Figure S30: HPLC chromatogram of the $B(OC_6F_5)_3$/tetralin process to form F_5-BsubNc at T = 3.25 hours (MAX PLOT - 190 nm to 800 nm) HPLC run conducted with C18 functionalized silica as the stationary phase and 80:20 ACN:DMF (V:V) as the mobile phase.

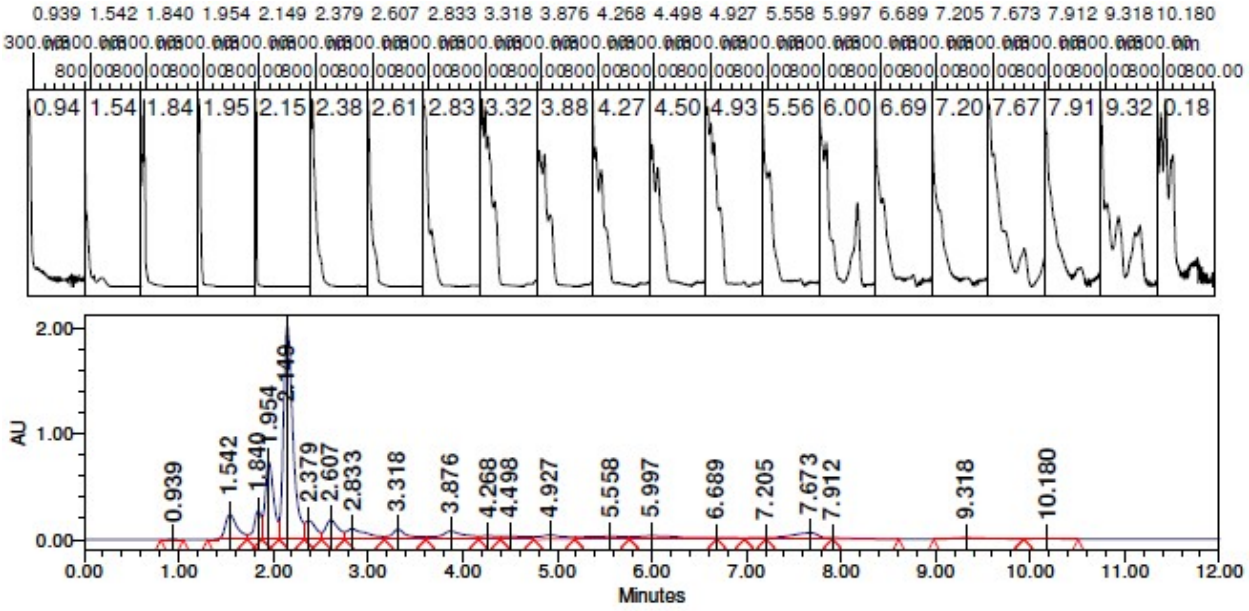

Figure S31: HPLC chromatogram of the $B(OC_6F_5)_3$/tetralin process to form F_5-BsubNc at T = 3.5 hours (MAX PLOT - 190 nm to 800 nm) HPLC run conducted with C18 functionalized silica as the stationary phase and 80:20 ACN:DMF (V:V) as the mobile phase.

Degradation of F_5-BsubNc from the $B(OC_6F_5)_3$ / Tetralin Process After Solvent Removal

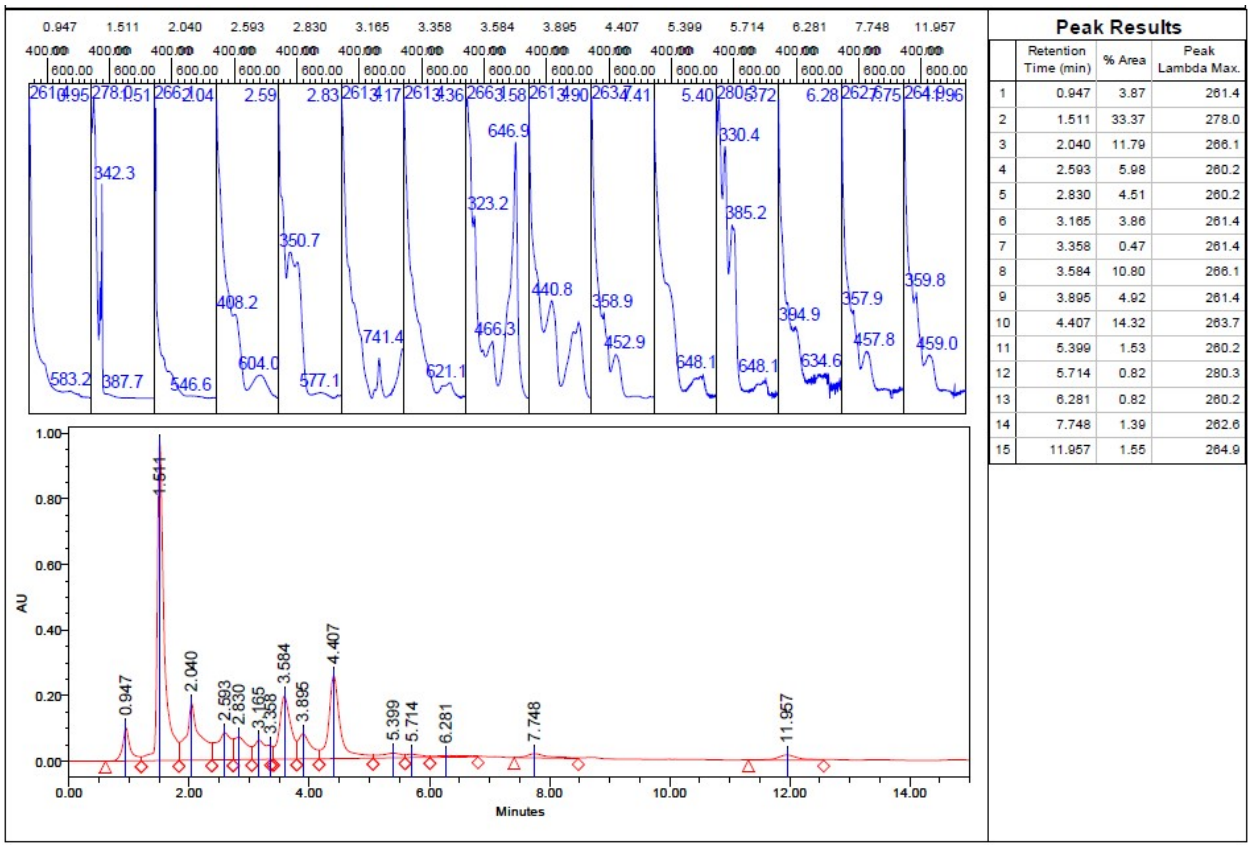

Figure S32: HPLC chromatogram after solvent removal using a rotary evaporator (MAX PLOT 260 nm and 750 nm). HPLC run conducted with C18 functionalized silica as the stationary phase and 80:20 ACN:DMF (V:V) as the mobile phase.

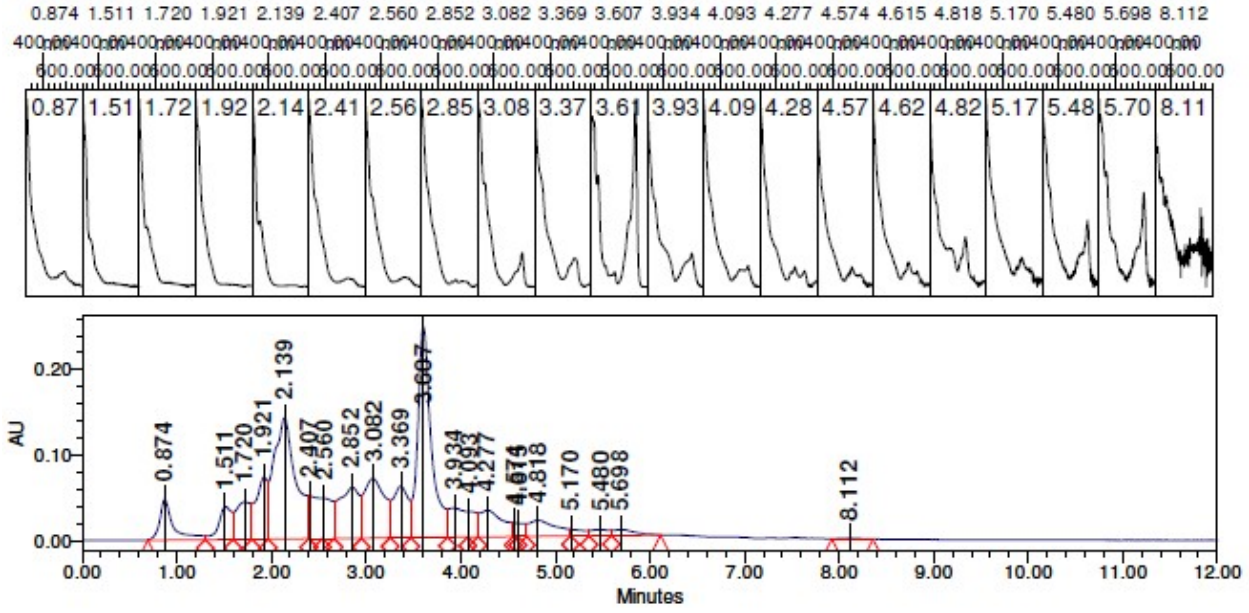

Figure S33: HPLC chromatogram after solvent removal by short path distillation (MAX PLOT 260 nm and 750 nm). HPLC run conducted with C18 functionalized silica as the stationary phase and 80:20 ACN:DMF (V:V) as the mobile phase.

Sublimation of F_5-BsubNc from the Tetralin Process

F_5-BsubNc crude from the tetralin process was loaded into an apparatus designed in house which is operated under vacuum with a controlled flow of nitrogen gas (100 mTorr) generating an internal pressure of 120 mTorr. The temperature was increased from room temperature to 560 ºC to promote sublimation.

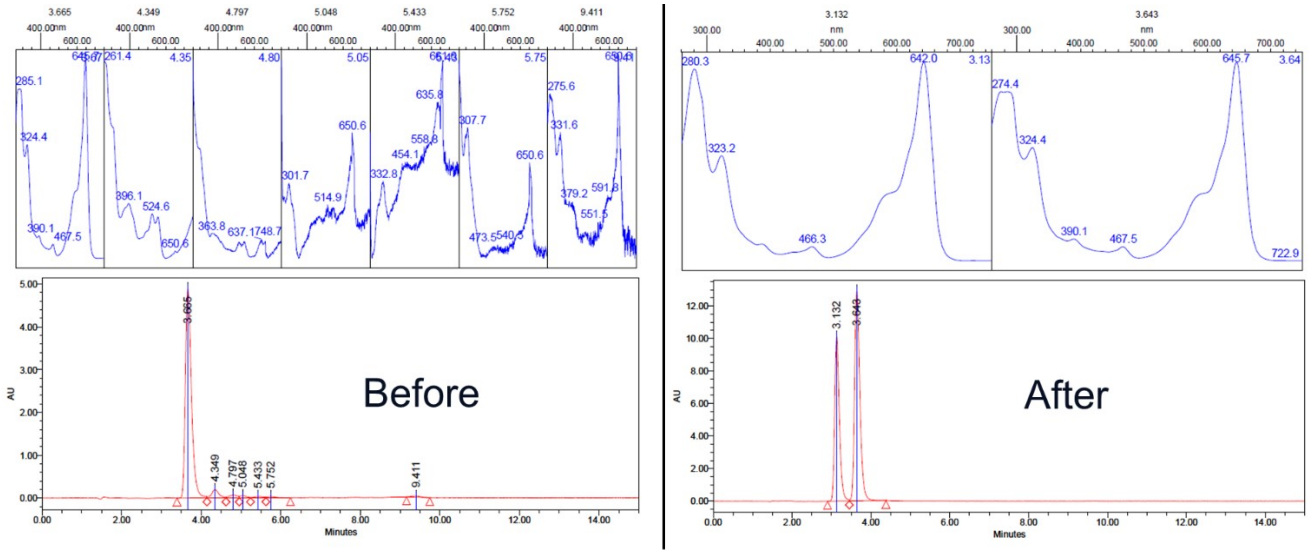

Figure S34: HPLC of crude from the tetralin process before and after train sublimation. Chromatogram extracted between 600 nm and 700 nm. HPLC runs conducted with C18 functionalized silica as the stationary phase and 80:20 ACN:DMF (V:V) as the mobile phase.

Train Sublimation with CO_2 Carrier Gas

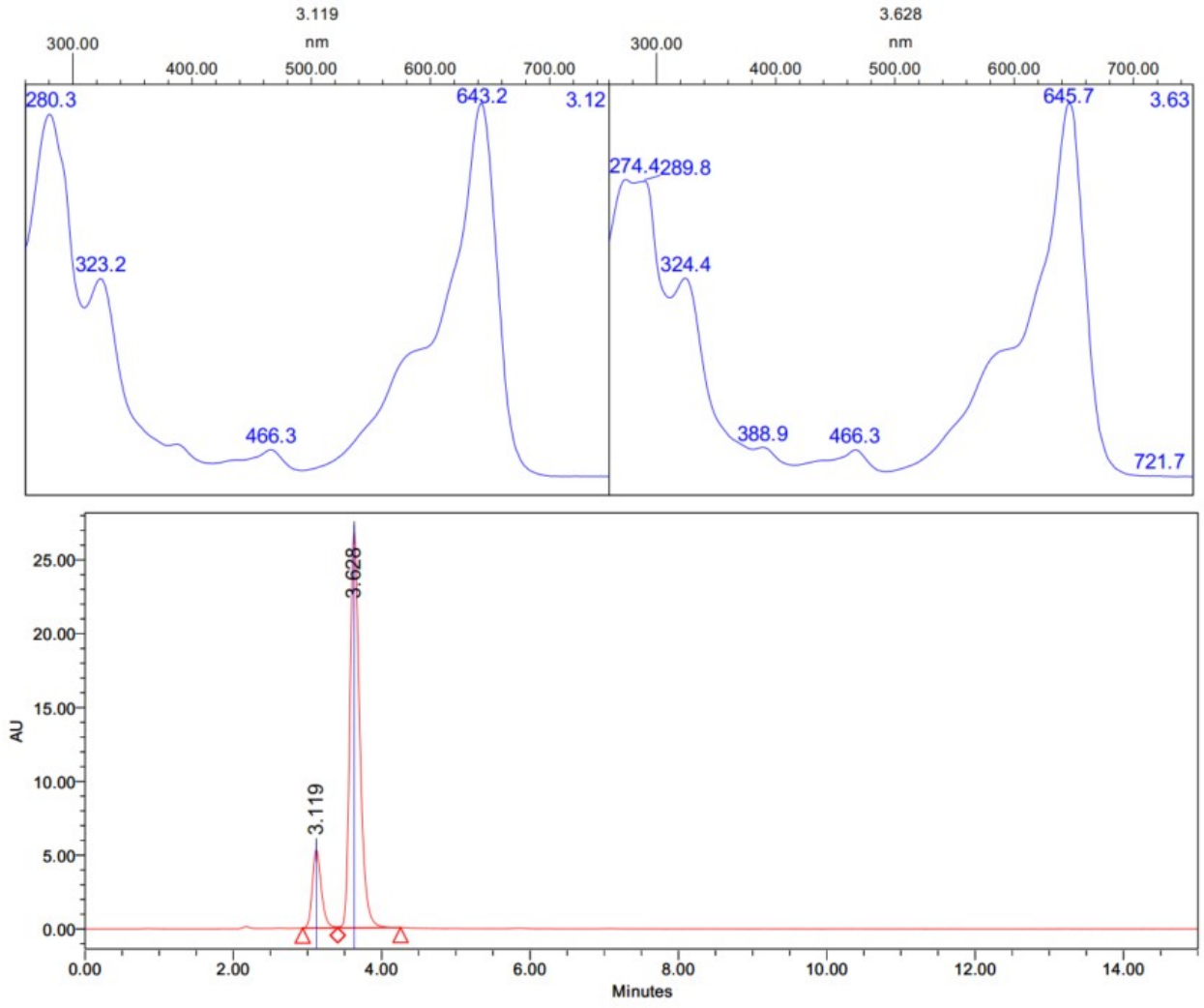

Figure S35: HPLC of sublimed material from the $B(OC_6F_5)_3$/tetralin process using CO_2 as the carrier gas. Chromatogram extracted between 600 nm and 700 nm. Material collected on the insert with BsubNc closest to the boat. HPLC run conducted with C18 functionalized silica as the stationary phase and 80:20 ACN:DMF (V:V) as the mobile phase.

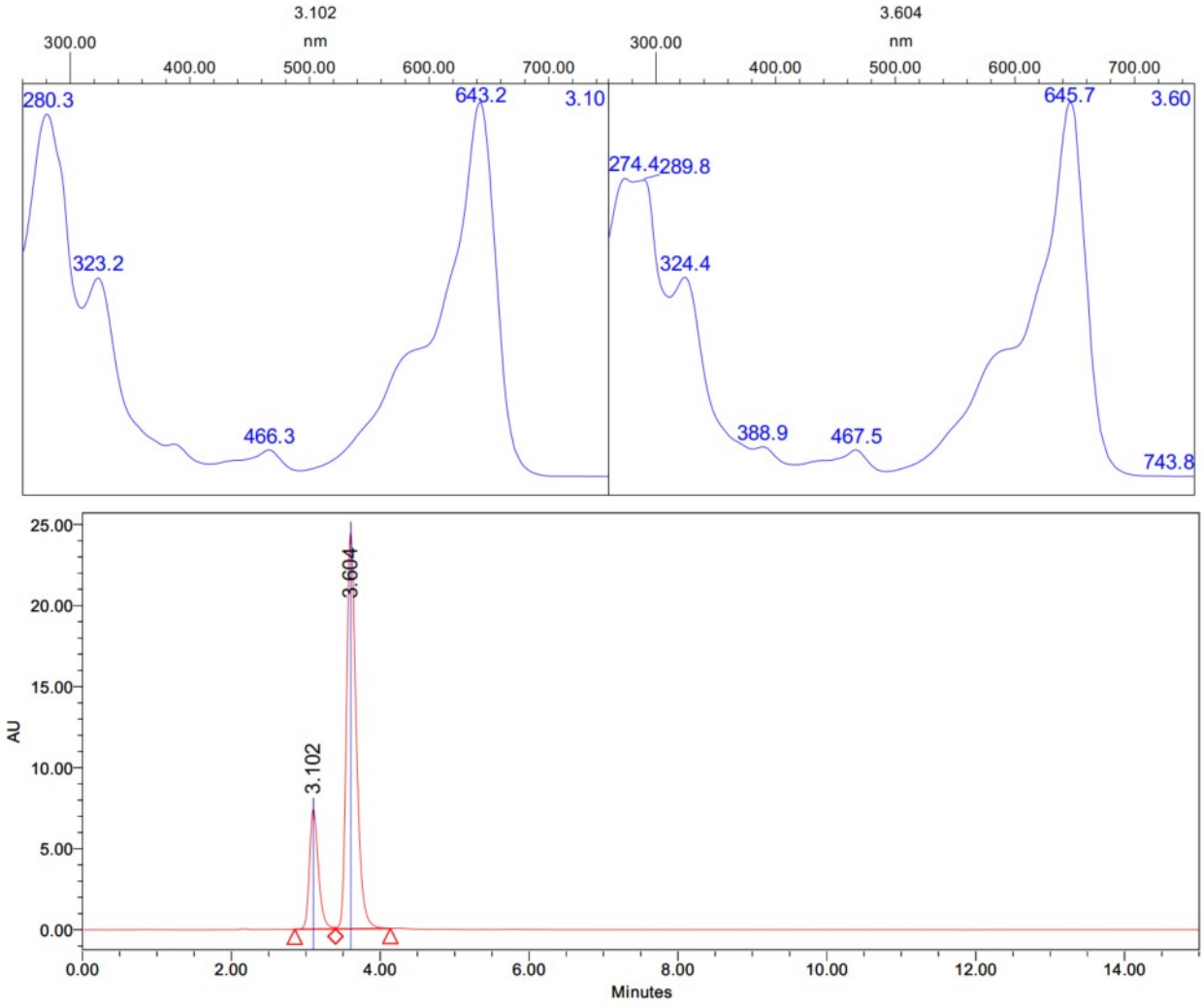

Figure S36: HPLC of sublimed material from the $B(OC_6F_5)_3$/tetralin process using CO_2 as the carrier gas. Chromatogram extracted between 600 nm and 700 nm. Material collected on the insert with BsubNc furthest from the boat. HPLC run conducted with C18 functionalized silica as the stationary phase and 80:20 ACN:DMF (V:V) as the mobile phase.

The Second Sublimation of F_5-BsubNc Toward Full Conversion to F-BsubNc

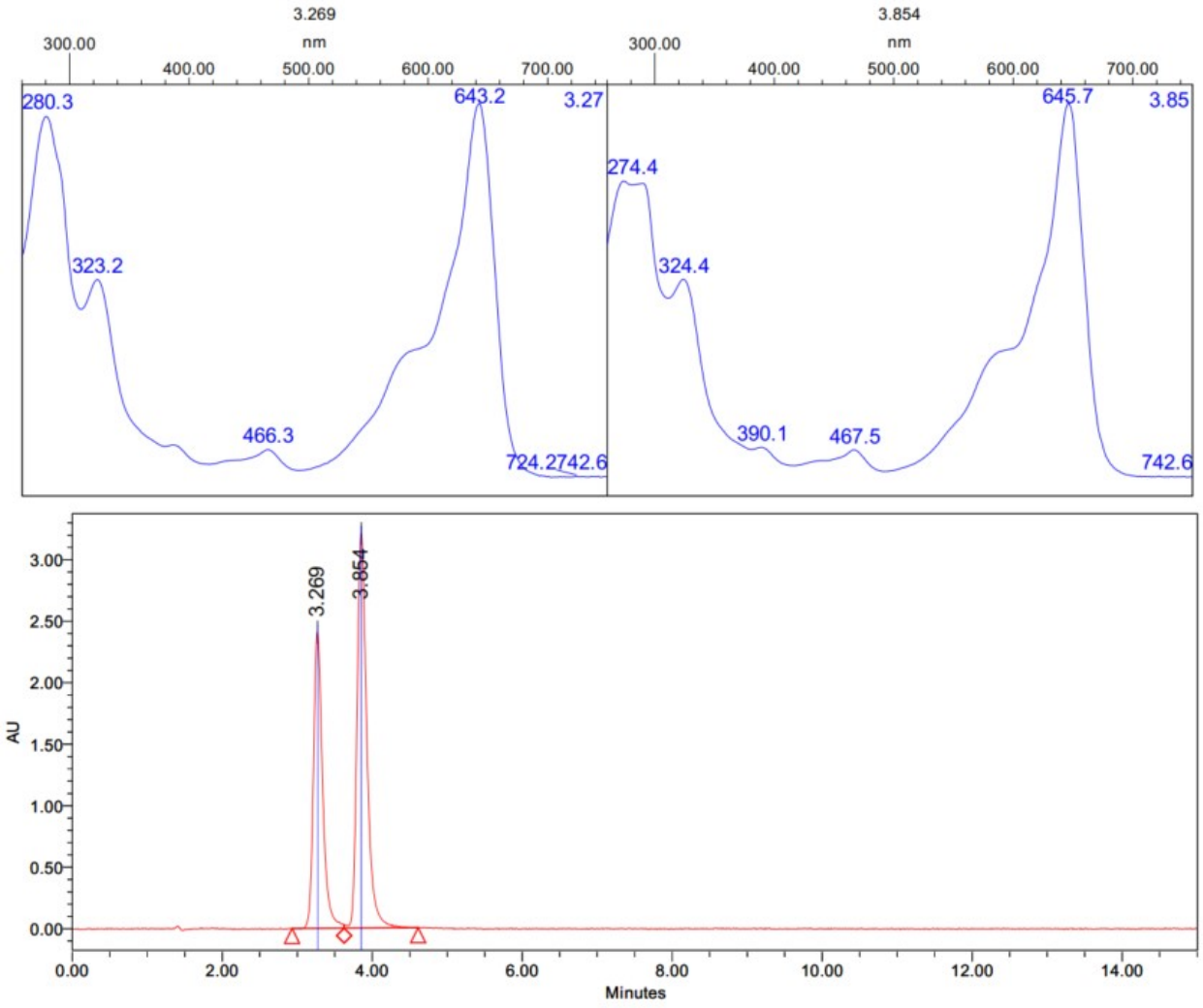

Figure S37: HPLC of twice sublimed material from the tetralin process. Chromatogram extracted between 600 nm and 700 nm. HPLC run conducted with C18 functionalized silica as the stationary phase and 80:20 ACN:DMF (V:V) as the mobile phase.

Triplicate F_5-BsubNc Syntheses

Reaction 1 after 1.5 hours at reflux

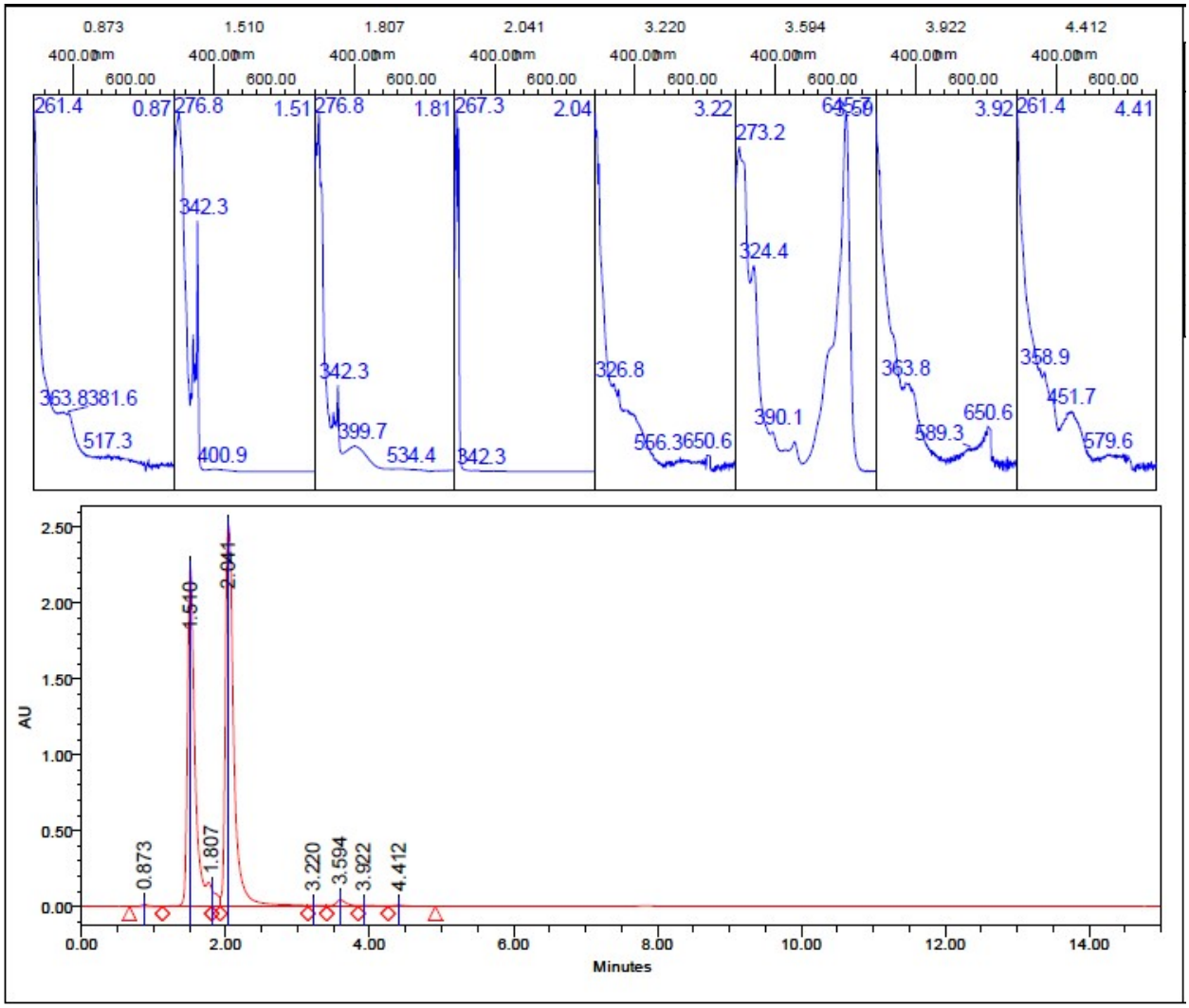

Figure S38: HPLC chromatogram max plot (260 nm and 750 nm). HPLC run conducted with C18 functionalized silica as the stationary phase and 80:20 ACN:DMF (V:V) as the mobile phase.

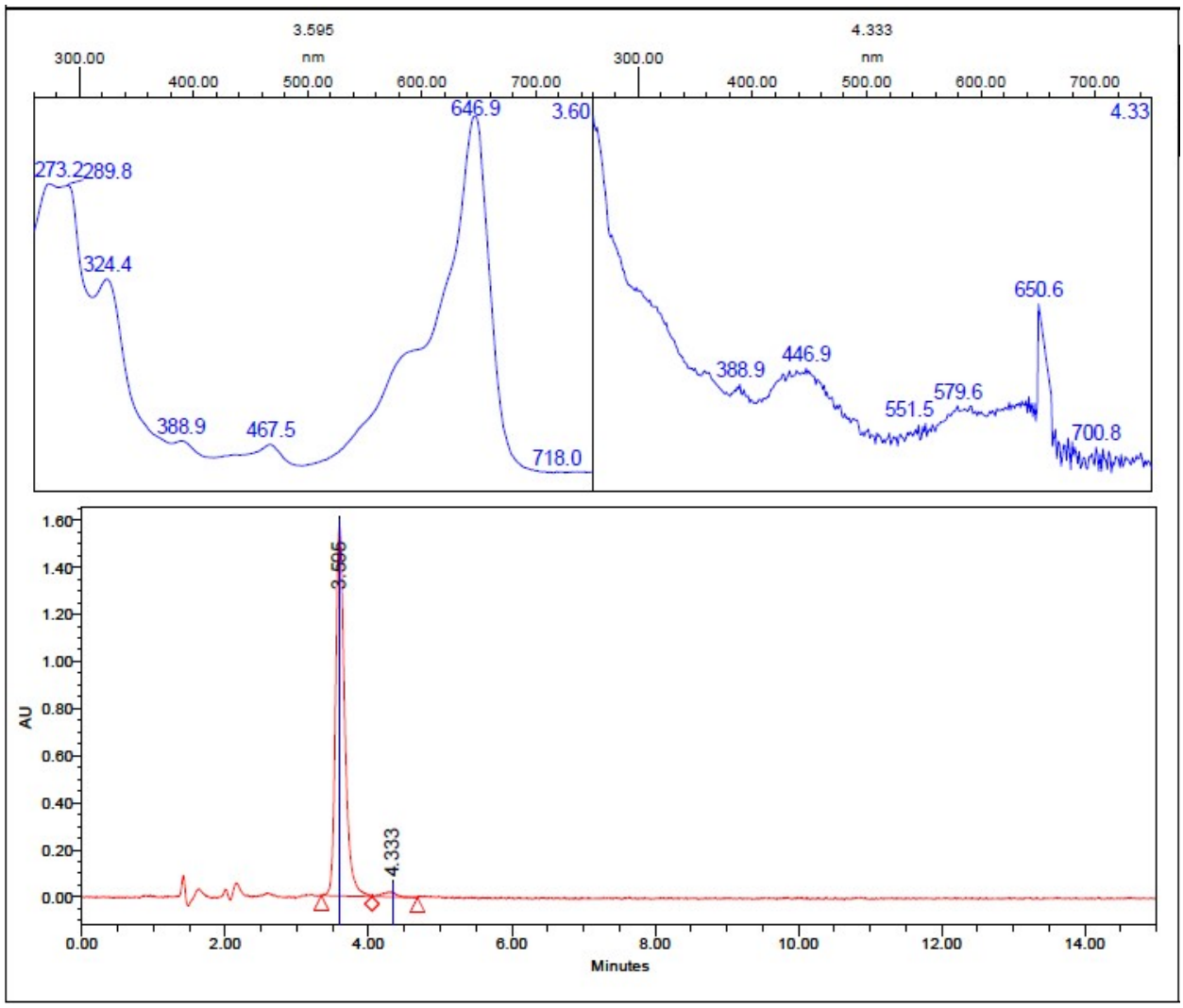

Figure S39: HPLC chromatogram extracted between 600 nm and 700 nm. HPLC run conducted with C18 functionalized silica as the stationary phase and 80:20 ACN:DMF (V:V) as the mobile phase.

Reaction 1 Immediately Before Solvent Removal Using a Rotary Evaporator

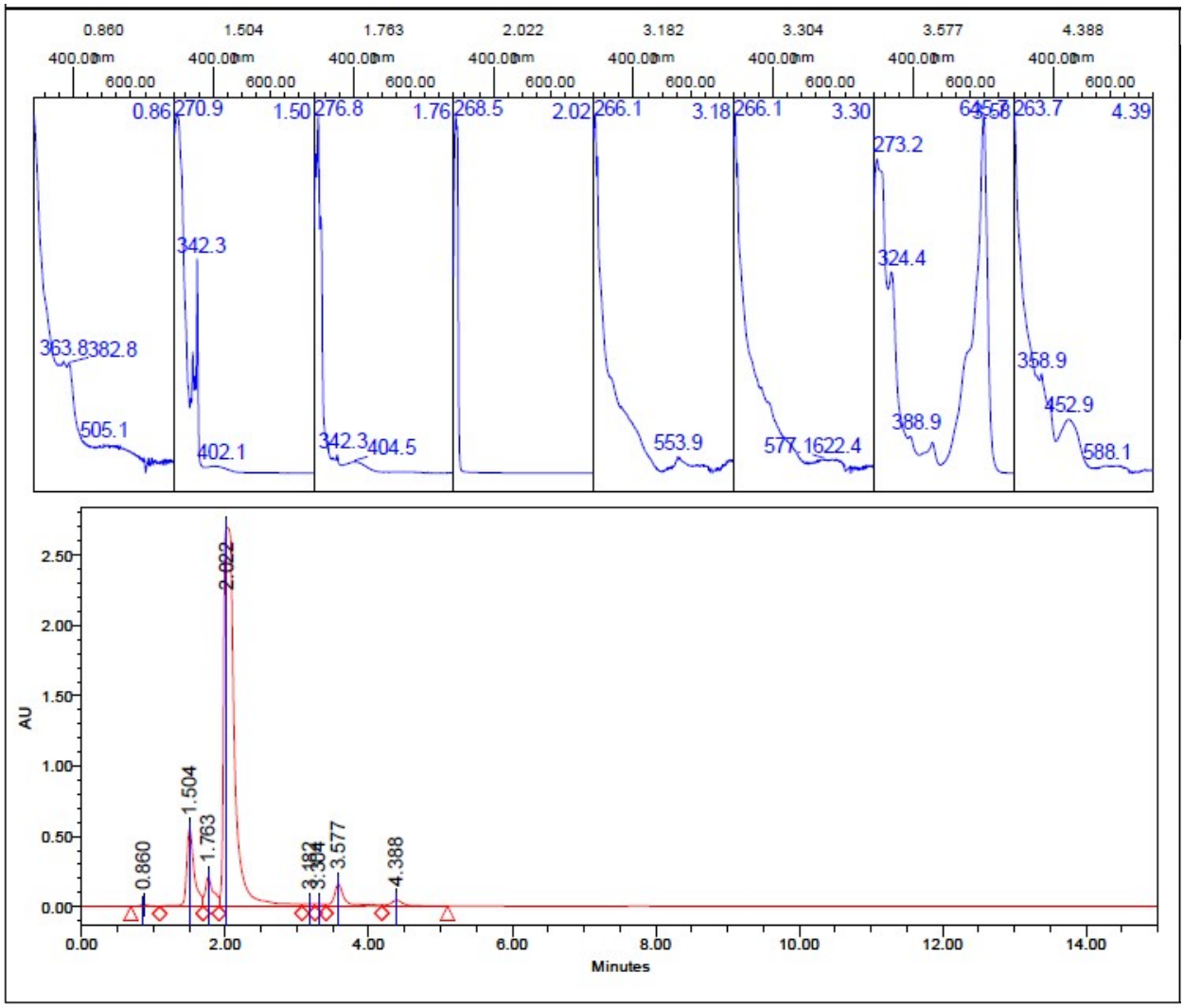

Figure S40: HPLC chromatogram max plot (260 nm and 750 nm). HPLC run conducted with C18 functionalized silica as the stationary phase and 80:20 ACN:DMF (V:V) as the mobile phase.

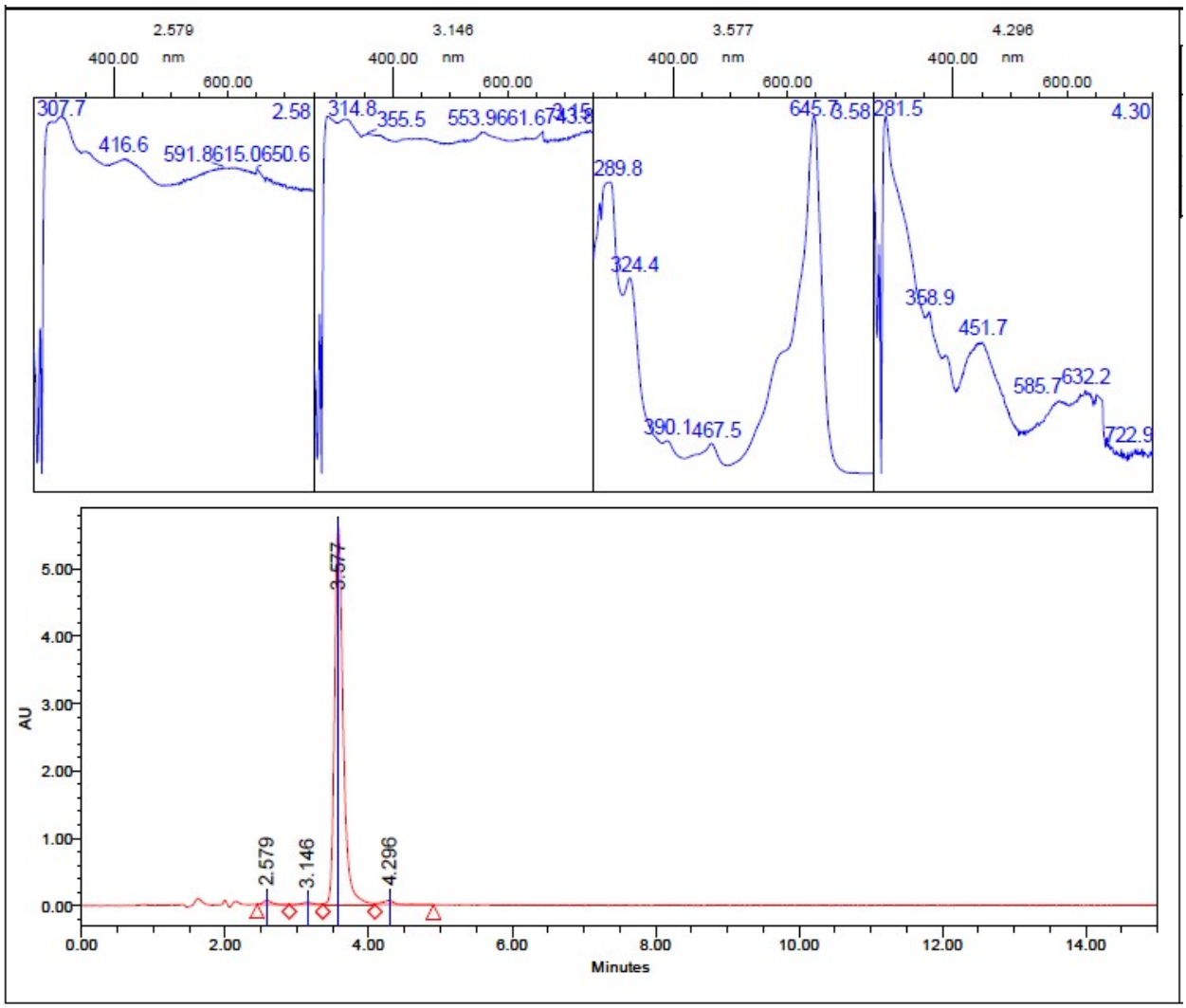

Figure S41: HPLC chromatogram extracted between 600 nm and 700 nm. HPLC run conducted with C18 functionalized silica as the stationary phase and 80:20 ACN:DMF (V:V) as the mobile phase.

Reaction 1 After Solvent Removal Using a Rotary Evaporator

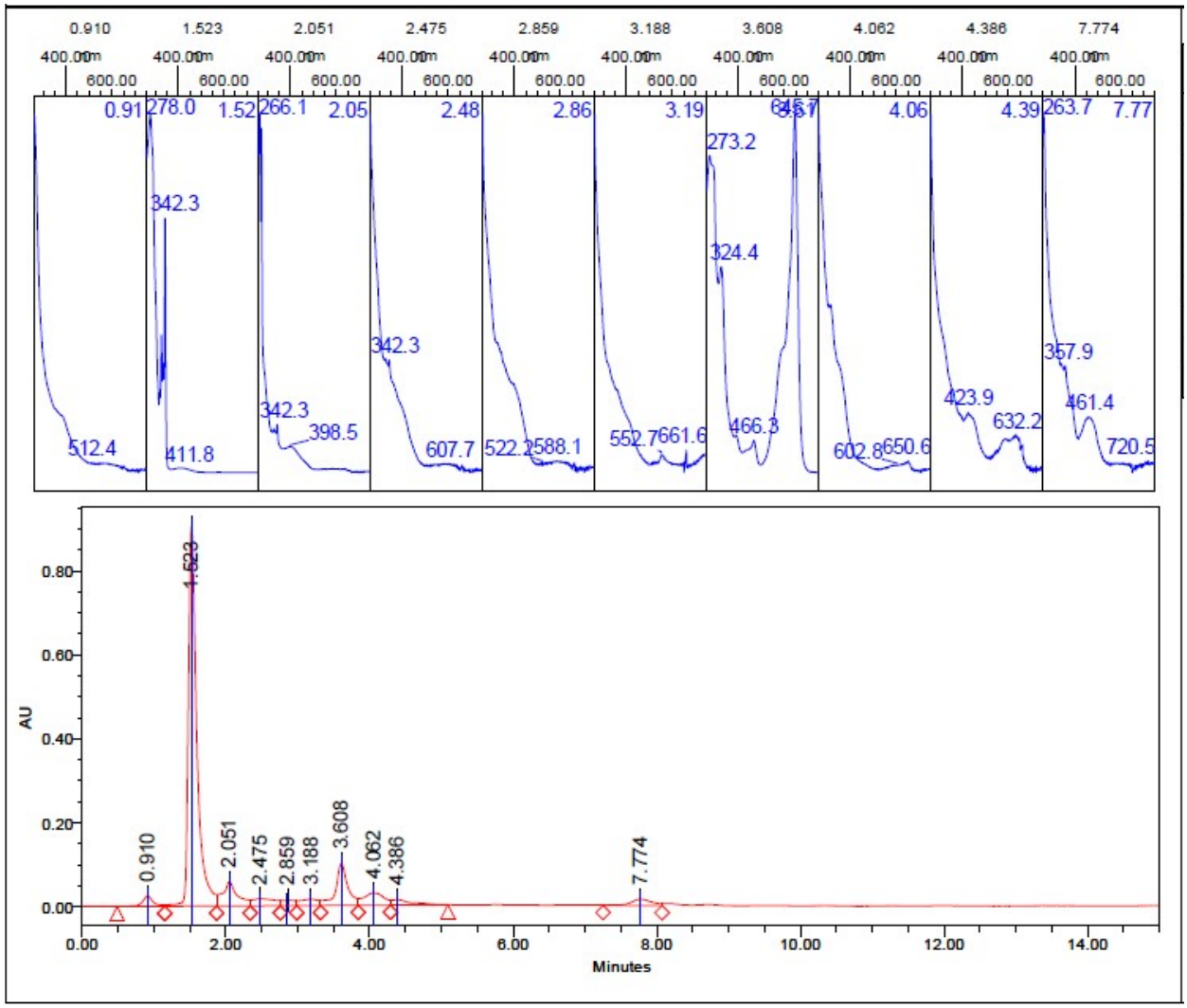

Figure S42: HPLC chromatogram max plot (260 nm and 750 nm). HPLC run conducted with C18 functionalized silica as the stationary phase and 80:20 ACN:DMF (V:V) as the mobile phase.

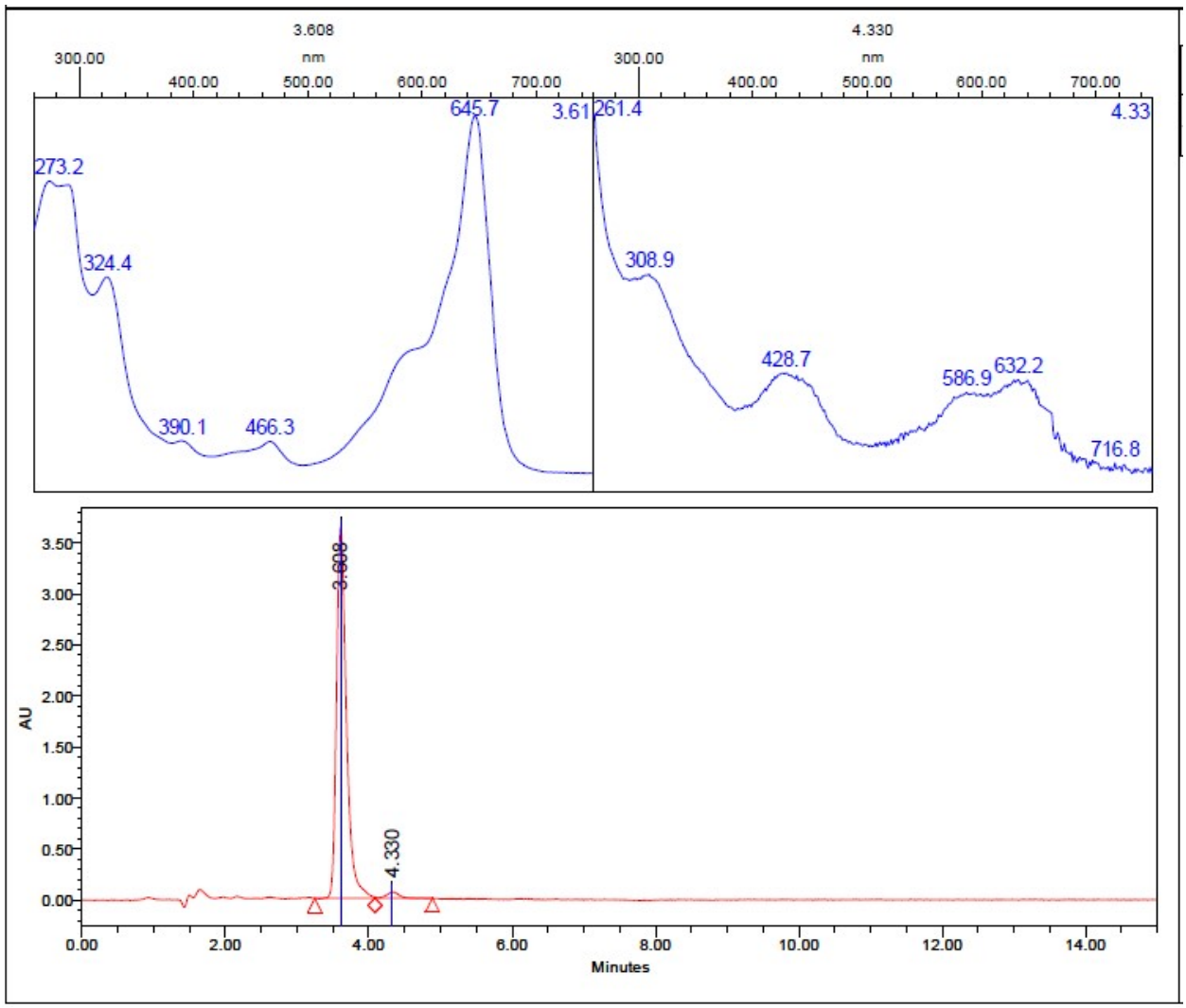

Figure S43: HPLC chromatogram extracted between 600 nm and 700 nm. HPLC run conducted with C18 functionalized silica as the stationary phase and 80:20 ACN:DMF (V:V) as the mobile phase.

Reaction 2 After 1.5 Hours at Reflux

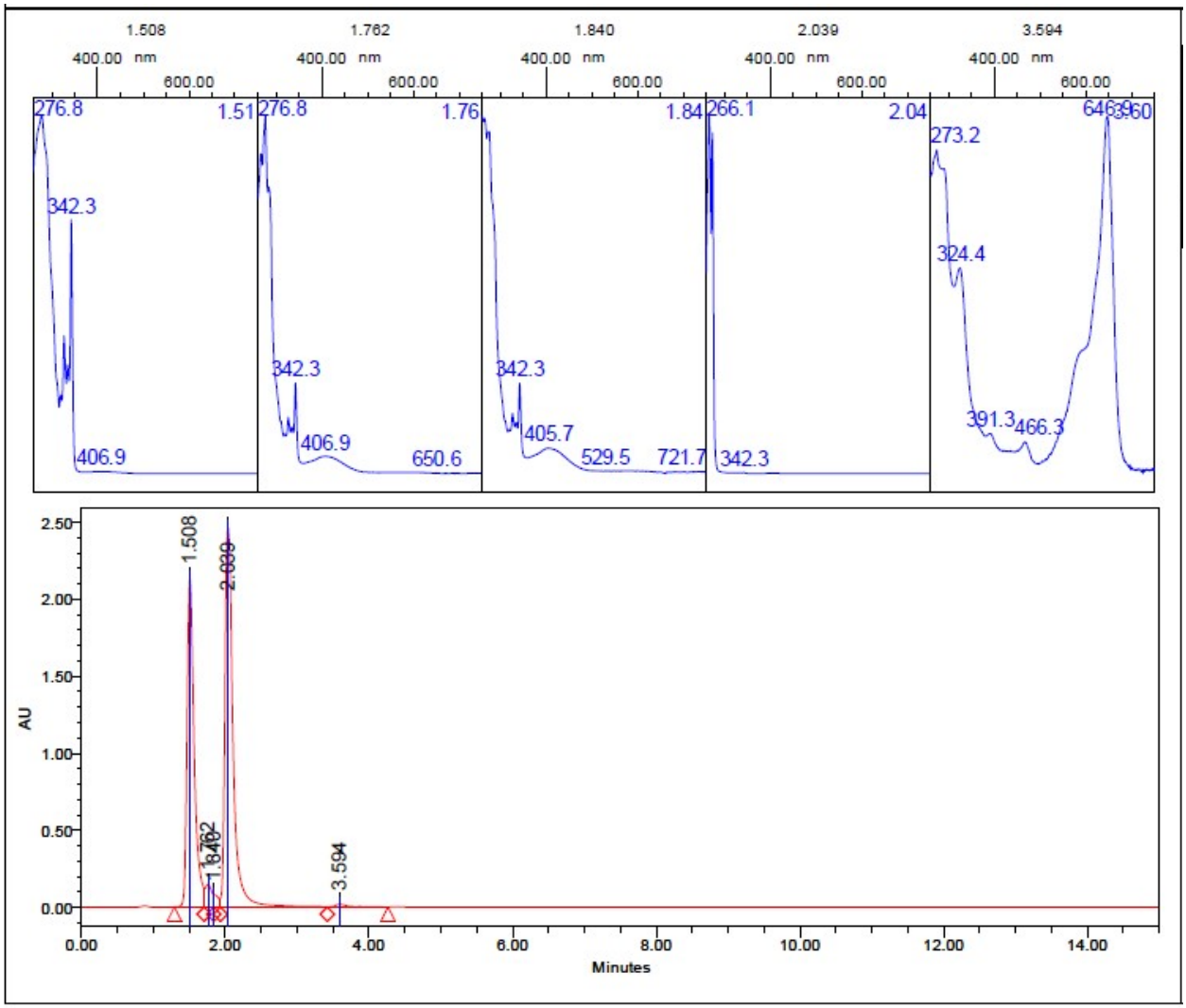

Figure S44: HPLC chromatogram max plot (260 nm and 750 nm). HPLC run conducted with C18 functionalized silica as the stationary phase and 80:20 ACN:DMF (V:V) as the mobile phase.

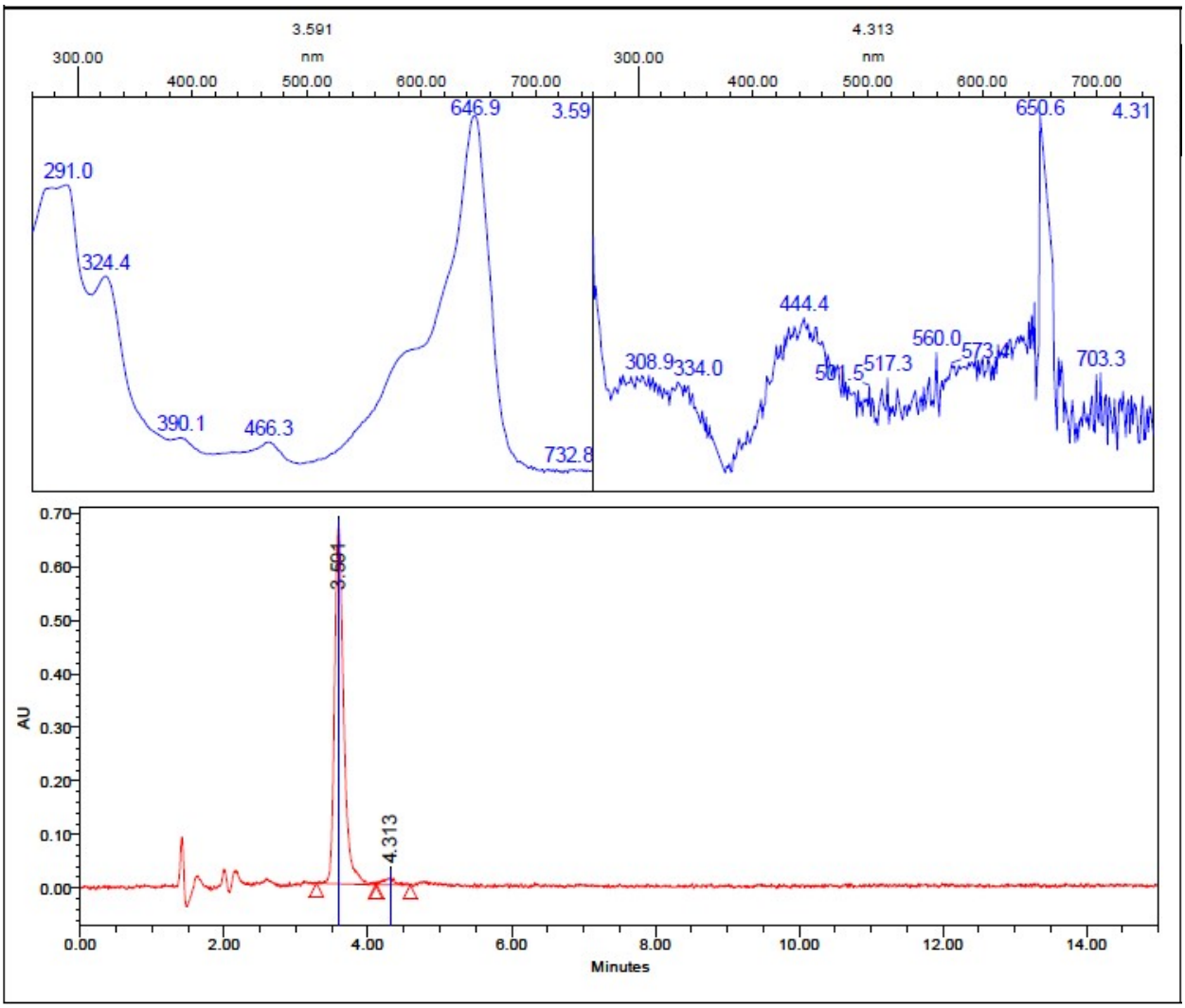

Figure S45: HPLC chromatogram extracted between 600 nm and 700 nm. HPLC run conducted with C18 functionalized silica as the stationary phase and 80:20 ACN:DMF (V:V) as the mobile phase.

Reaction 2 Immediately Before Solvent Removal Using a Rotary Evaporator

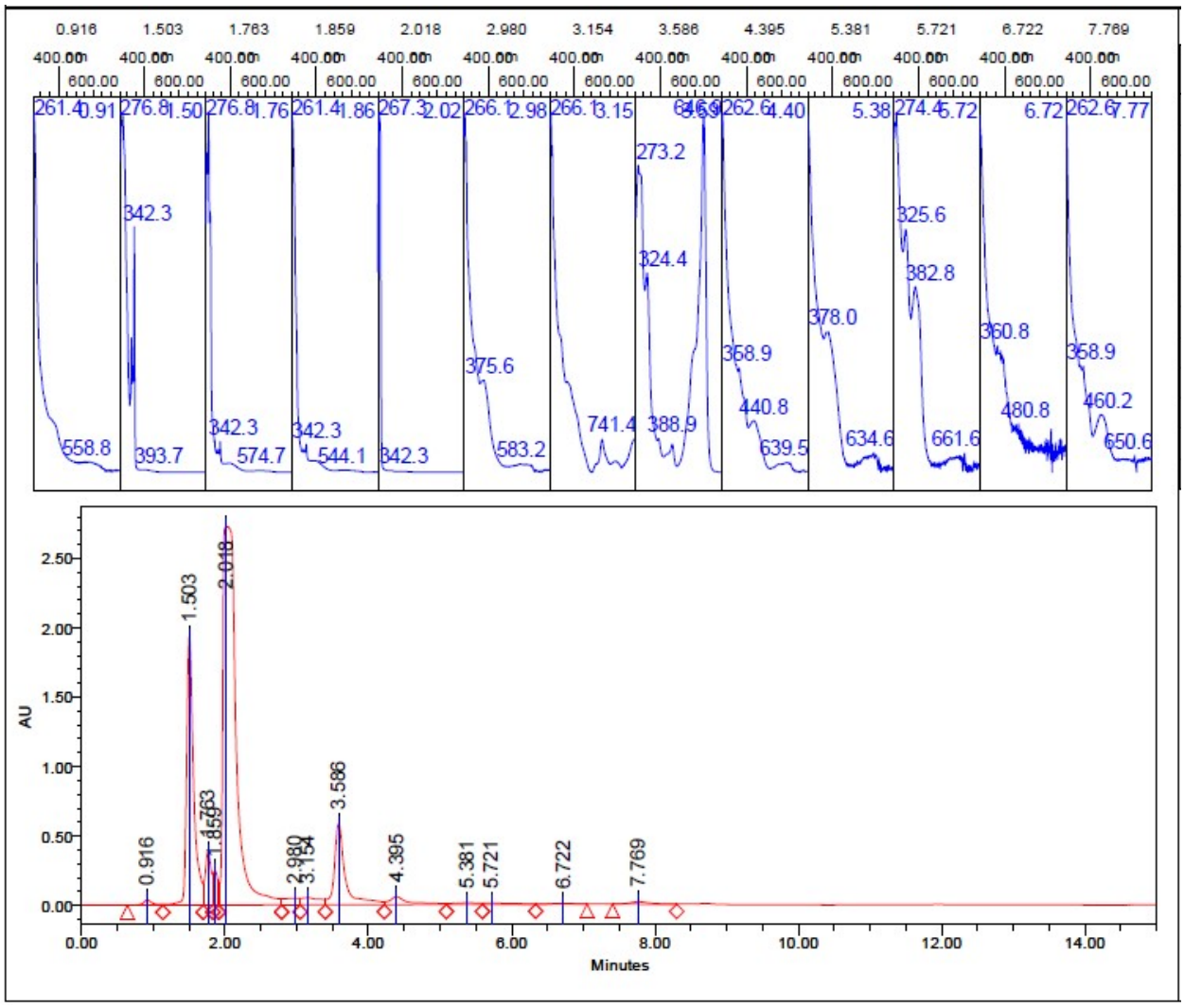

Figure S46: HPLC chromatogram max plot (260 nm and 750 nm). HPLC run conducted with C18 functionalized silica as the stationary phase and 80:20 ACN:DMF (V:V) as the mobile phase.

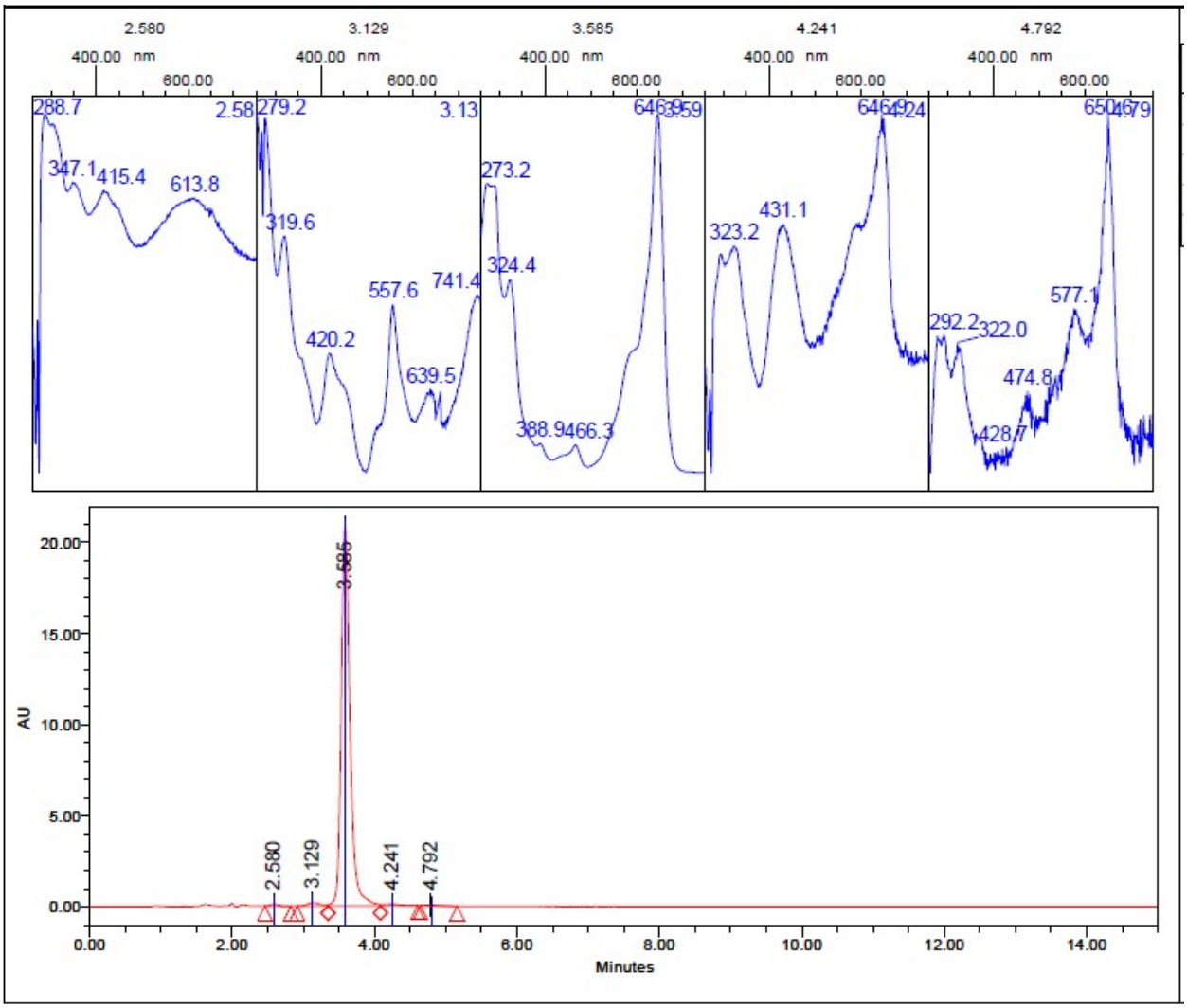

Figure S47: HPLC chromatogram extracted between 600 nm and 700 nm. HPLC run conducted with C18 functionalized silica as the stationary phase and 80:20 ACN:DMF (V:V) as the mobile phase.

Reaction 2 After Solvent Removal Using a Rotary Evaporator

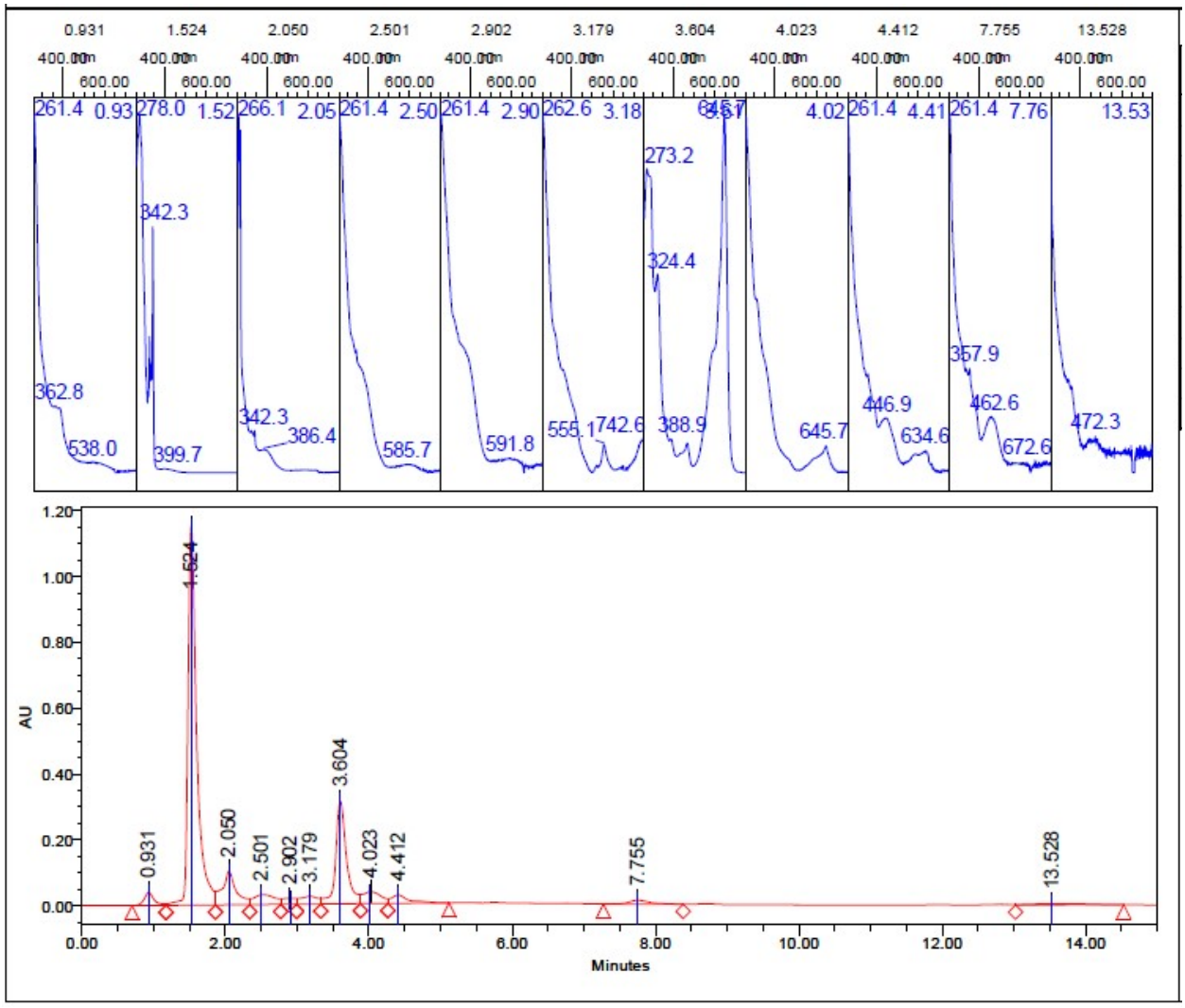

Figure S48: HPLC chromatogram max plot (260 nm and 750 nm). HPLC run conducted with C18 functionalized silica as the stationary phase and 80:20 ACN:DMF (V:V) as the mobile phase.

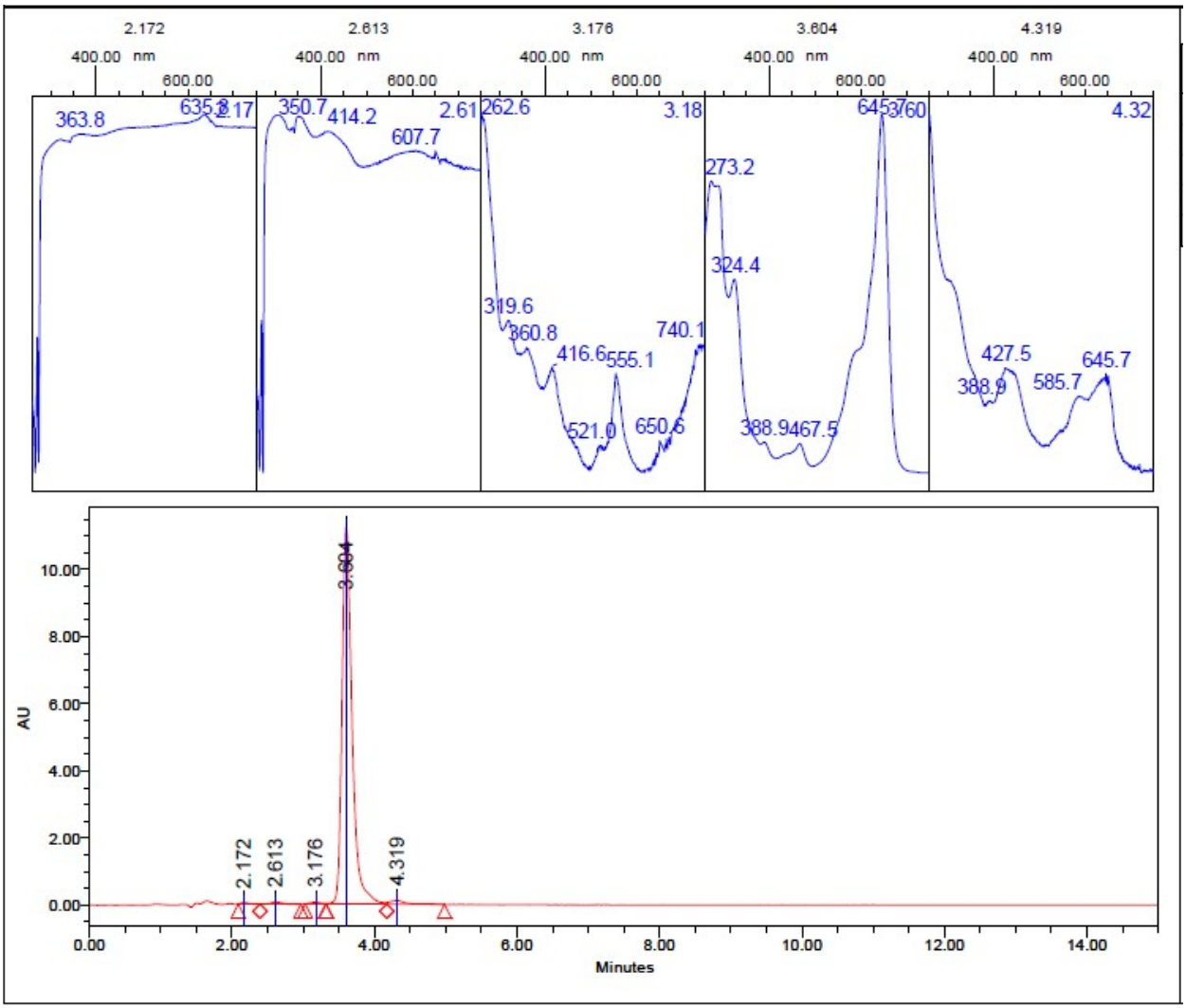

Figure S49: HPLC chromatogram extracted between 600 nm and 700 nm. HPLC run conducted with C18 functionalized silica as the stationary phase and 80:20 ACN:DMF (V:V) as the mobile phase.

Reaction 3 After 1.5 Hours at Reflux

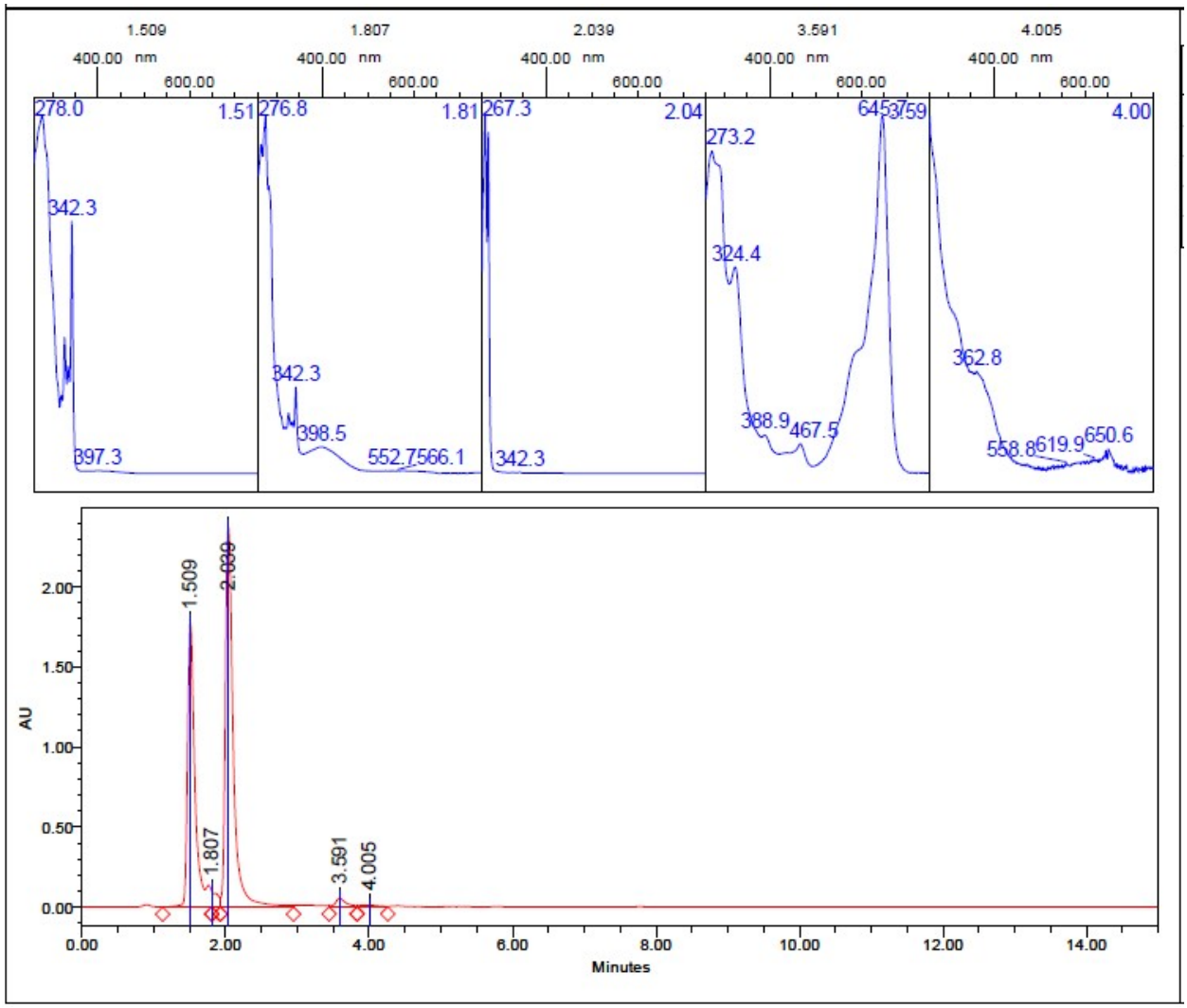

Figure S50: HPLC chromatogram max plot (260 nm and 750 nm). HPLC run conducted with C18 functionalized silica as the stationary phase and 80:20 ACN:DMF (V:V) as the mobile phase.

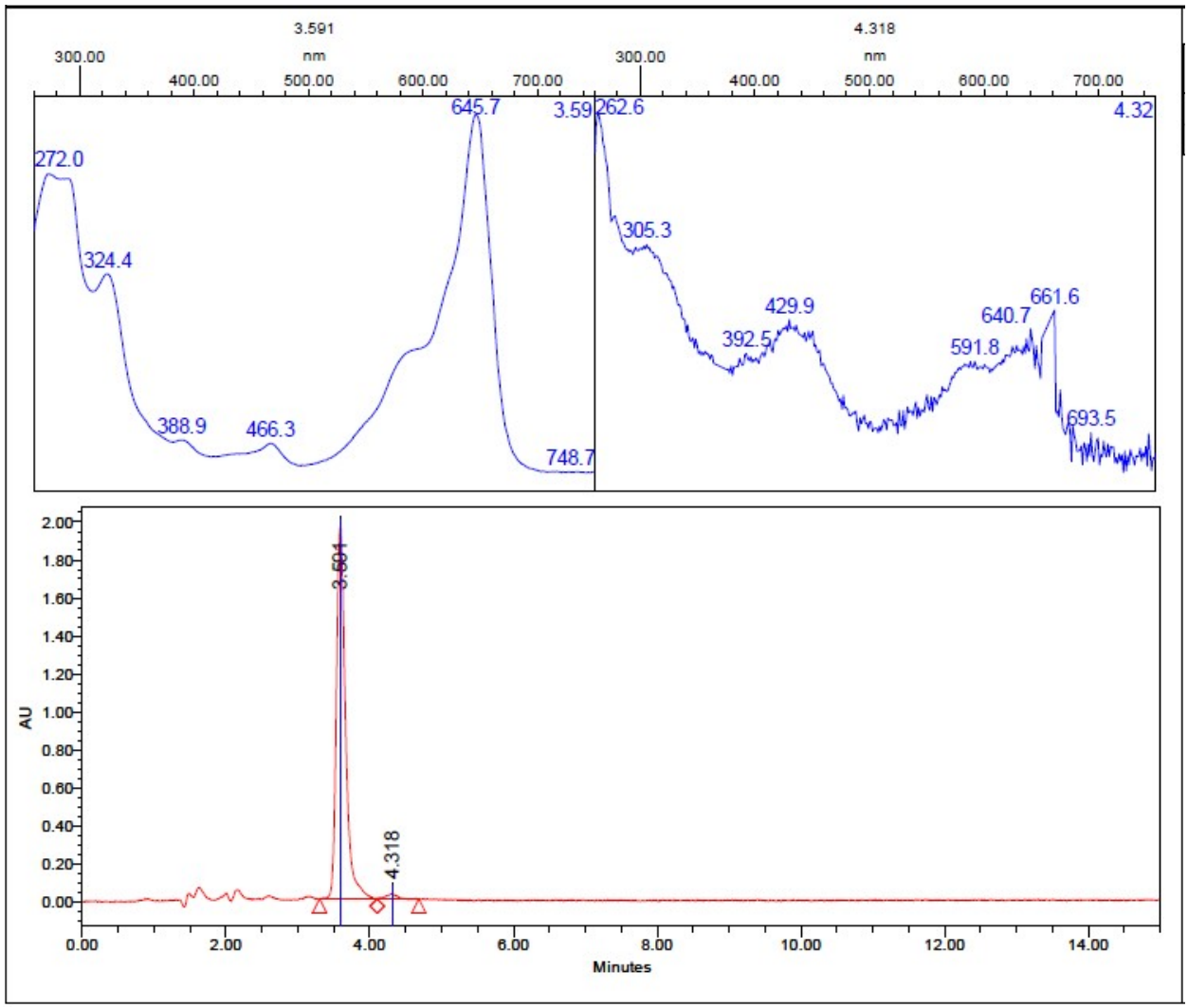

Figure S51: HPLC chromatogram extracted between 600 nm and 700 nm. HPLC run conducted with C18 functionalized silica as the stationary phase and 80:20 ACN:DMF (V:V) as the mobile phase.

Reaction 3 Immediately Before Solvent Removal Using a Rotary Evaporator

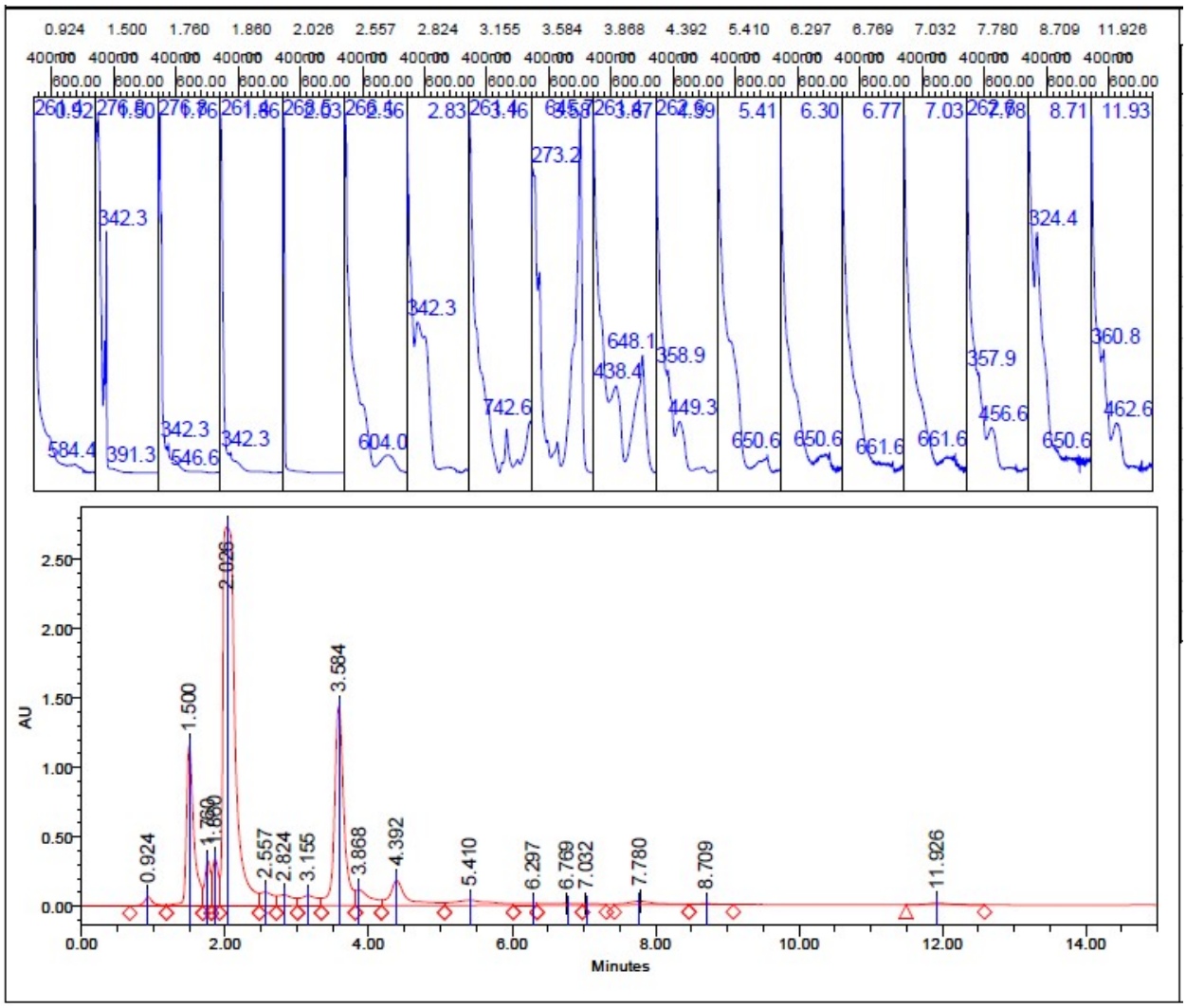

Figure S52: HPLC chromatogram max plot (260 nm and 750 nm). HPLC run conducted with C18 functionalized silica as the stationary phase and 80:20 ACN:DMF (V:V) as the mobile phase.

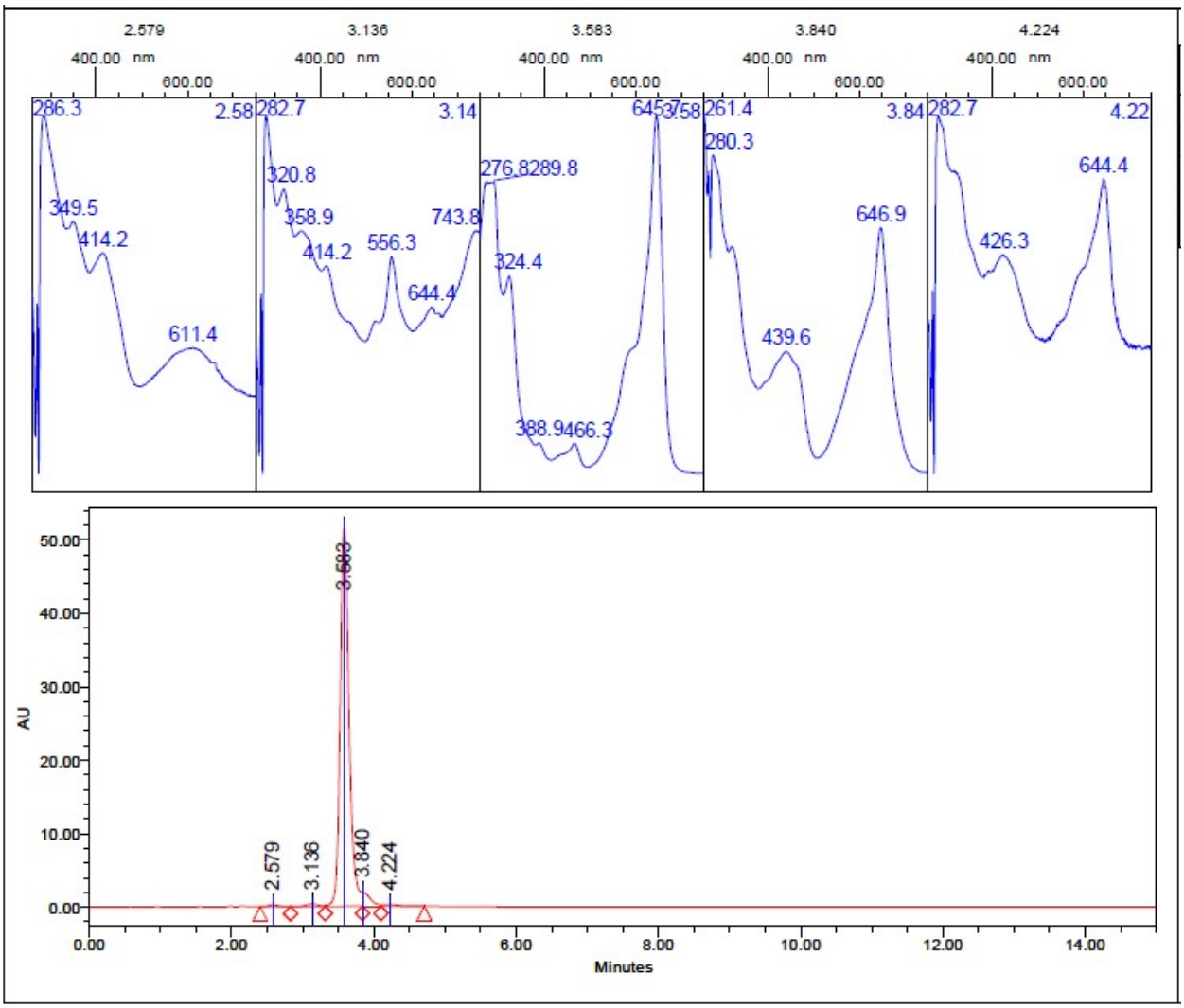

Figure S53: HPLC chromatogram extracted between 600 nm and 700 nm. HPLC run conducted with C18 functionalized silica as the stationary phase and 80:20 ACN:DMF (V:V) as the mobile phase.

Reaction 3 After Solvent Removal Using a Rotary Evaporator

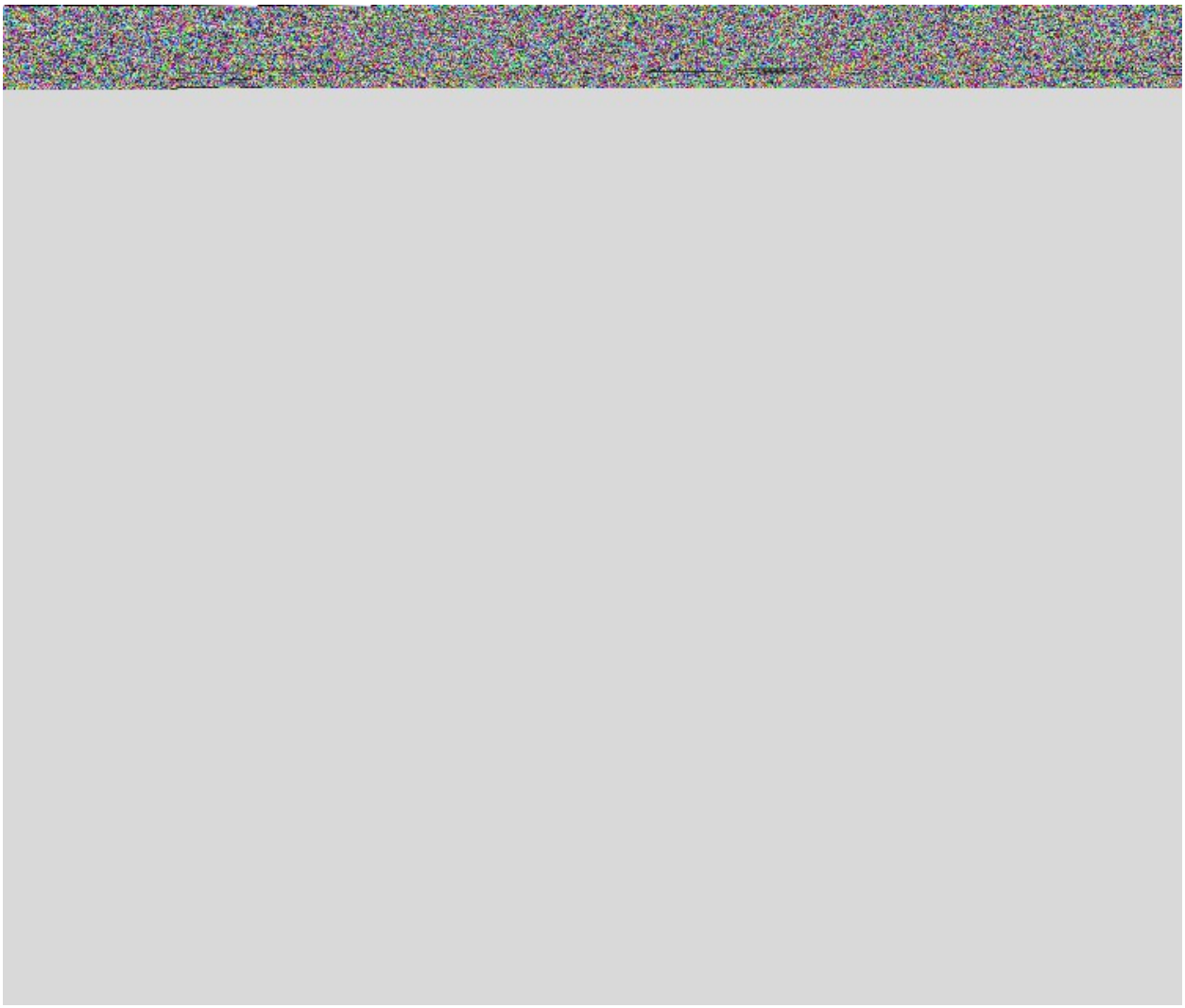

Figure S54: HPLC chromatogram max plot (260 nm and 750 nm). HPLC run conducted with C18 functionalized silica as the stationary phase and 80:20 ACN:DMF (V:V) as the mobile phase.

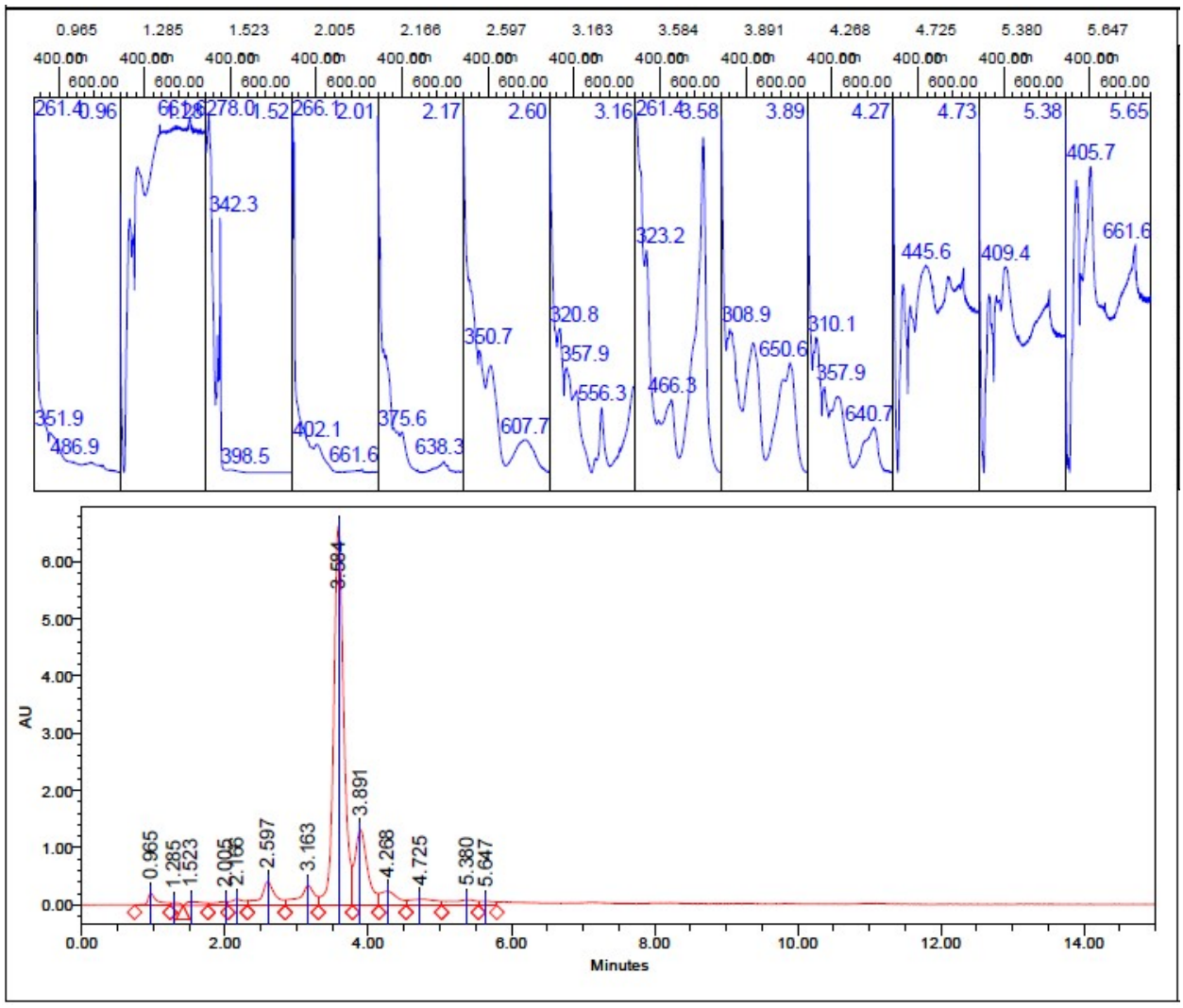

Figure S55: HPLC chromatogram extracted between 600 nm and 700 nm. HPLC run conducted with C18 functionalized silica as the stationary phase and 80:20 ACN:DMF (V:V) as the mobile phase.

Characterization of BsubNcs from the $B(OC_6F_5)_3$ / Tetralin Process

NMR Spectroscopy of F_5-BsubNc

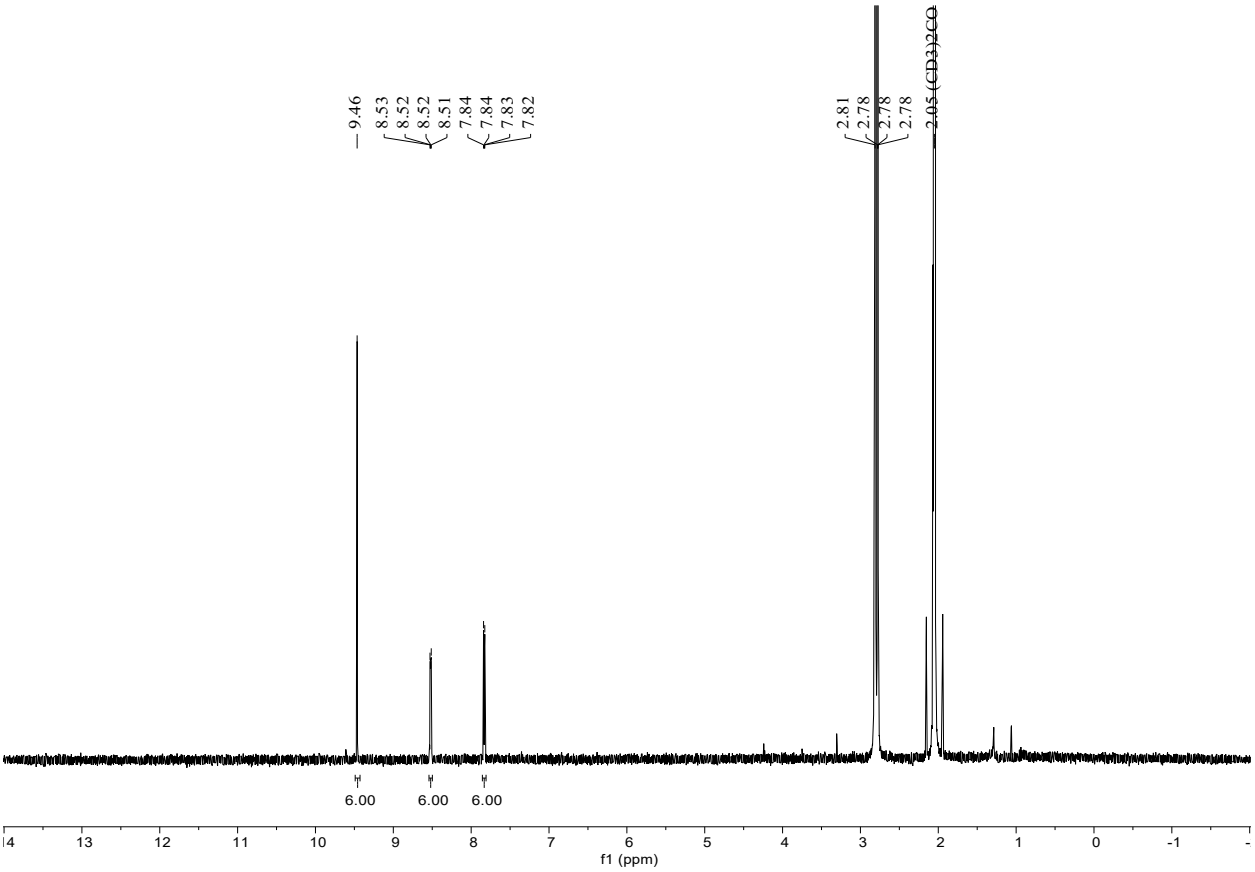

Figure S56: ^{1}H NMR spectrum (600 MHz) of F_5-BsubNc in acetone-d_6.

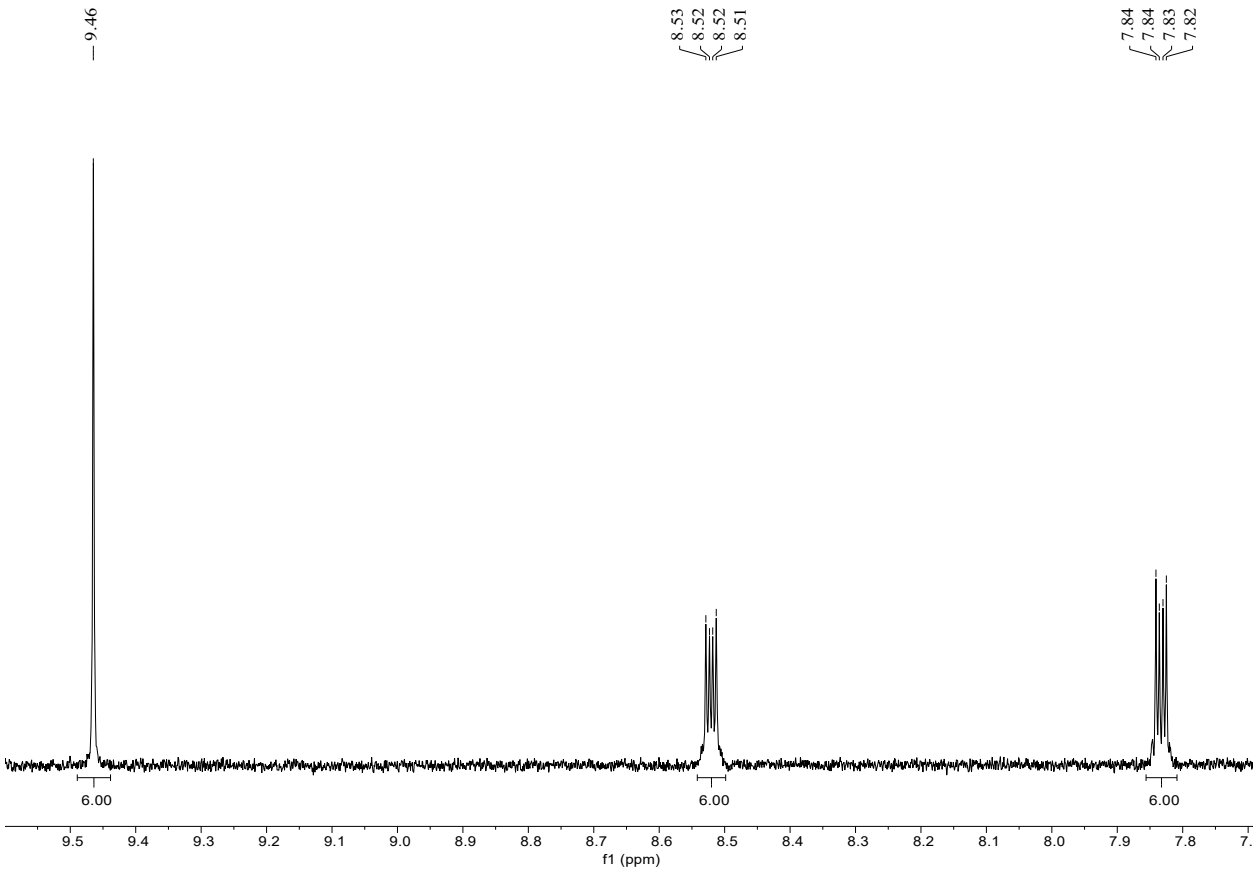

Figure S57: Zoom of F_5-BsubNc NMR spectrum (600 MHz) showing macrocycle peaks in acetone-d_6.

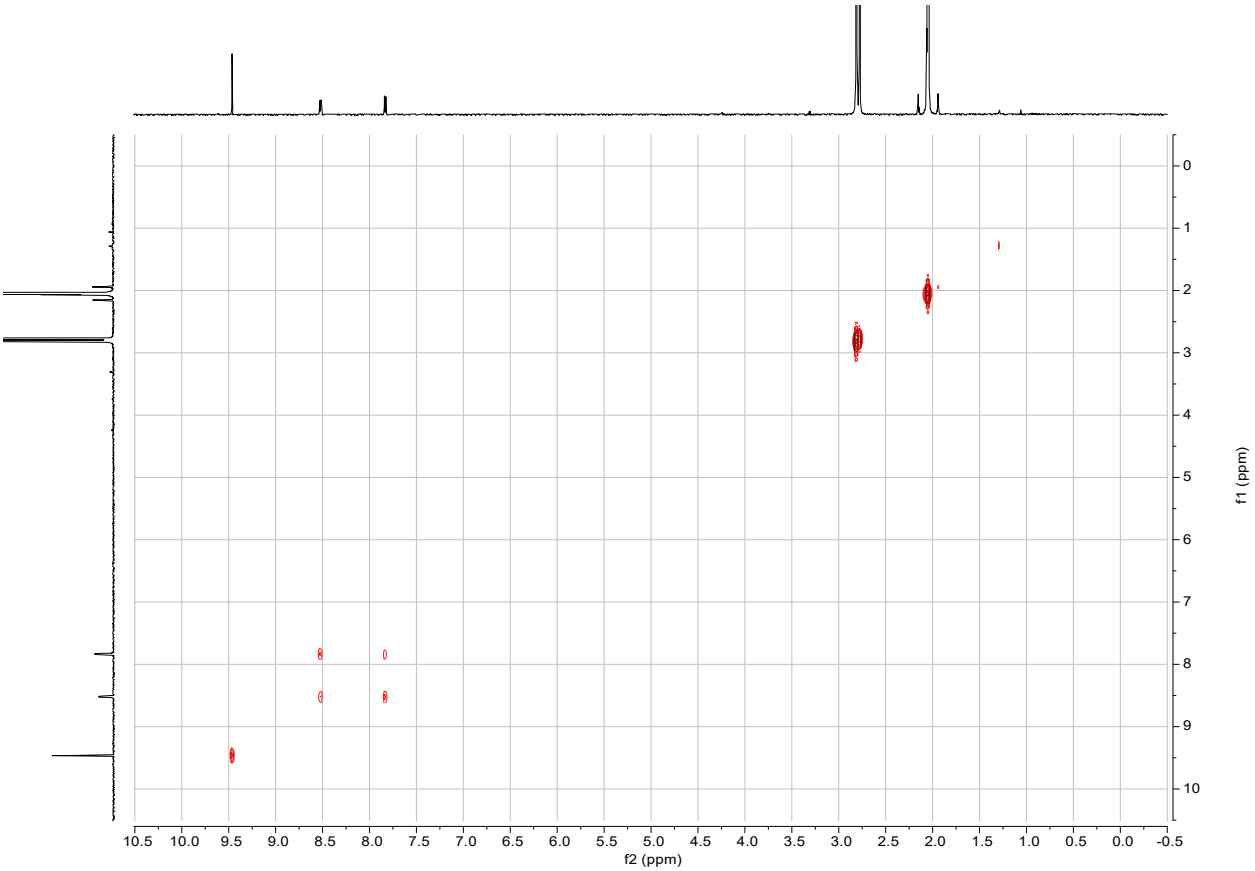

Figure S58: 2D COSY NMR spectrum (600 MHz) of F_5-BsubNc in acetone-d6.

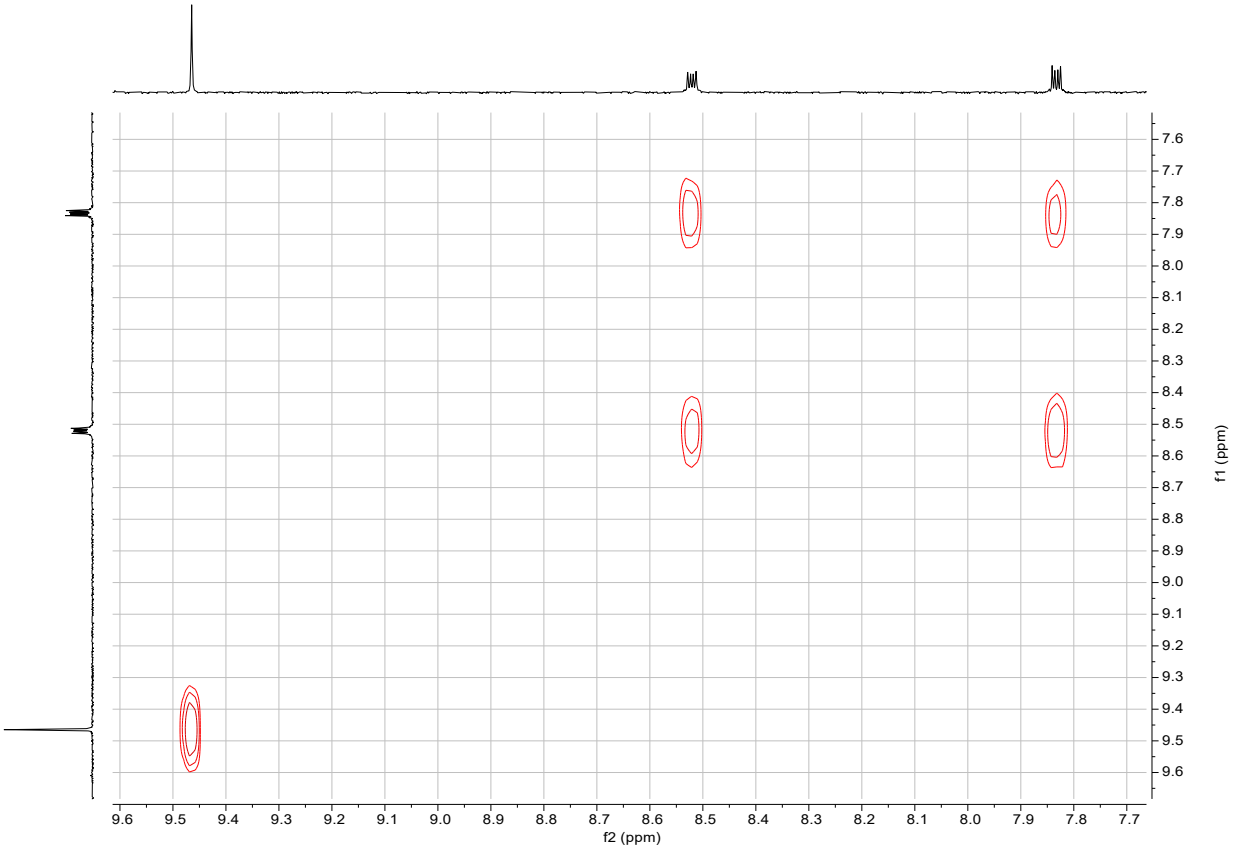

Figure S59: Zoom of the 2D COSY NMR spectrum of F_5-BsubNc (600 MHz) in acetone-d6.

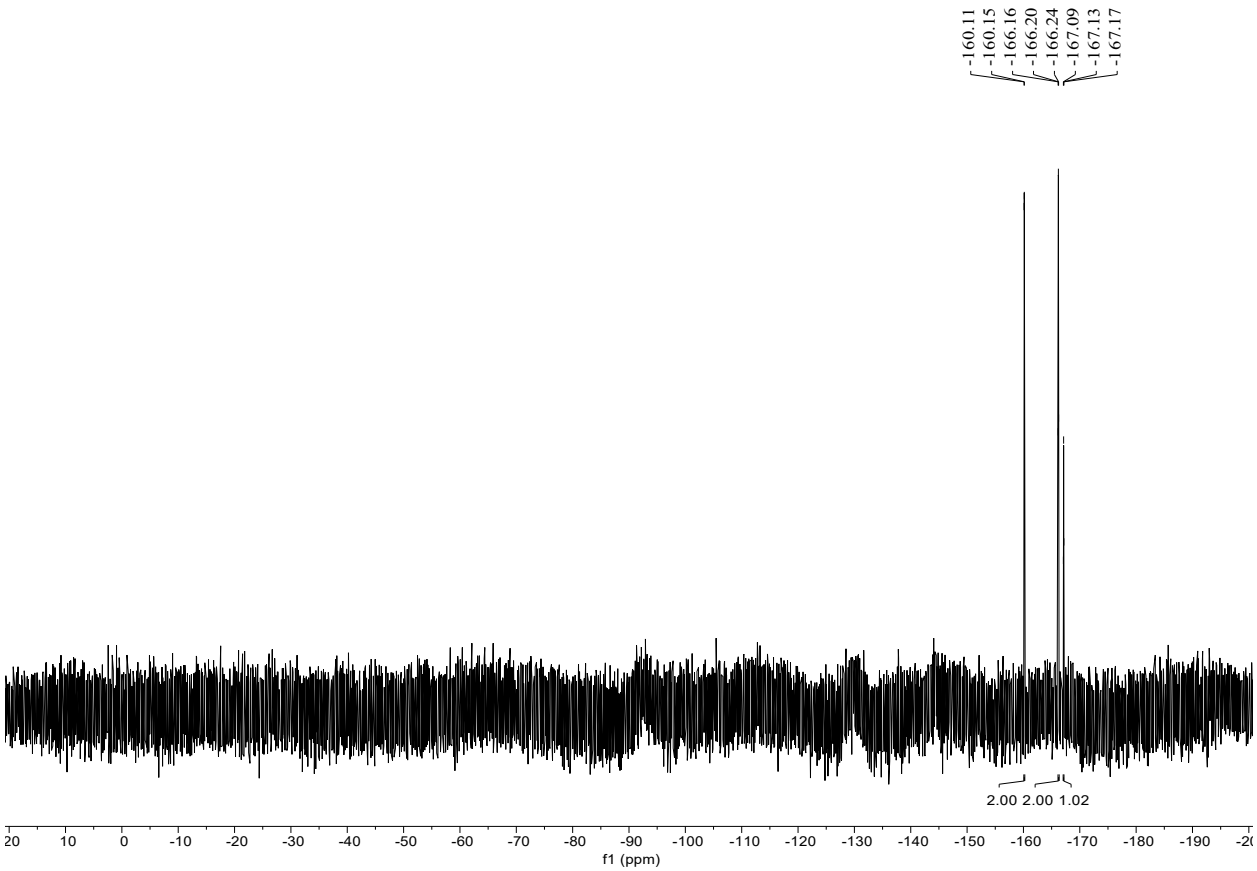

Figure S60: ^{19}F NMR spectrum of F_5-BsubNc (600 MHz) in acetone-d6.

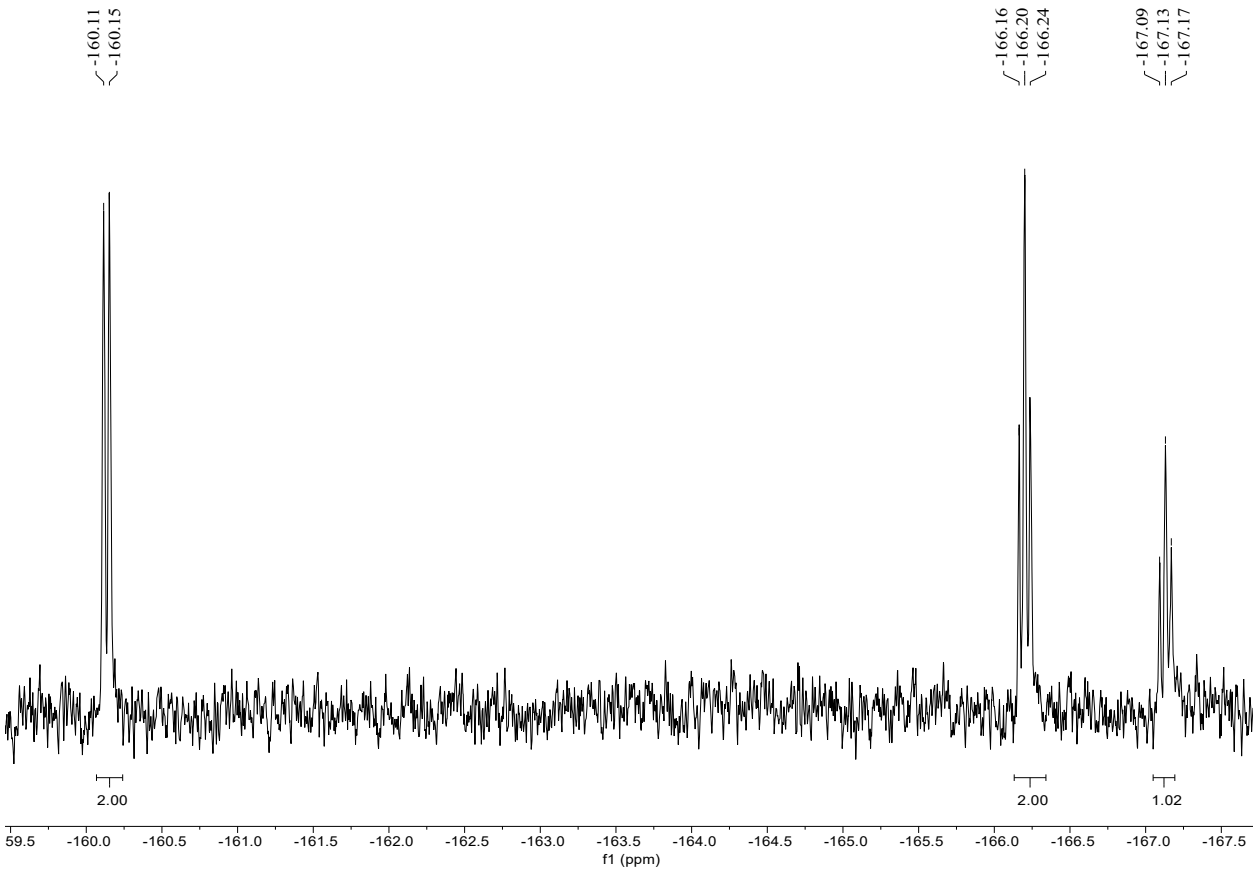

Figure S61: Zoom of the ^{19}F NMR spectrum (600 MHz) of F_5-BsubNc in acetone-d6.

NMR Spectroscopy of F-BsubNc

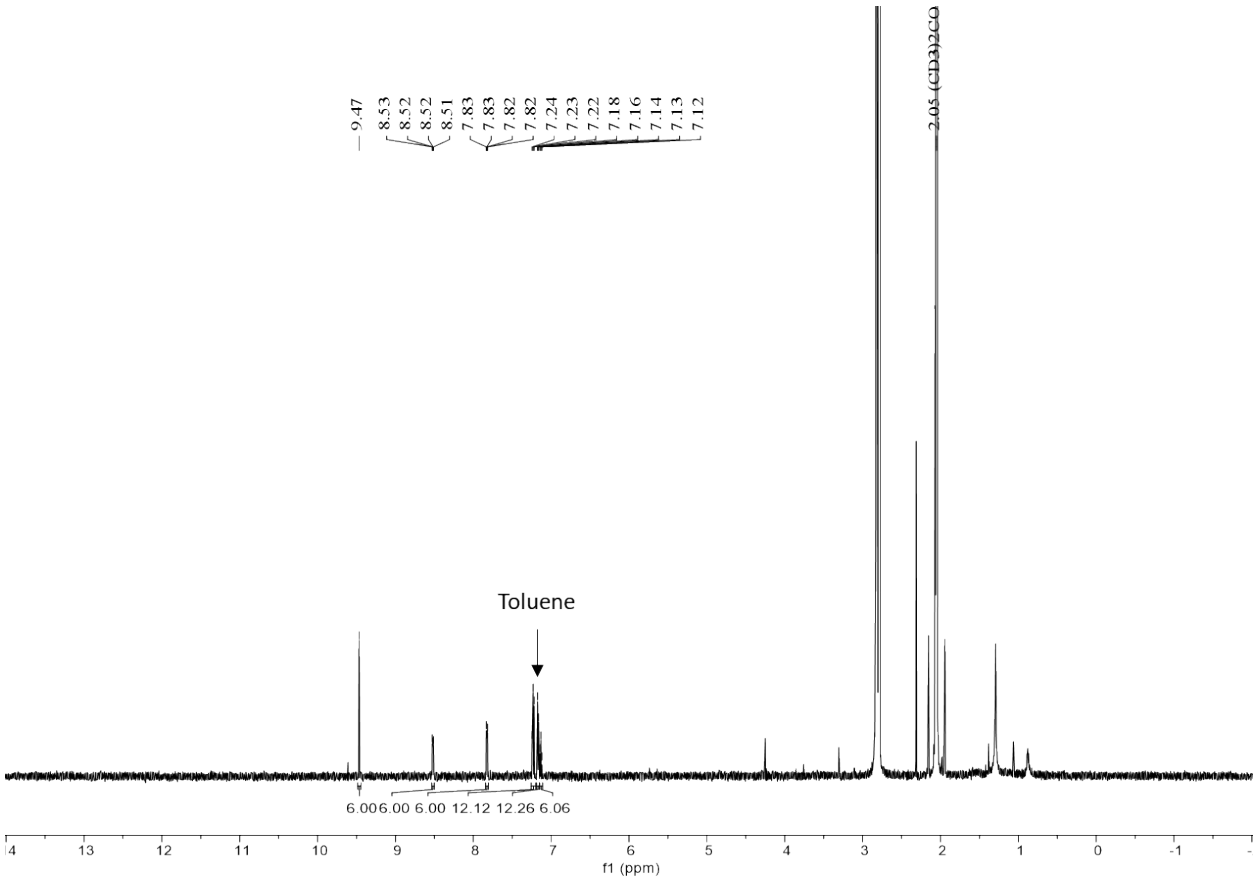

Figure S62: ^{1}H NMR spectrum (600 MHz) of F-BsubNc in acetone-d6.

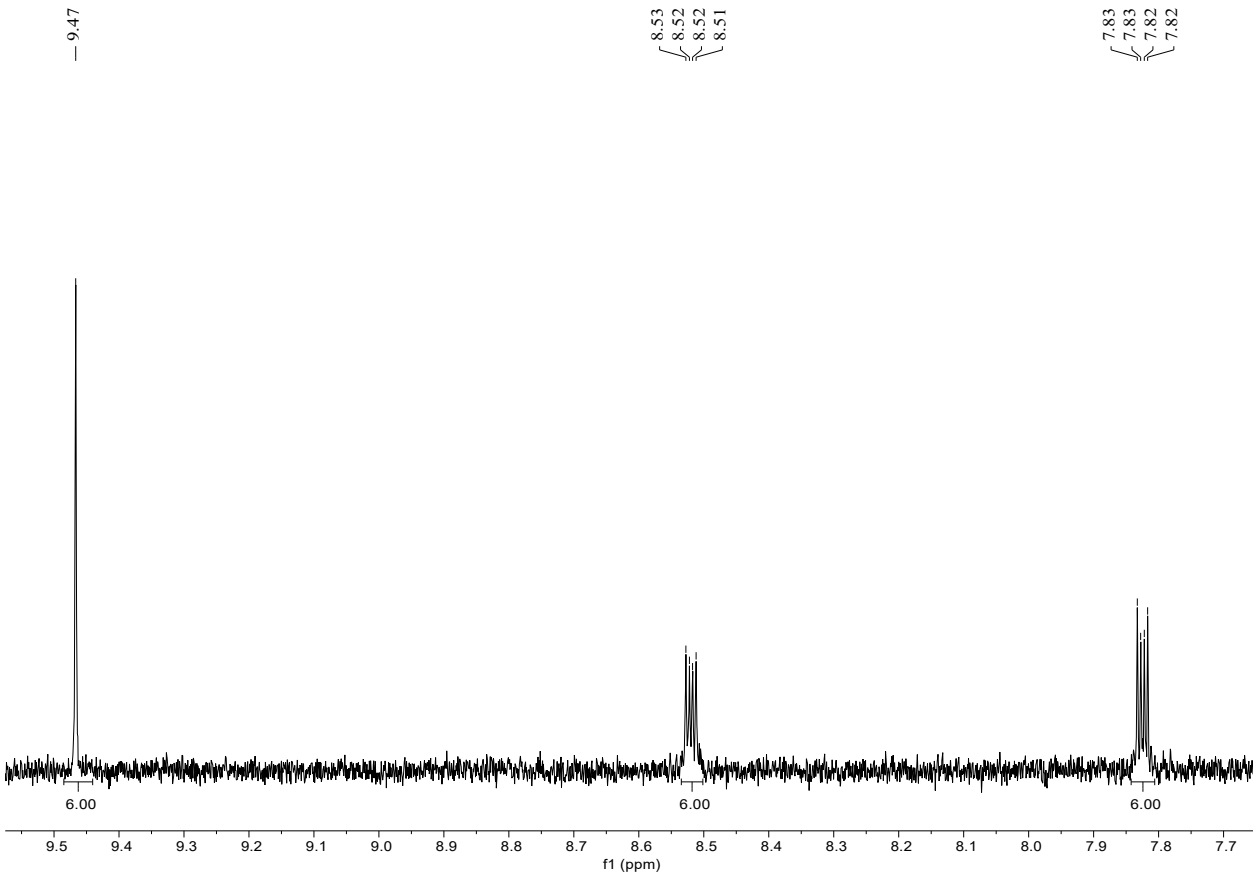

Figure S63: Zoom of the ^{1}H NMR spectrum (600 MHz) of F-BsubNc in acetone-d6.

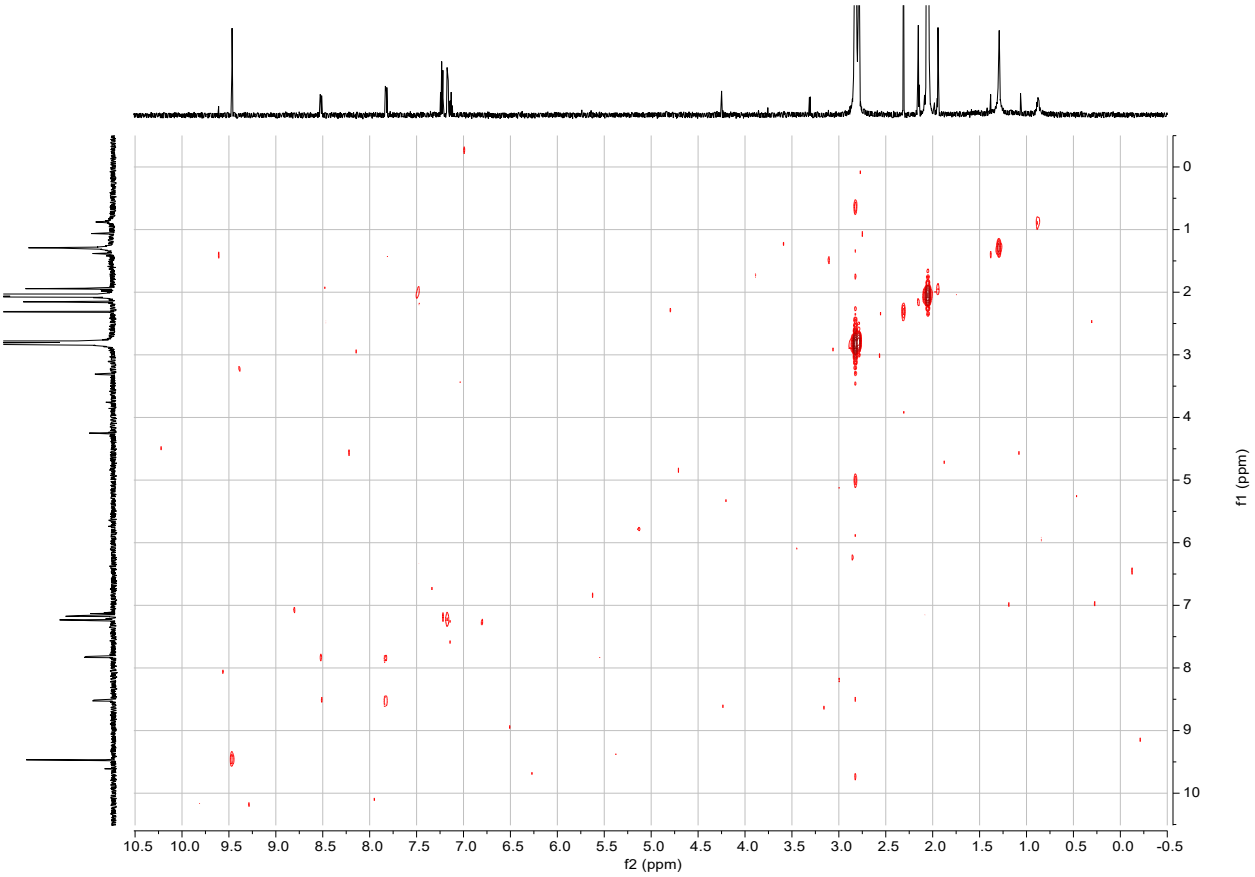

Figure S64: 2D gCOSY NMR spectrum (600 MHz) of F-BsubNc in acetone-d6.

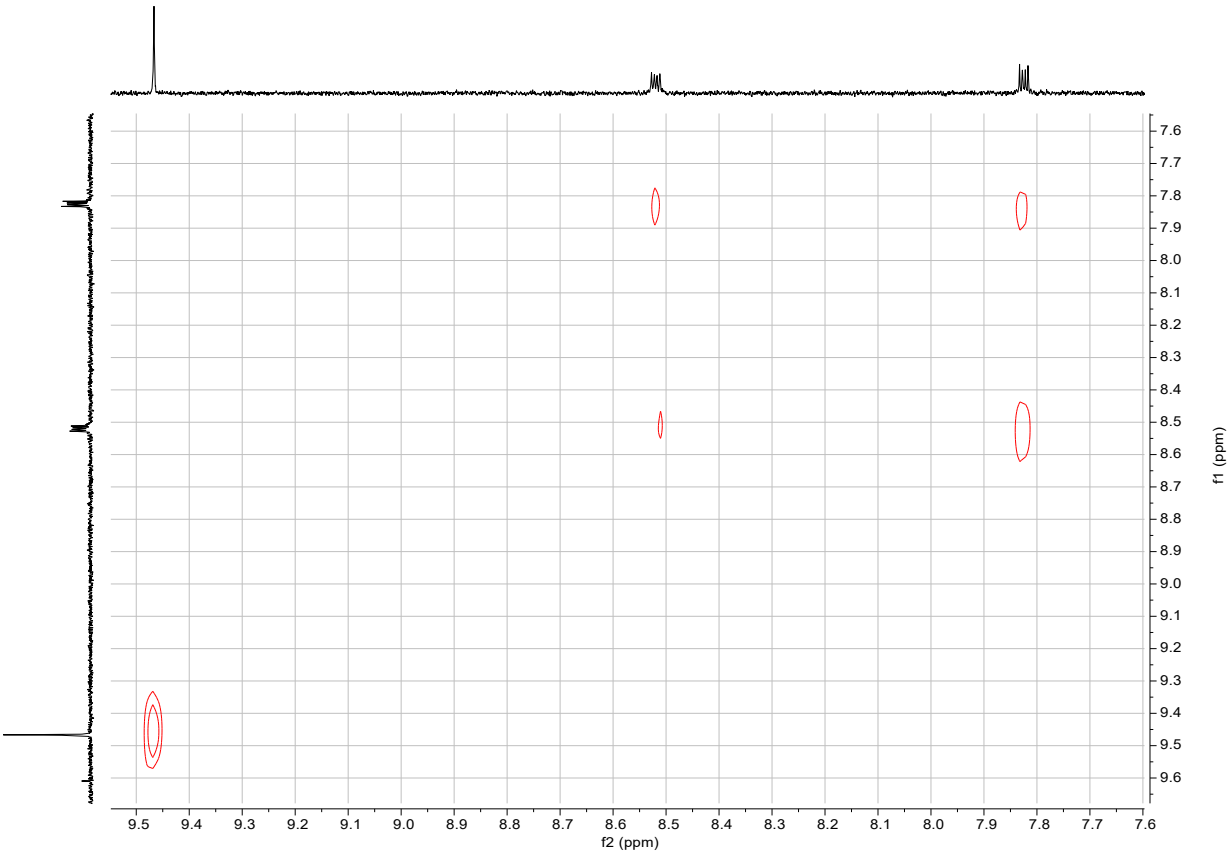

Figure S65: Zoom of the 2D gCOSY NMR spectrum (600 MHz) of F-BsubNc in acetone-d6.

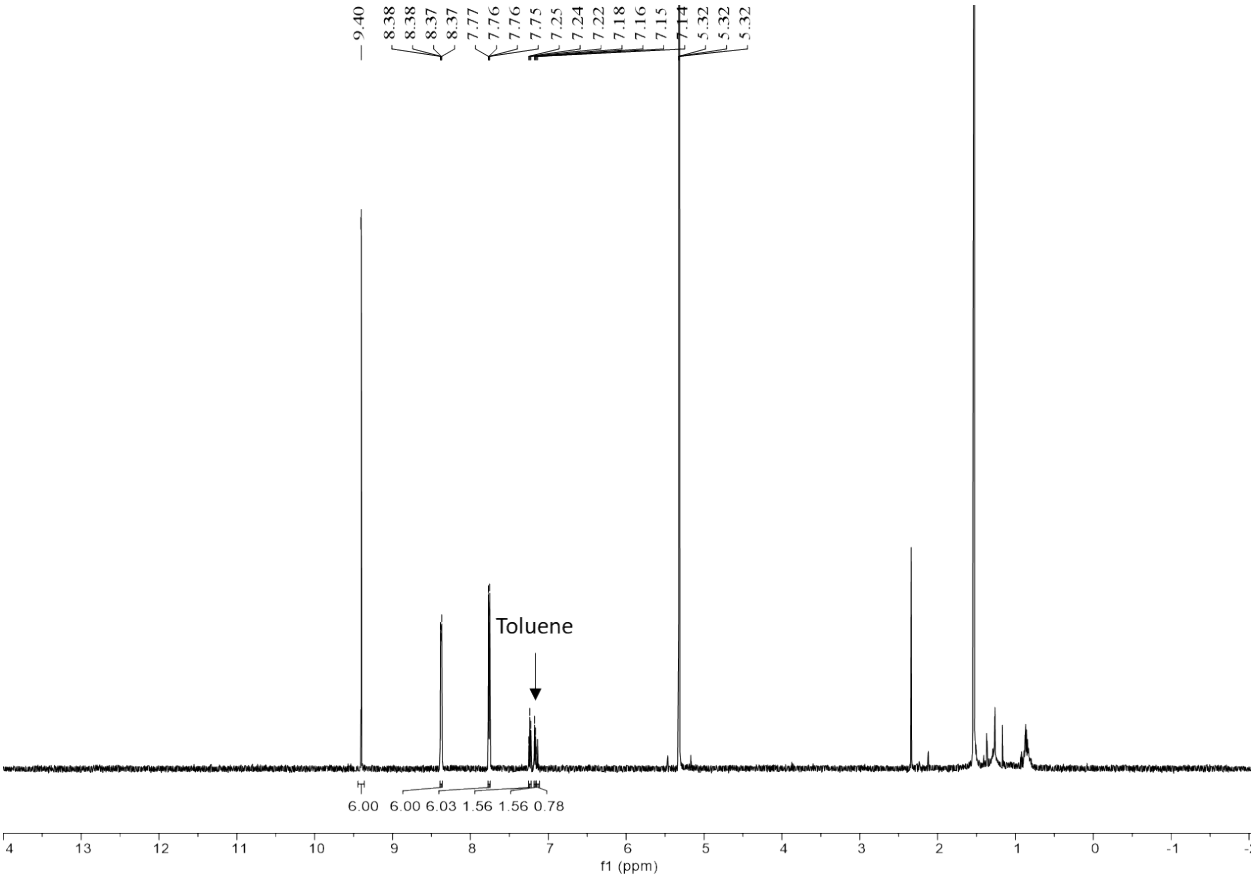

Figure S66: ^{1}H NMR spectrum (600 MHz) of F-BsubNc in DCM-d2.

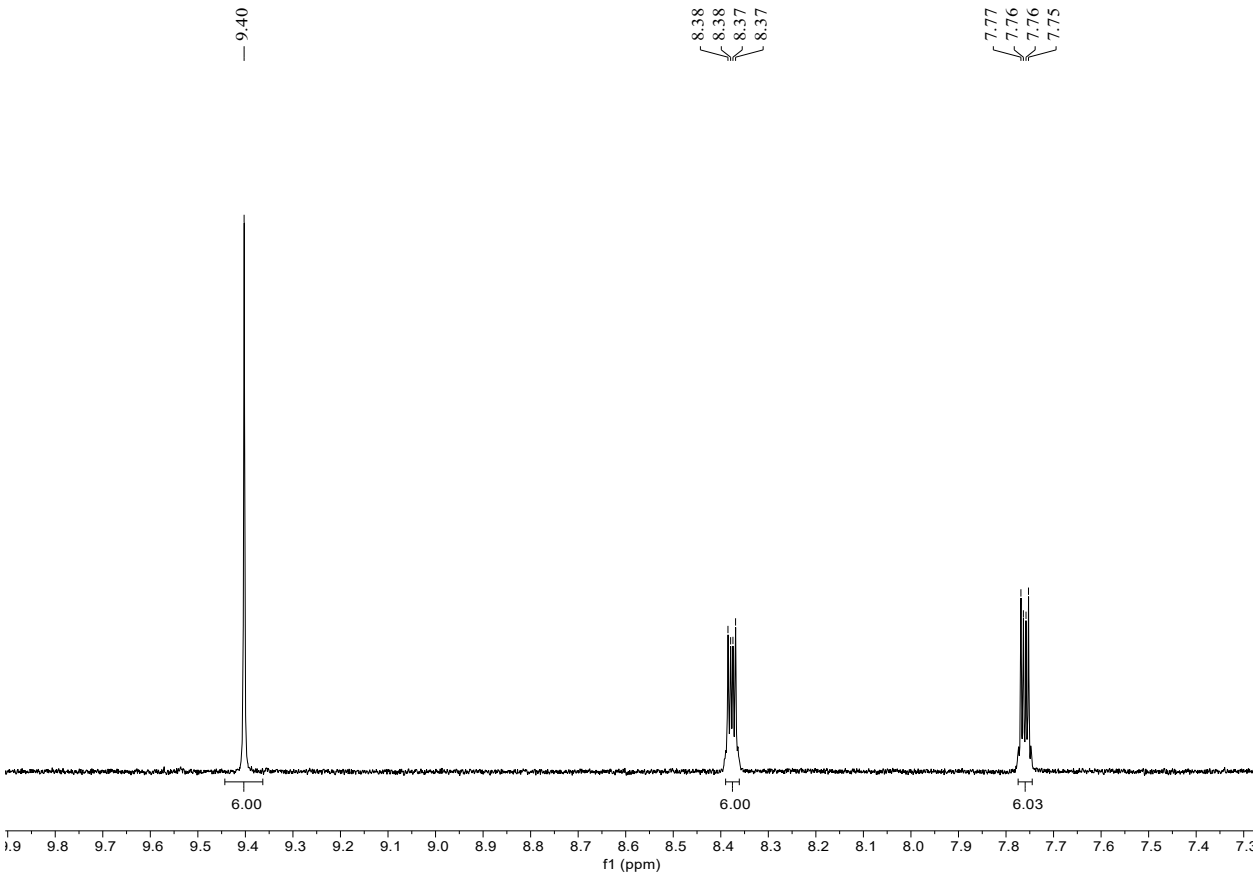

Figure S67: Zoom of the ^{1}H NMR spectrum (600 MHz) of F-BsubNc in DCM-d2.

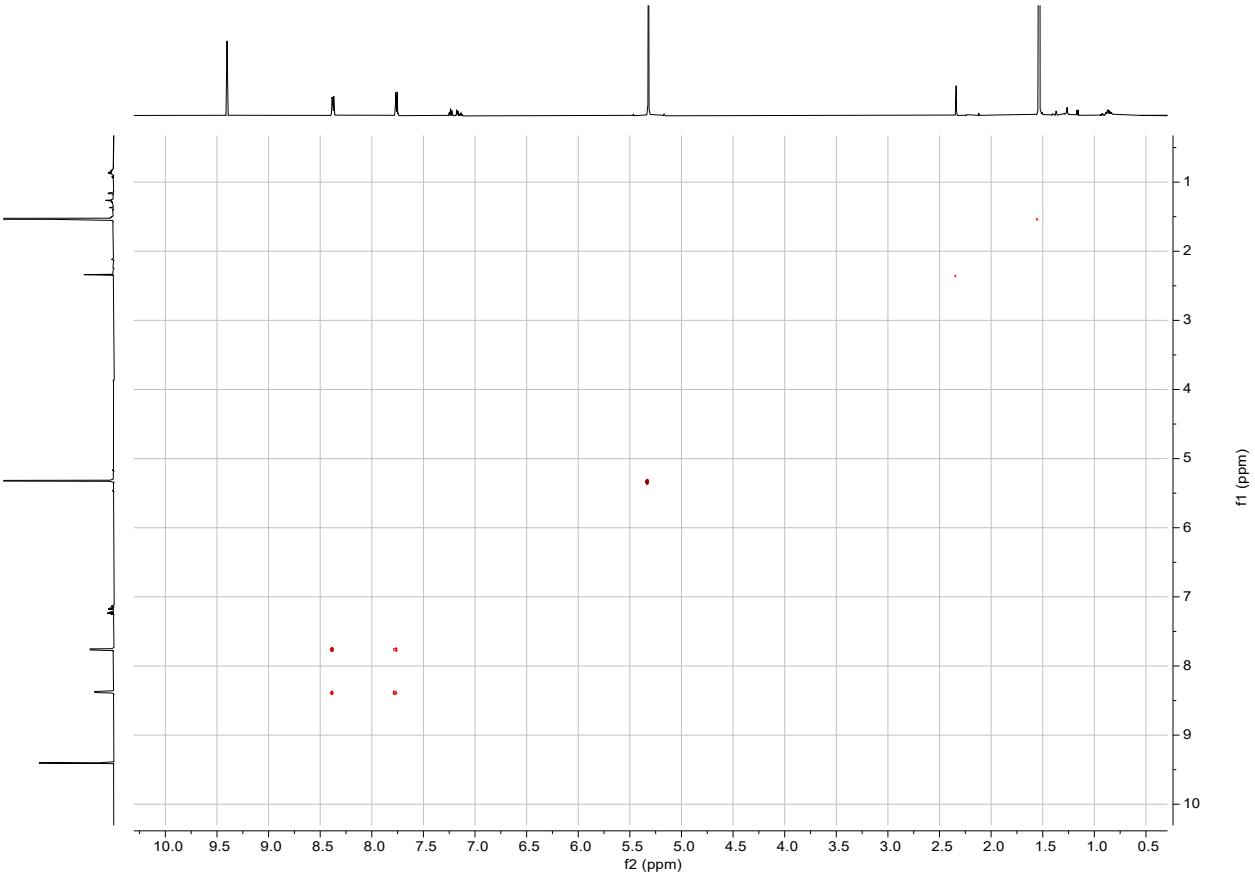

Figure S68: 2D gCOSY NMR spectrum (600 MHz) of F-BsubNc in DCM-d2.

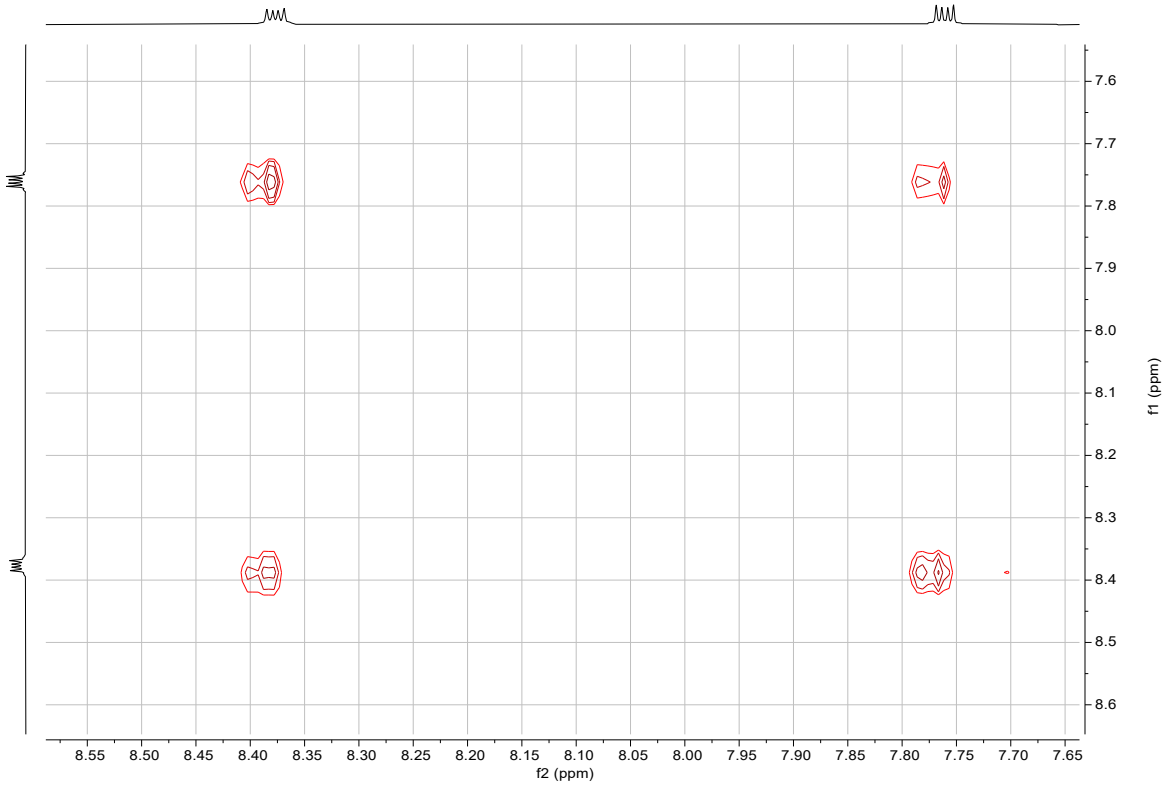

Figure S69: Zoom of the 2D gCOSY NMR spectrum (600 MHz) of F-BsubNc in DCM-d2.

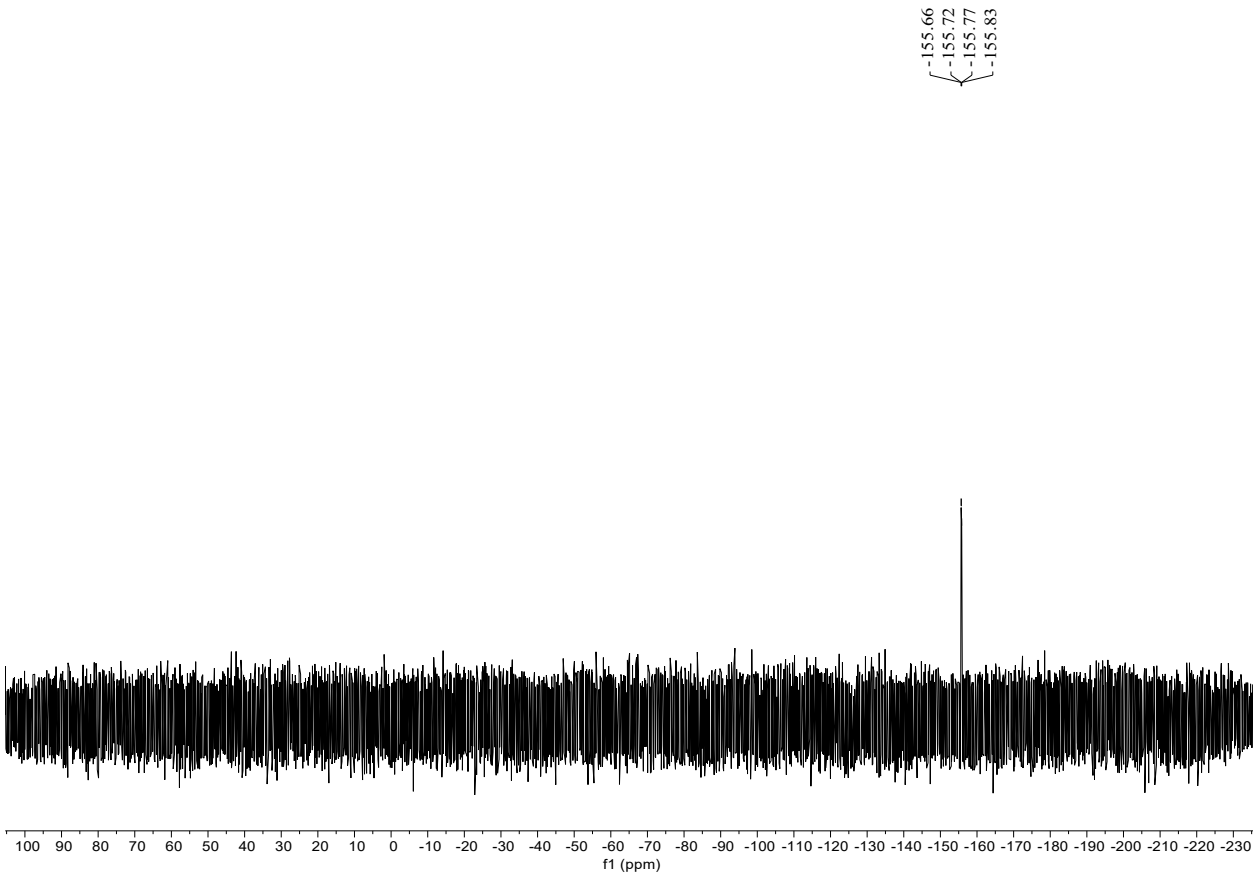

Figure S70: ^{19}F NMR spectrum (600 MHz) of F-BsubNc in DCM-d2.

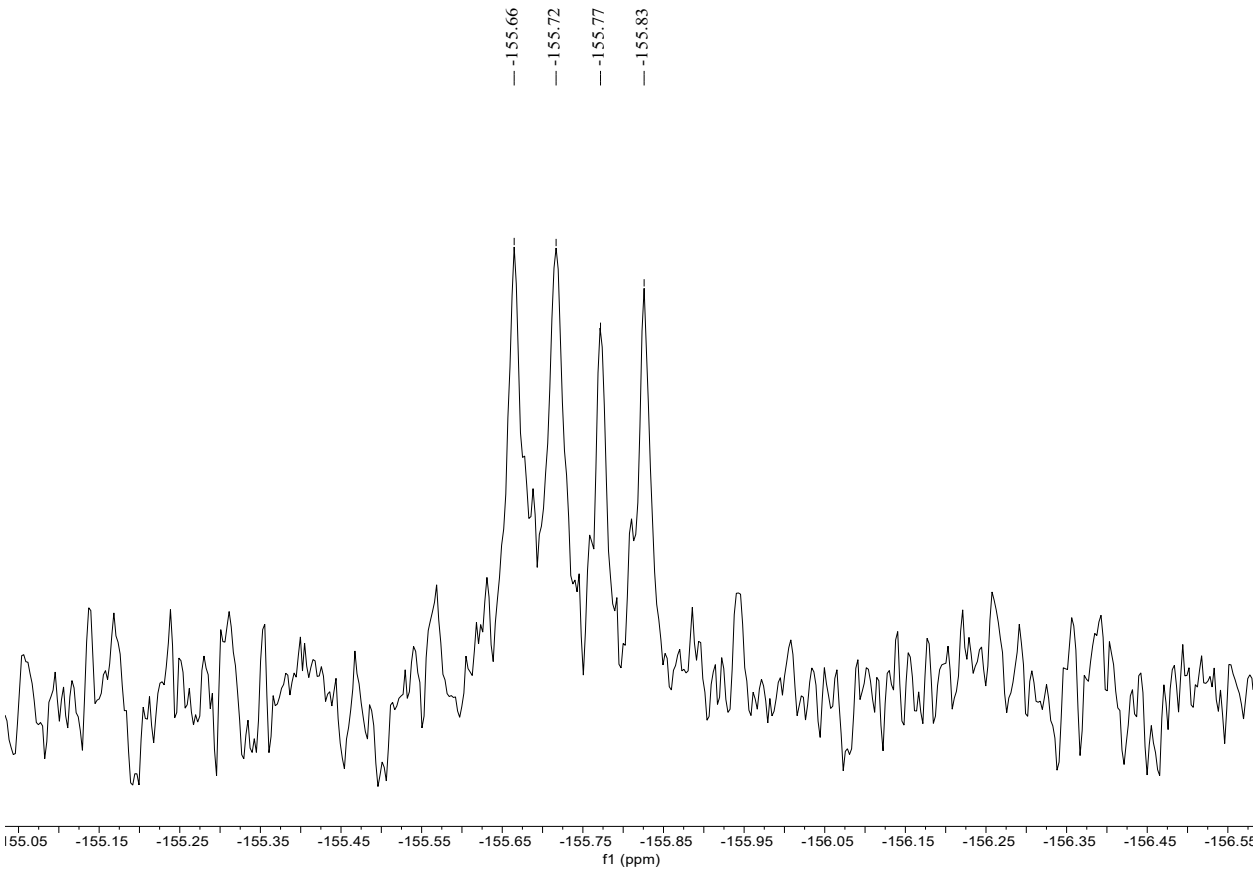

Figure S71: Zoom of the ^{19}F NMR spectrum (600 MHz) of F-BsubNc in DCM-d2.

NMR Spectroscopy of the BsubNc Precursor 2,3-Dicyanonaphthalene

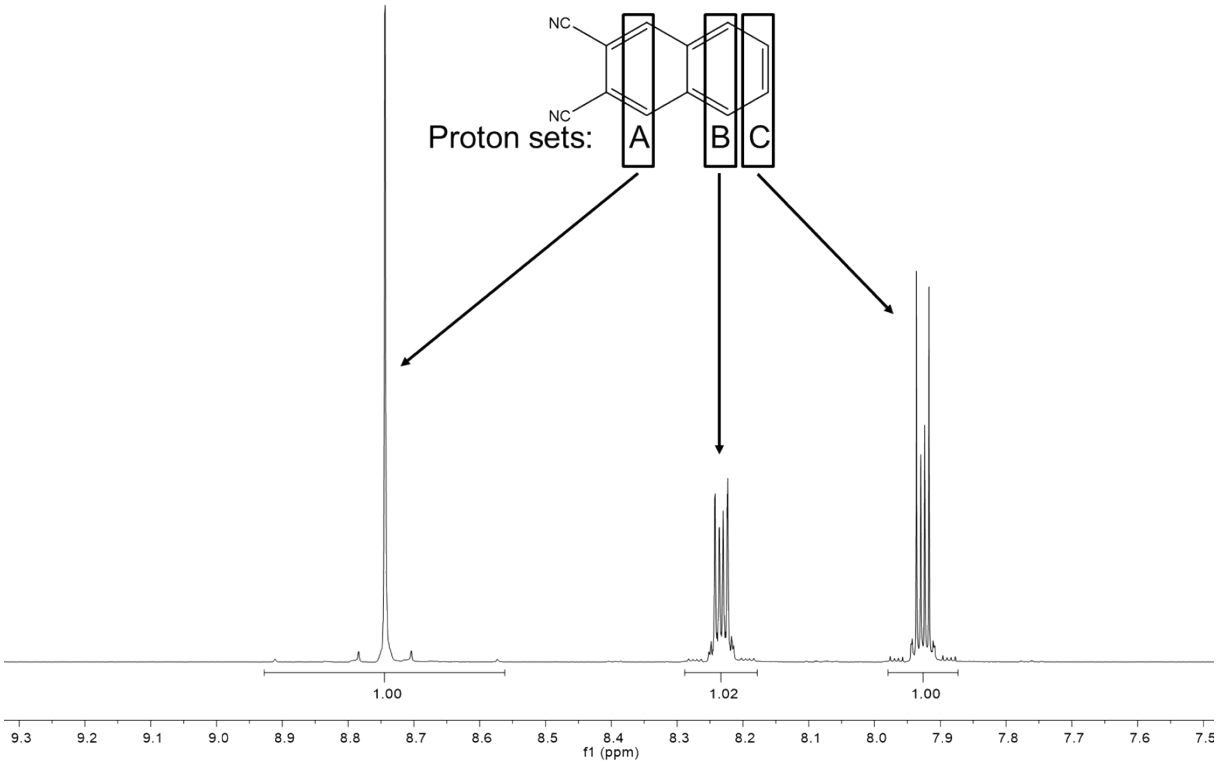

Figure S72: Zoom of the ^{1}H NMR spectrum (500 MHz) of 2,3-dicyanonaphthalene showing long range coupling.

MS of F_5-BsubNc

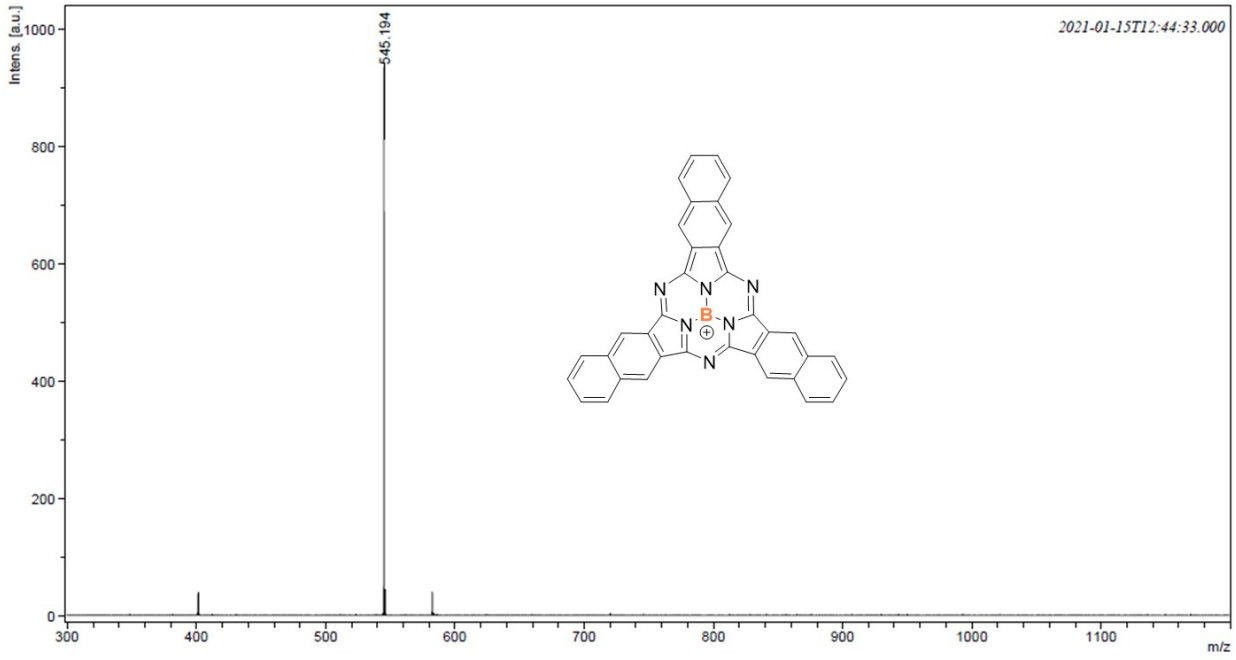

Figure S73: Laser desorption ionization mass spectrum of F_5-BsubNc.

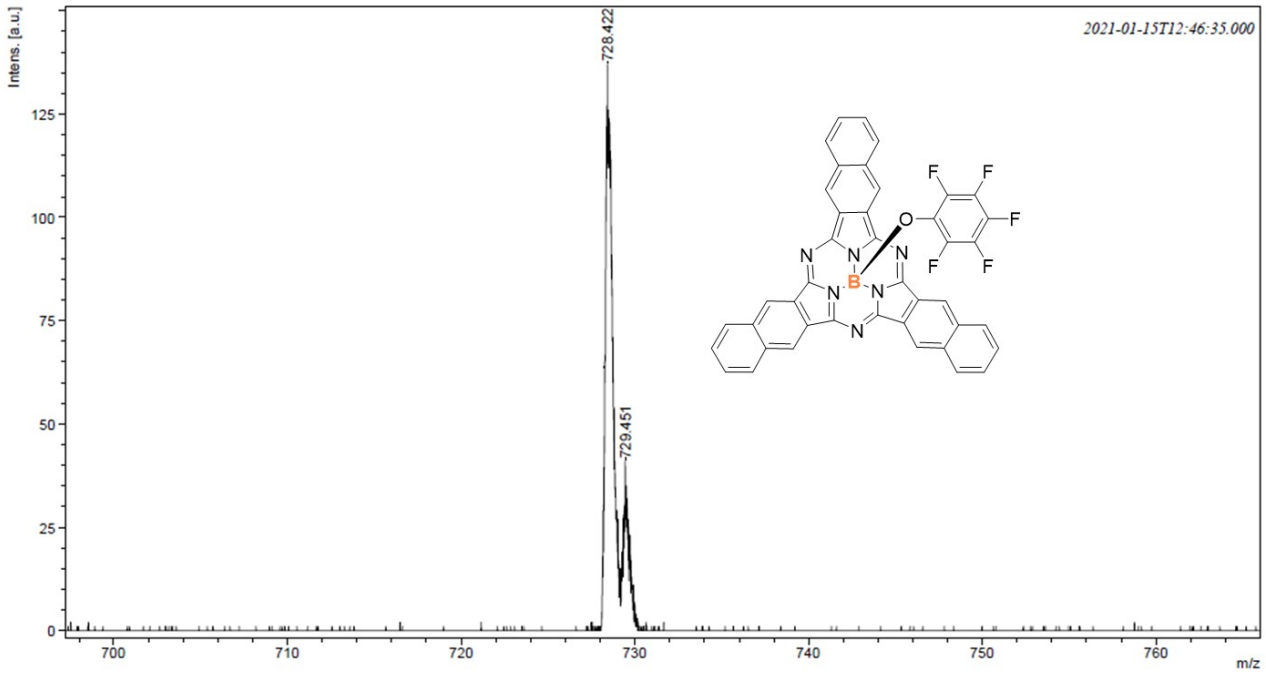

Figure S74: Matrix assisted (α-CHCA) laser desorption ionization mass spectrum of F_5-BsubNc.

MS of F-BsubNc

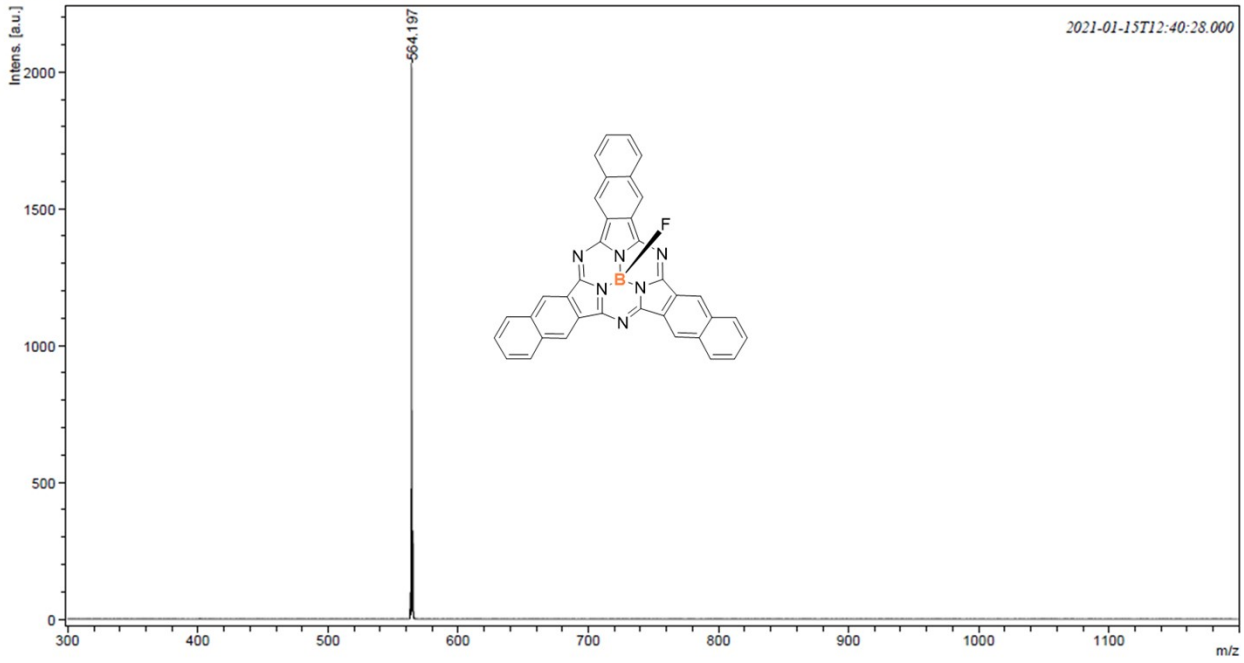

Figure S75: Laser desorption ionization mass spectrum of F-BsubNc.

Solution stability

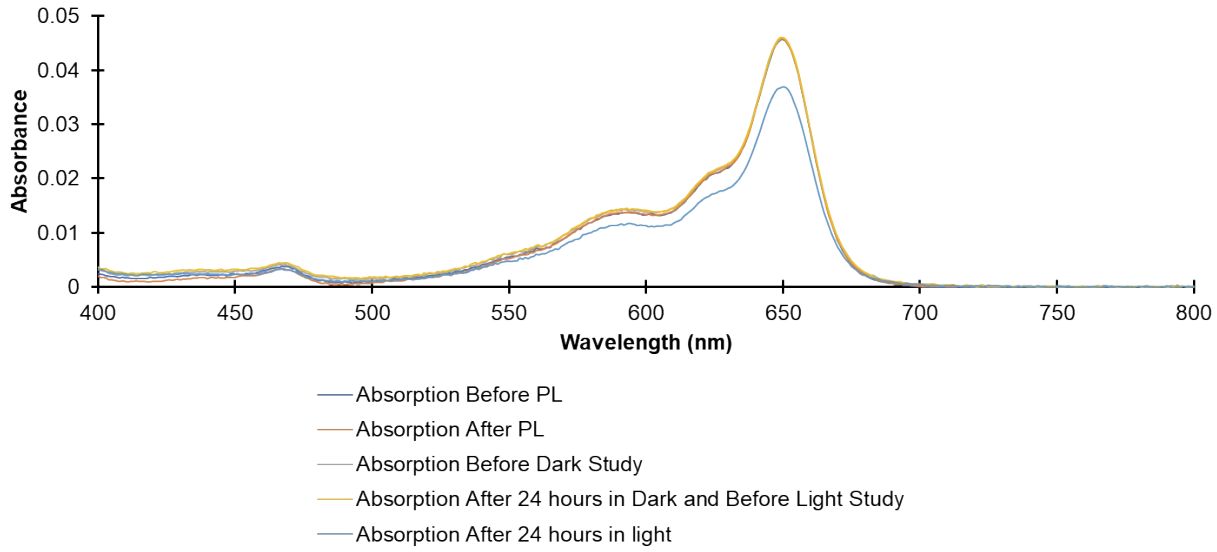

Figure S76: Absorption spectroscopy to measure the solution stability of F_5-BsubNc in the dark, under ambient light, as well as before and after photoluminescence spectroscopy. Measurements taken in toluene at room temperature.

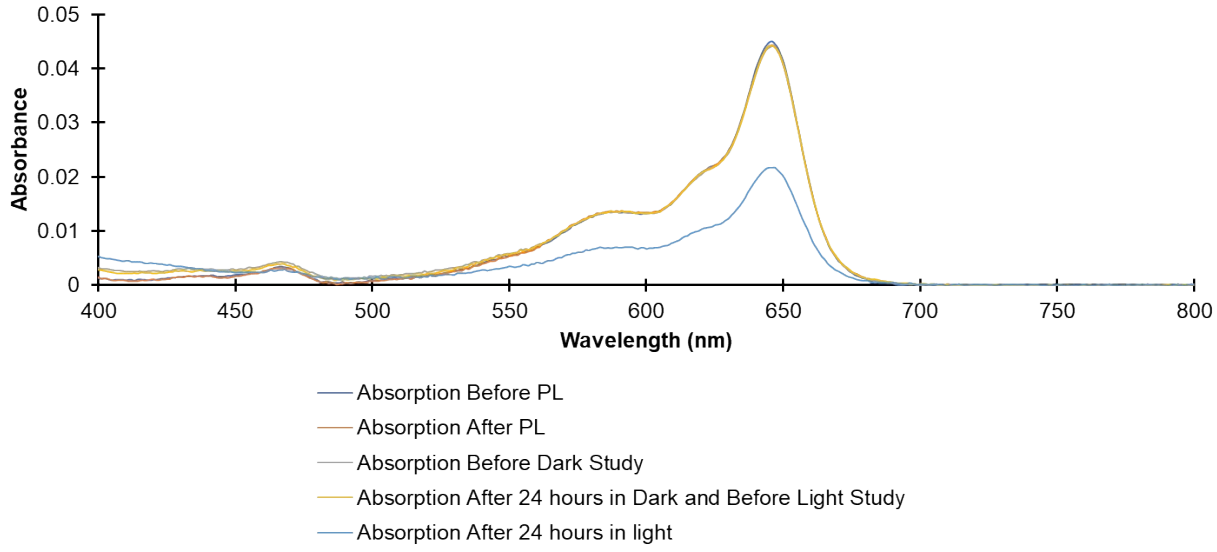

Figure S77: Absorption spectroscopy to measure the solution stability of F-BsubNc in the dark, under ambient light, as well as before and after photoluminescence spectroscopy. Measurements taken in toluene at room temperature.

Triphenyl Borate and 1,3-Diiminoisoindoline to Make PhO-BsubPc

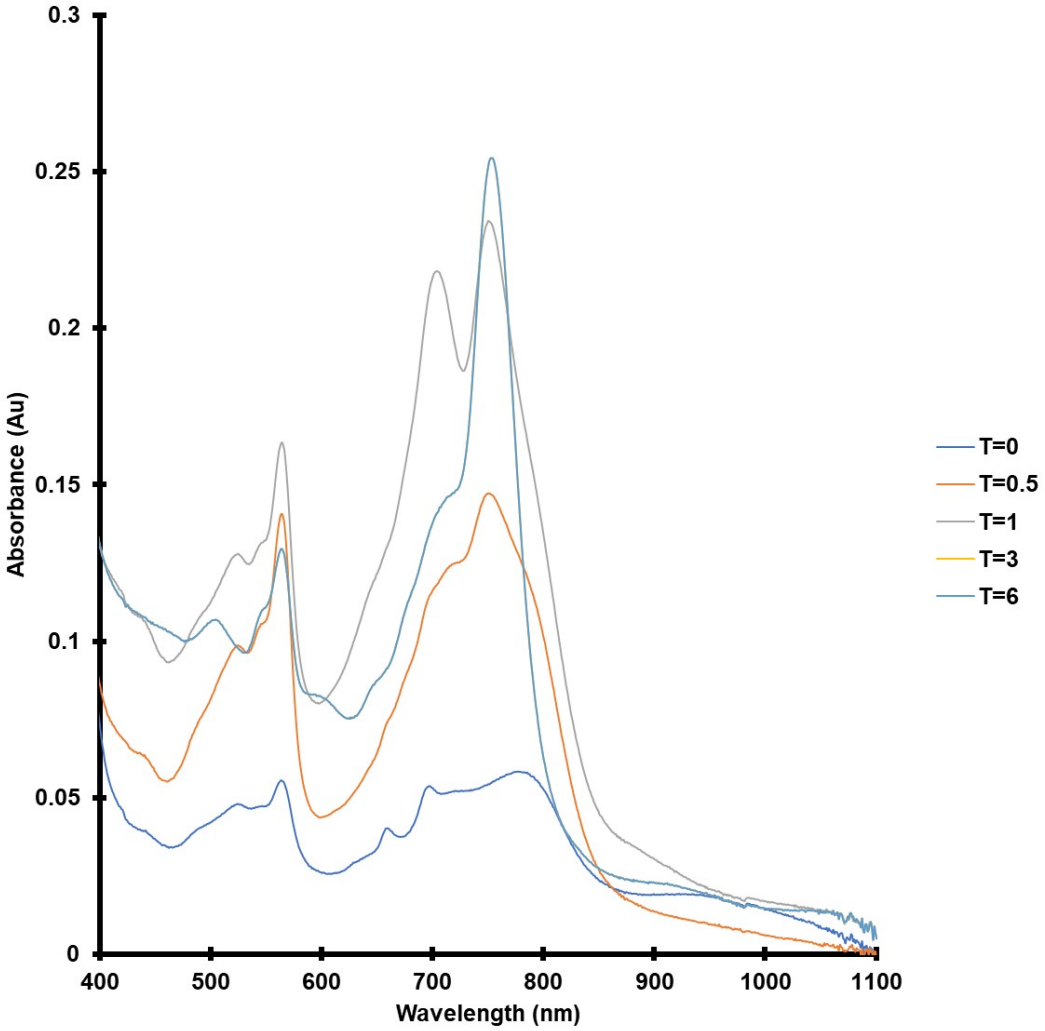

Figure S78: UV-Vis in chlorobenzene from the reaction of triphenyl borate and diiminoisoindoline to make PhO-BsubPc.

PhO-BsubNc Formation at High Temperature and Pressure with a Low Lewis Acidity Borate and Low Lewis Basicity Organic Precursor

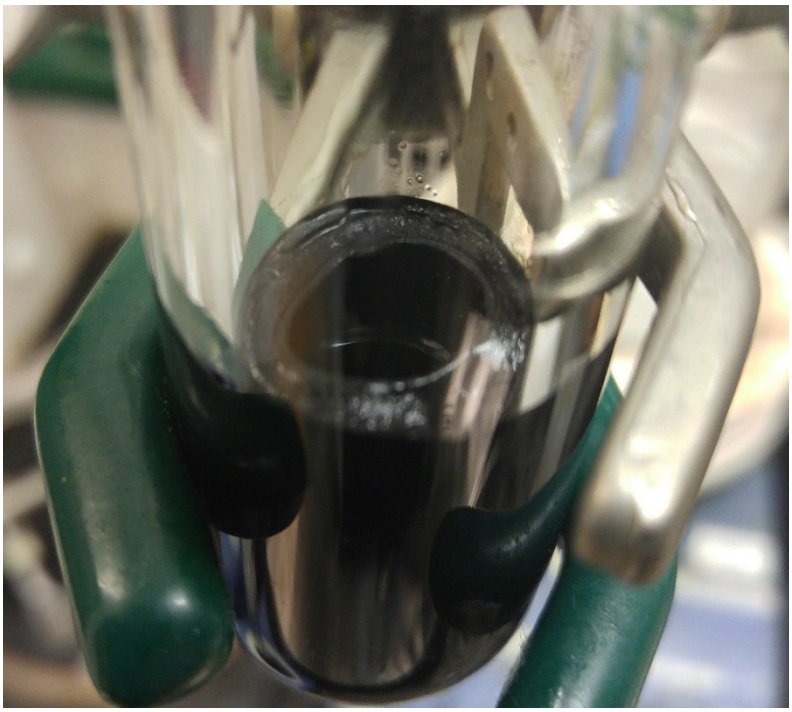

Figure S79: Photo of the PhO-BsubNc reaction mixture after completion of the reaction.

Figure S80: PhO-BsubNc reaction mixture dissolved in chlorobenzene.

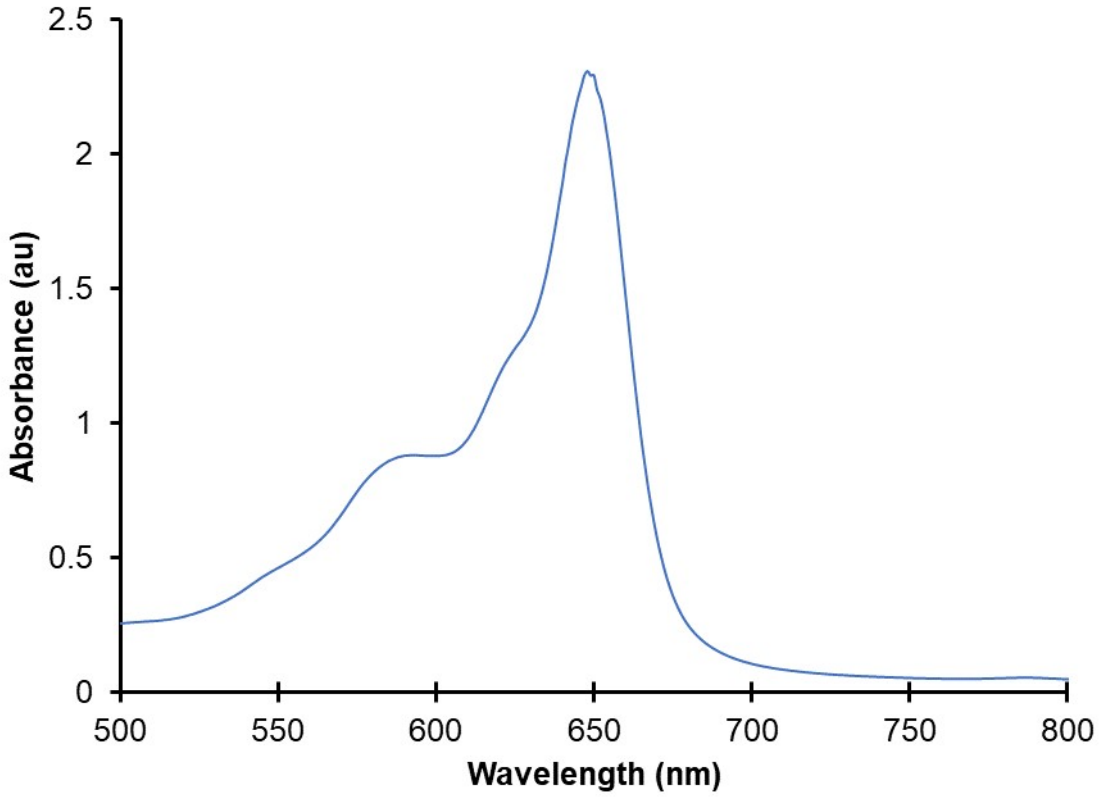

Figure S81: Absorption spectrum of the PhO-BsubNc reaction mixture in chlorobenzene.

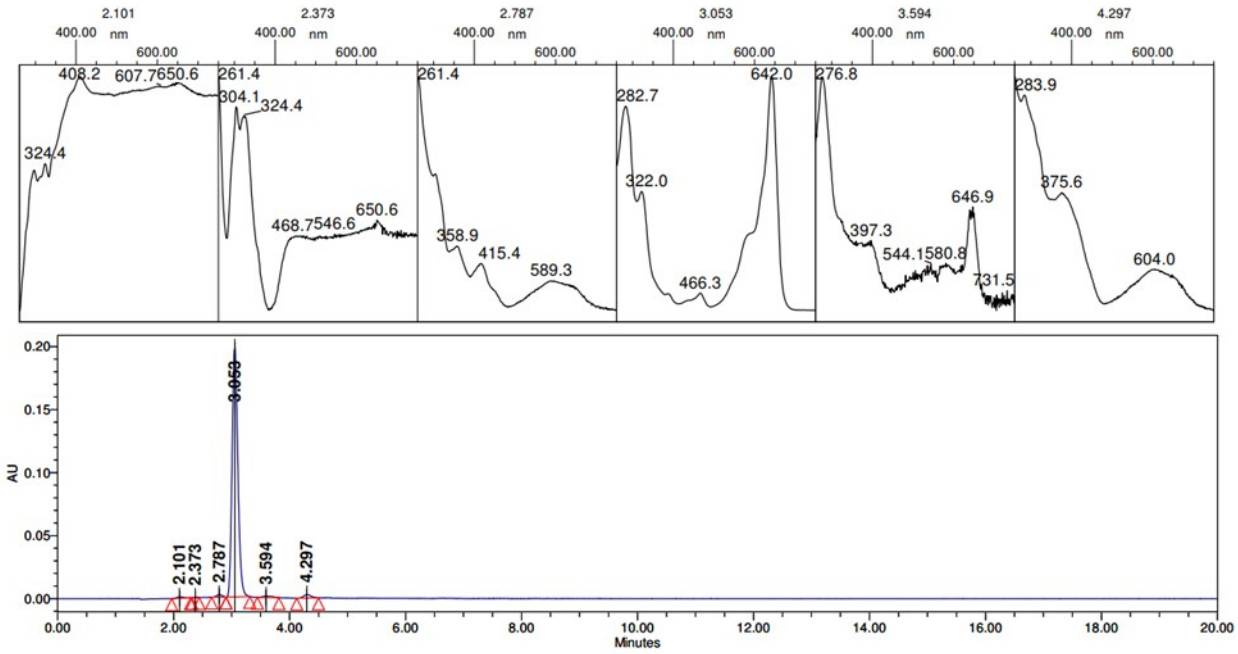

Figure S82: HPLC chromatogram of the PhO-BsubNc reaction crude. HPLC runs conducted with C18 functionalized silica as the stationary phase and 80:20 ACN:DMF (V:V) as the mobile phase.

Figure S83: Column chromatography of PhO-BsubNc reaction crude.

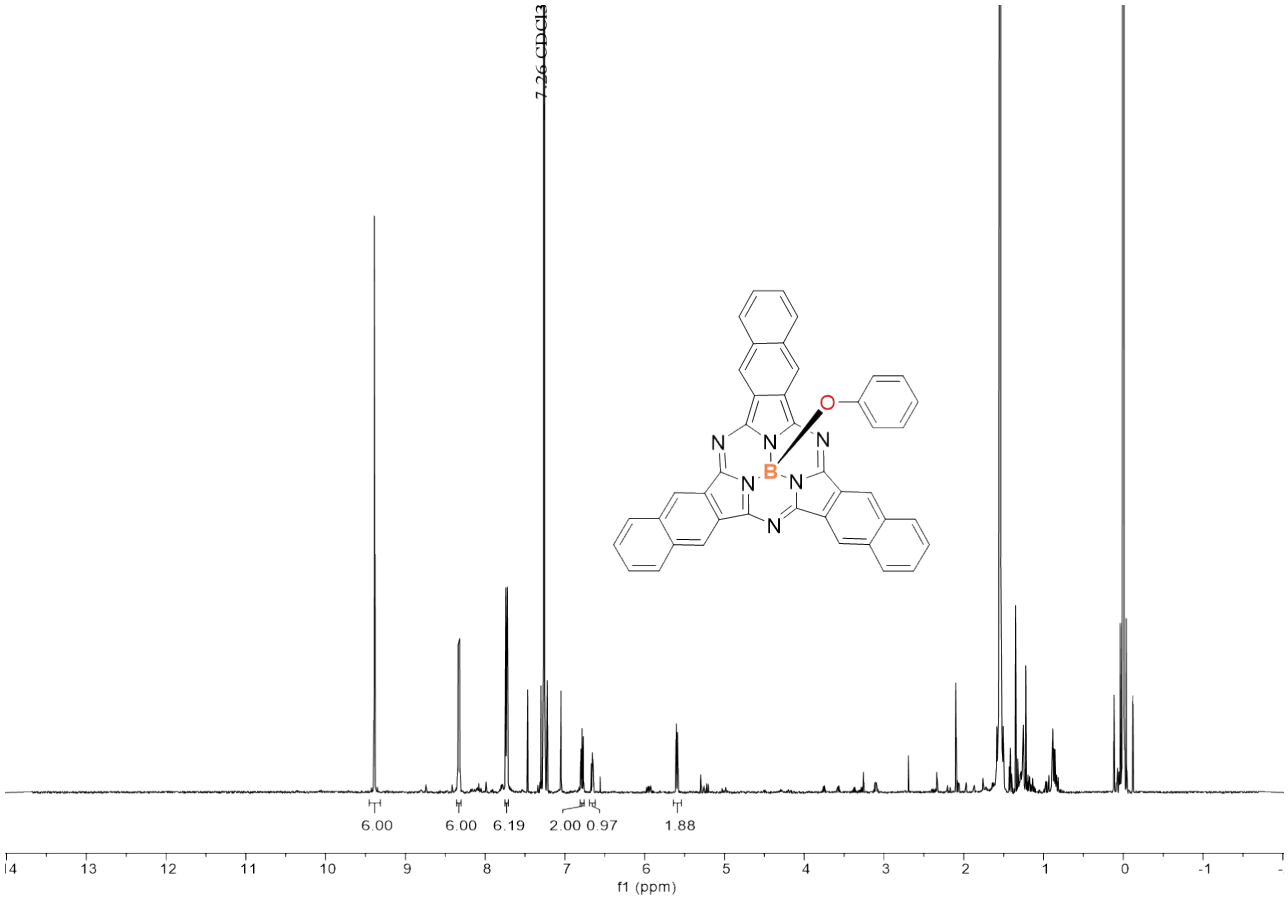

Figure S84: ^{1}H NMR spectrum (500 MHz) of PhO-BsubNc from column chromatography.

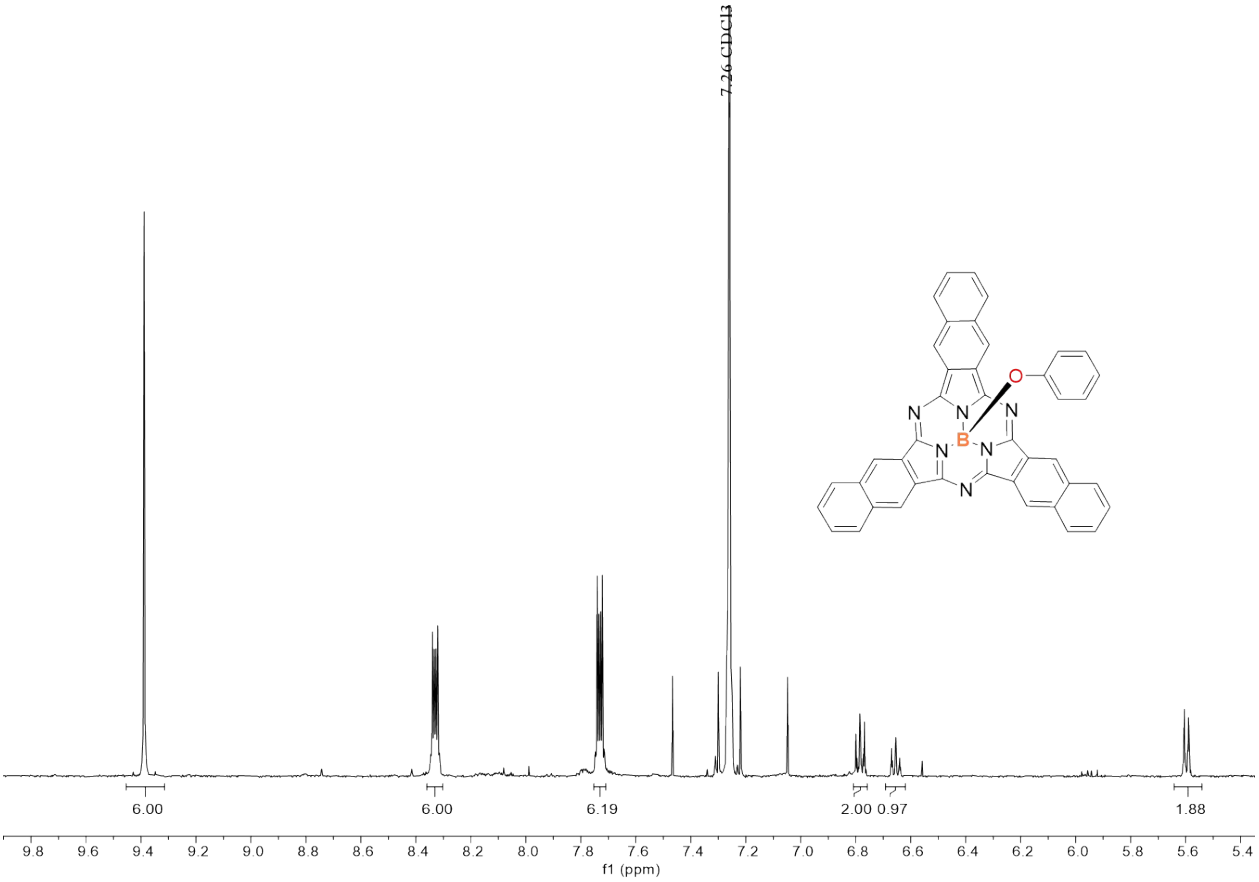

Figure S85: Zoom of the ^{1}H NMR spectrum (500 MHz) of PhO-BsubNc from column chromatography.

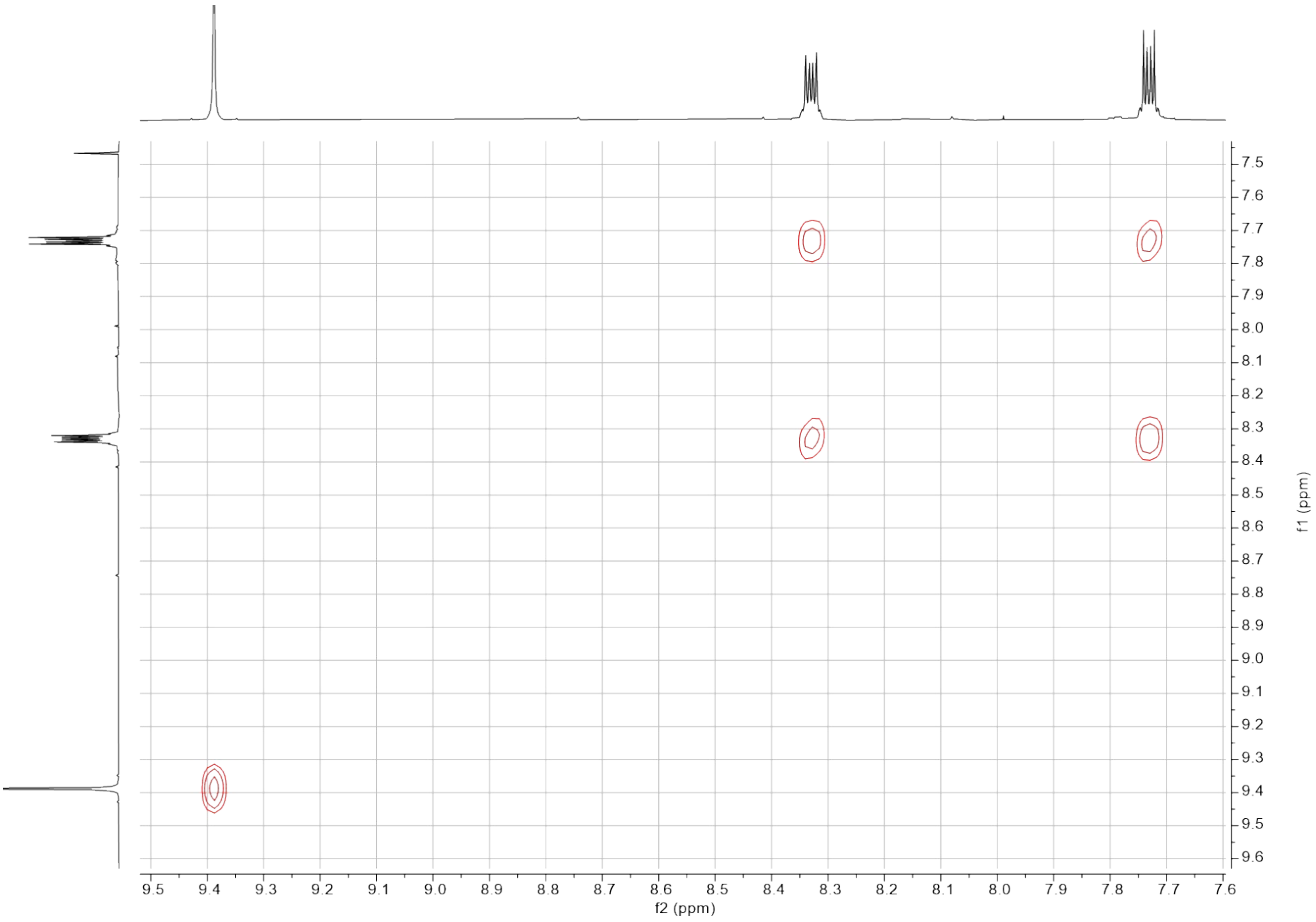

Figure S86: 2D COSY NMR spectrum (500 MHz) of PhO-BsubNc from column chromatography zoomed to the macrocyclic protons.

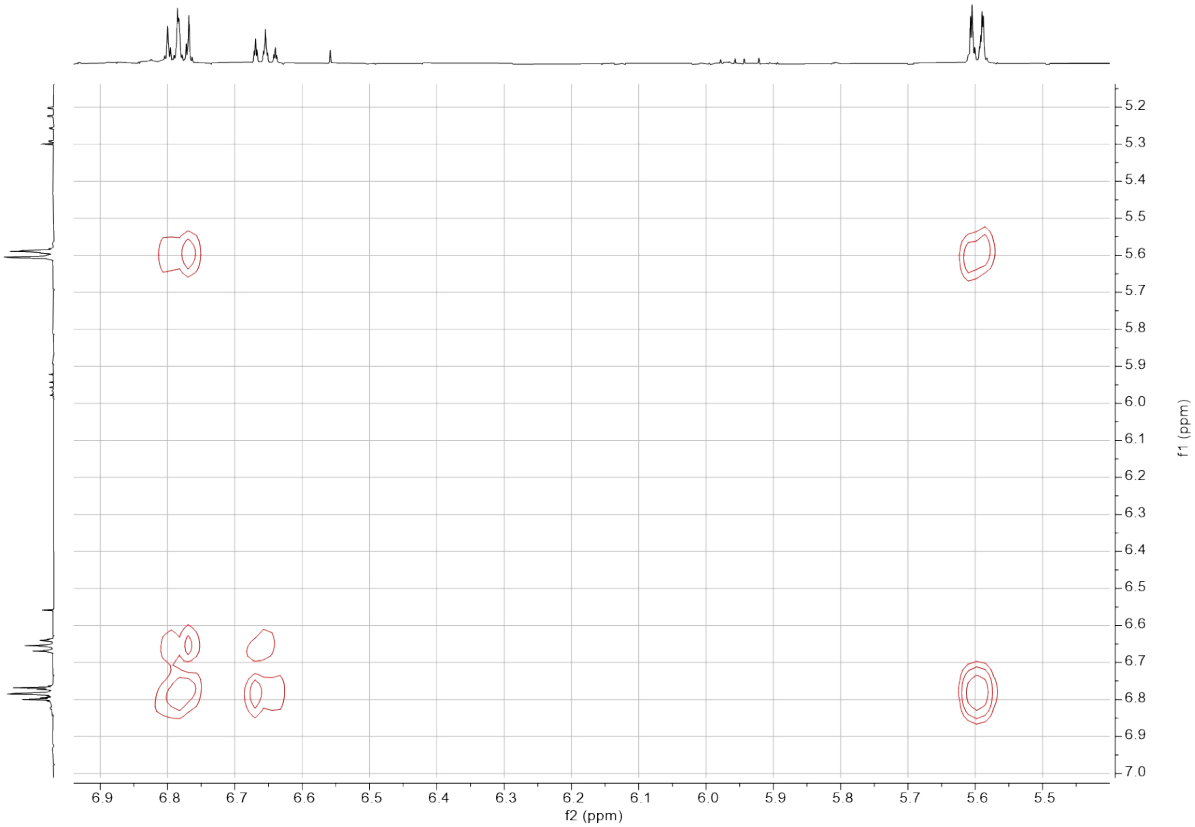

Figure S87: 2D COSY NMR spectrum (500 MHz) of PhO-BsubNc from column chromatography zoomed to the phenolic protons.

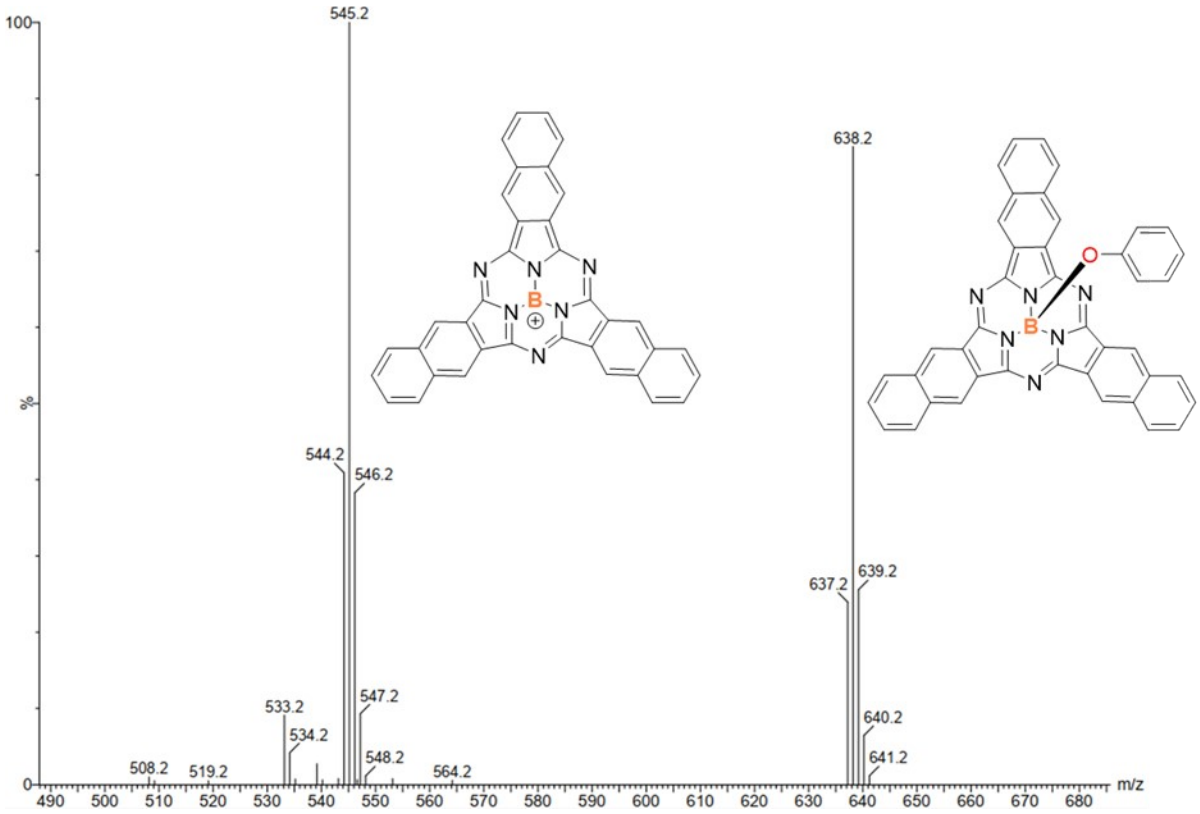

Figure S88: EI-MS of PhO-BsubNc from column chromatography.

Reaction of 2,3-DCN and Triphenyl Borate in DPGDME at Elevated Temperature and Pressure with Urea as an Additive.

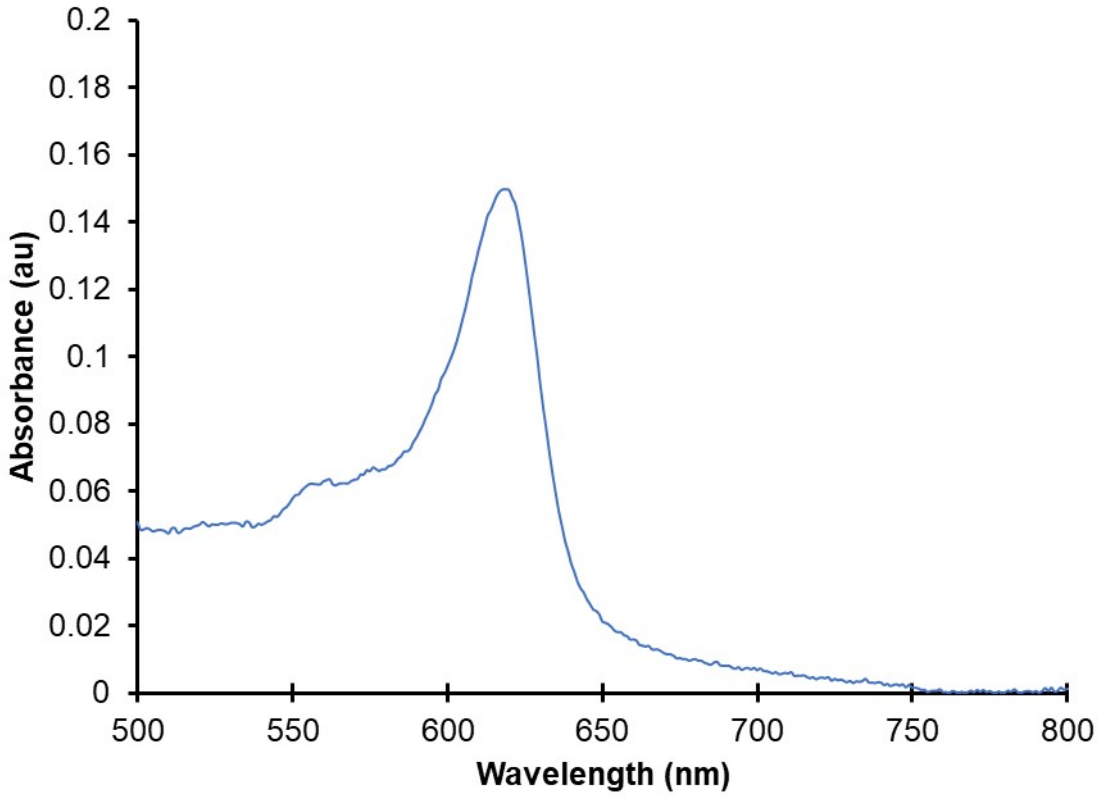

Figure S89: Absorption spectrum of the crude in chlorobenzene.

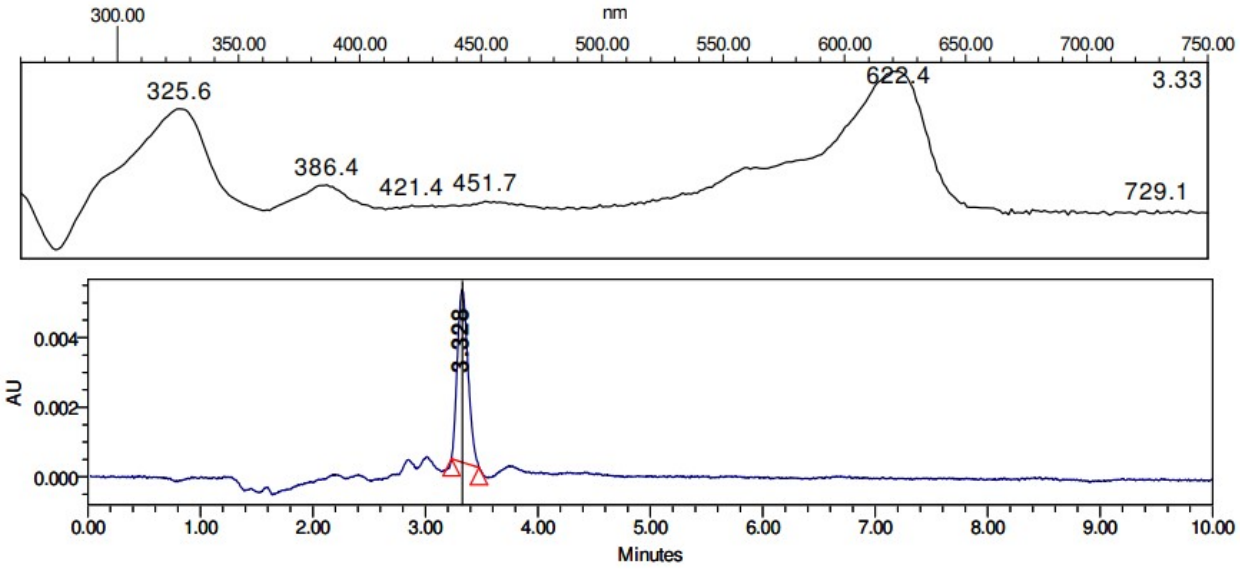

Figure S90: HPLC of the crude extracted between 600 nm and 700 nm. HPLC runs conducted with C18 functionalized silica as the stationary phase and 80:20 ACN:DMF (V:V) as the mobile phase.

Characterization of BsubPc/BsubNc Hybrid Reactions in DPGDME at Elevated Temperature and Pressure

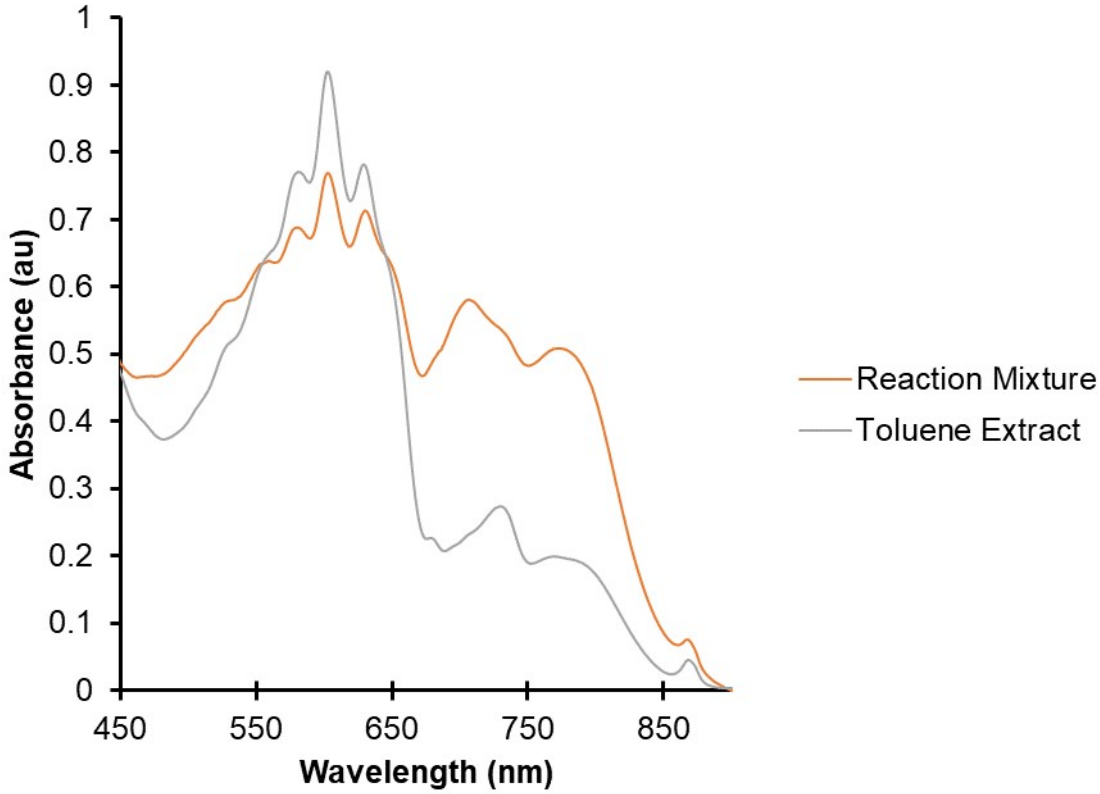

Figure S91: Absorption spectra of borates for hybrid synthesis reaction in chlorobenzene.

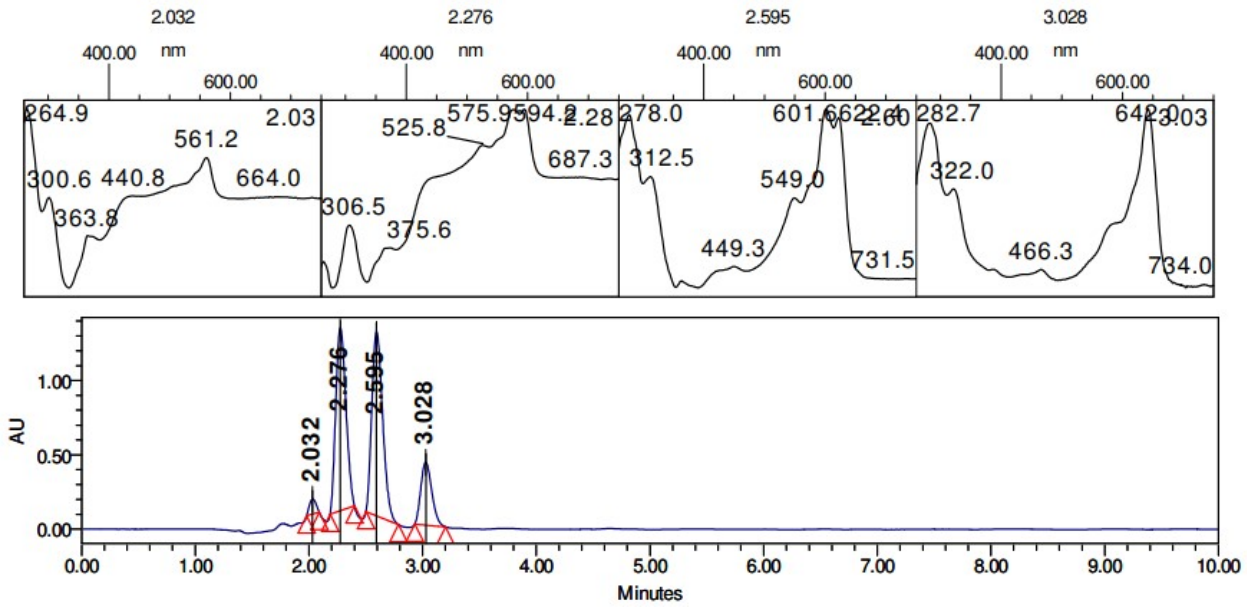

Figure S92: HPLC chromatogram extracted from 560 nm to 590 nm of the toluene extract from the borates for hybrid synthesis reaction. HPLC runs conducted with C18 functionalized silica as the stationary phase and 80:20 ACN:DMF (V:V) as the mobile phase.

Mixtures of Triphenyl Borate and Boron Trihalides

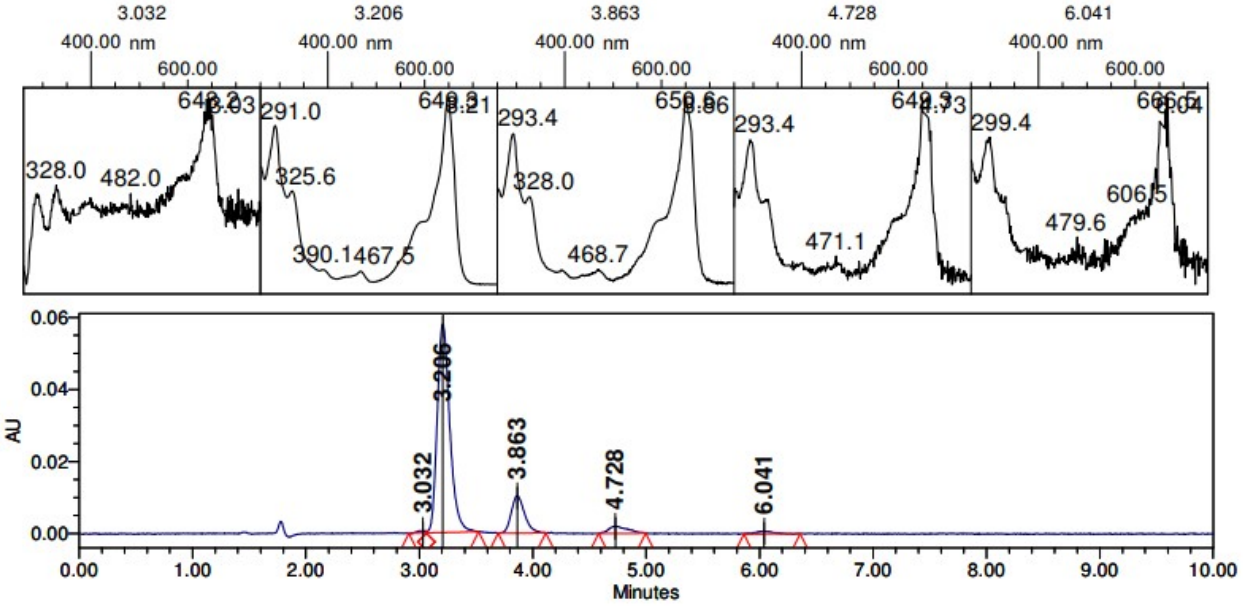

Figure S93: HPLC chromatogram extracted at 650 nm of the 1:2 BCl_3:$B(OPh)_3$ reaction to form BsubNc after 3 hours at reflux. HPLC run conducted with C18 functionalized silica as the stationary phase and 80:20 ACN:DMF (V:V) as the mobile phase.

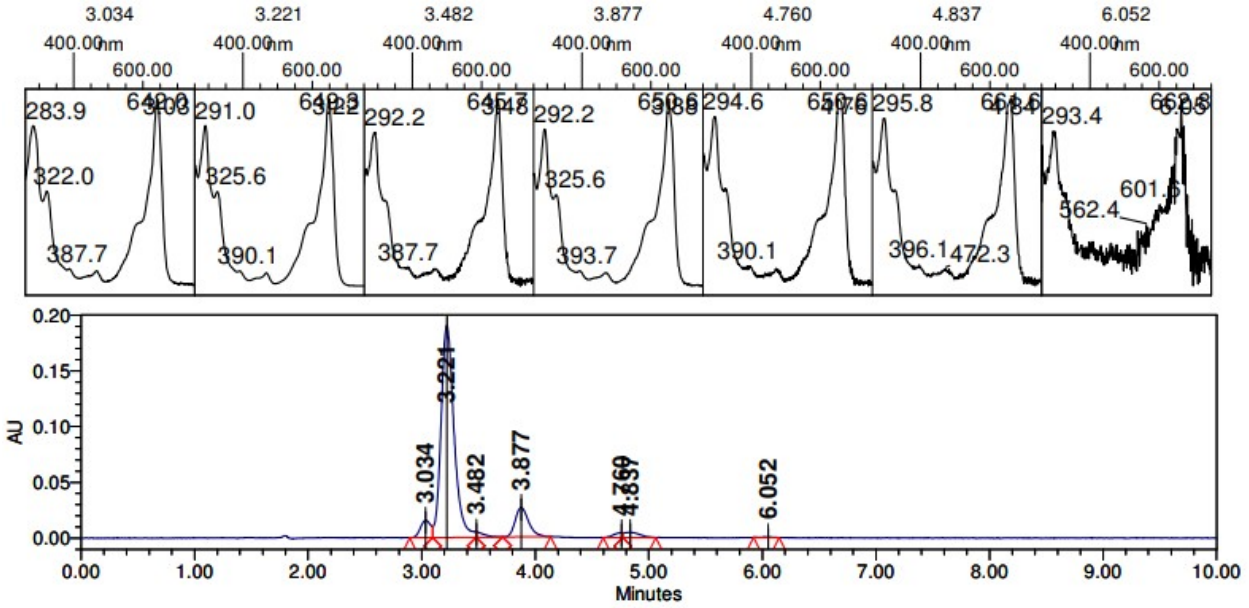

Figure S94: HPLC chromatogram extracted at 650 nm of the 1:1 BCl_3:$B(OPh)_3$ reaction to form BsubNc after 3 hours at reflux. HPLC run conducted with C18 functionalized silica as the stationary phase and 80:20 ACN:DMF (V:V) as the mobile phase.

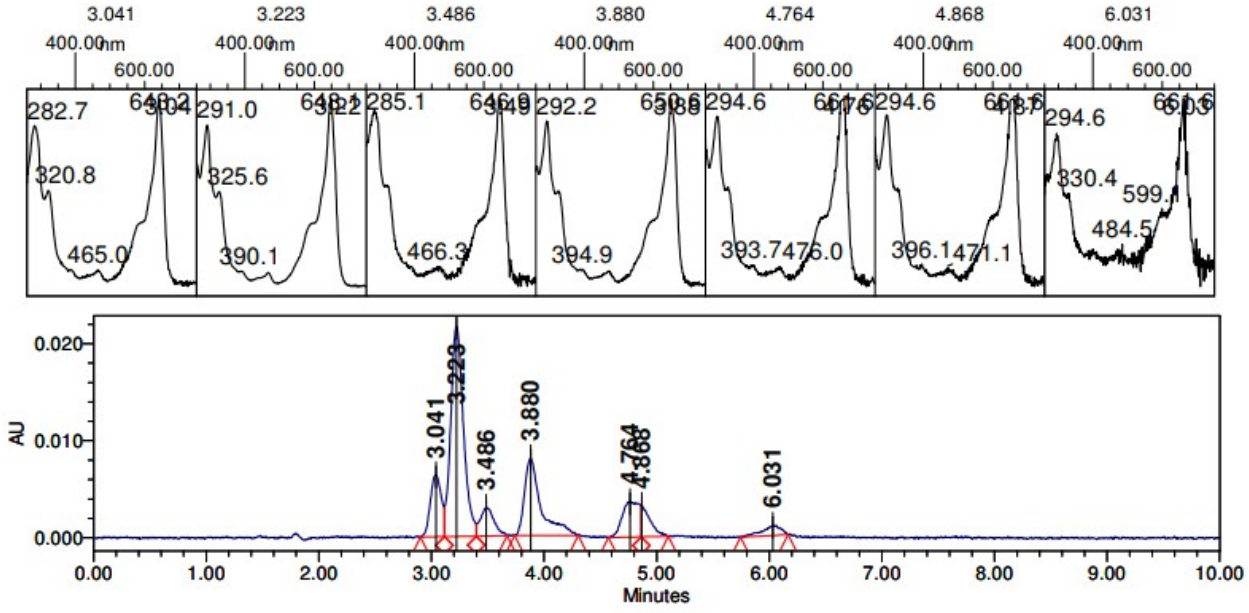

Figure S95: HPLC chromatogram extracted at 650 nm of the 2:1 BCl_3:$B(OPh)_3$ reaction to form BsubNc after 3 hours at reflux. HPLC run conducted with C18 functionalized silica as the stationary phase and 80:20 ACN:DMF (V:V) as the mobile phase.

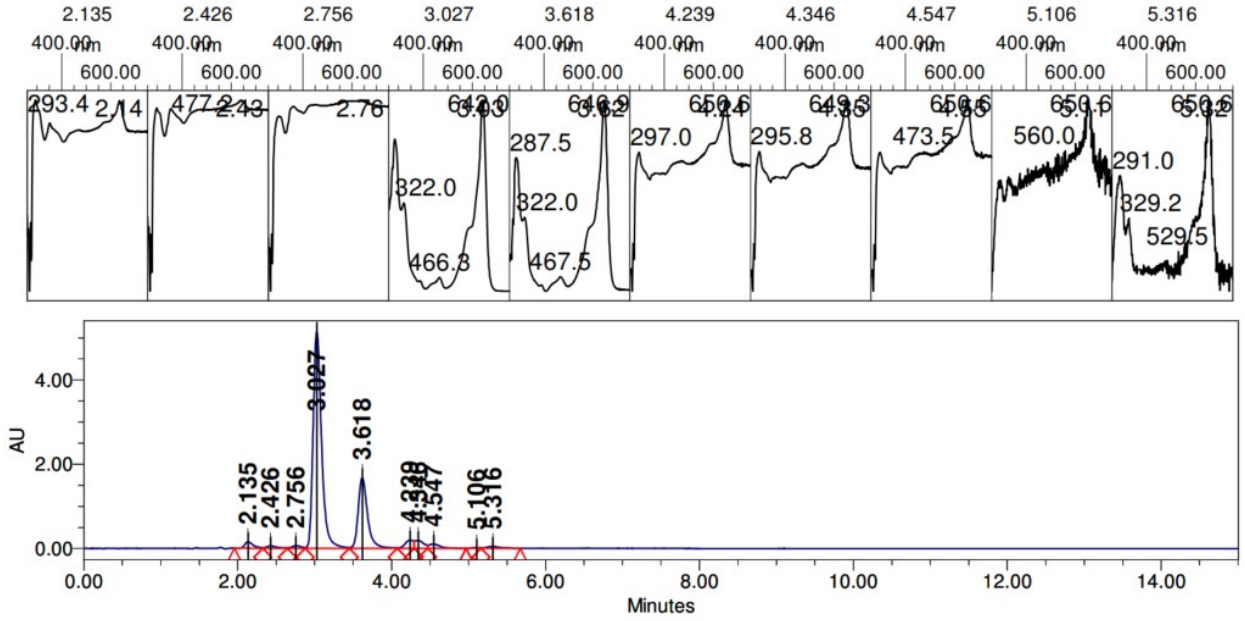

Figure S96: HPLC chromatogram extracted between 600 nm and 700 nm of the 1:2 BBr_3:$B(OPh)_3$ reaction to form BsubNc after 2 hours at reflux. HPLC run conducted with C18 functionalized silica as the stationary phase and 80:20 ACN:DMF (V:V) as the mobile phase.

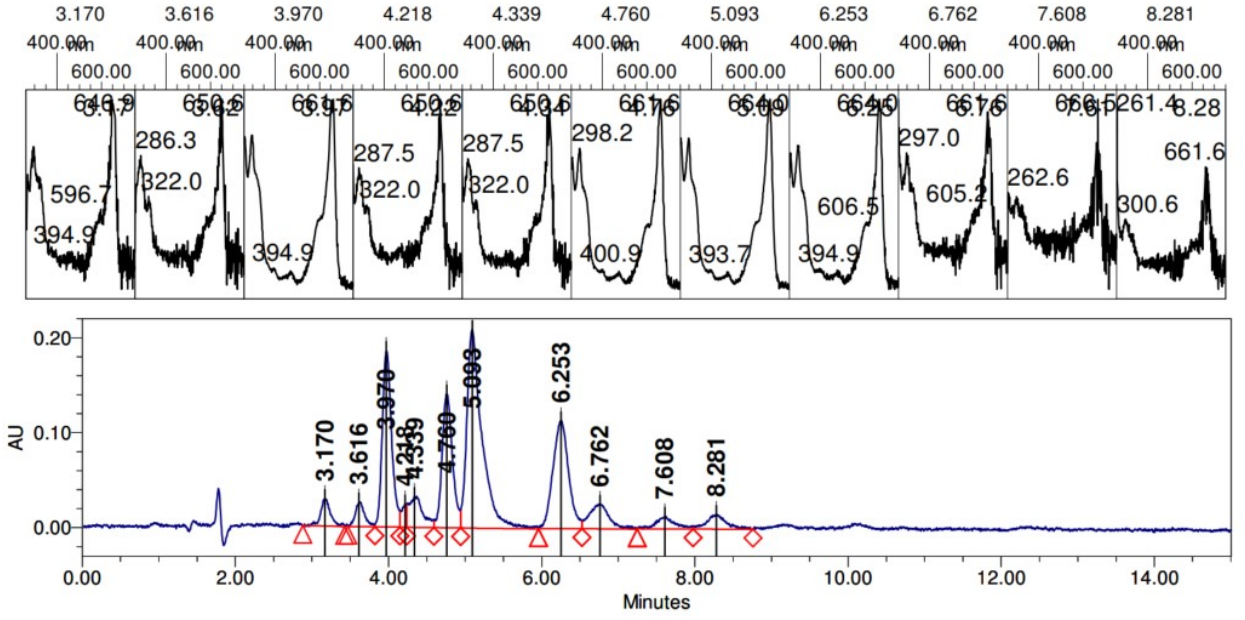

Figure S97: HPLC chromatogram extracted between 600 nm and 700 nm of the 1:1 BBr_3:$B(OPh)_3$ reaction to form BsubNc after 2 hours at reflux. HPLC run conducted with C18 functionalized silica as the stationary phase and 80:20 ACN:DMF (V:V) as the mobile phase.

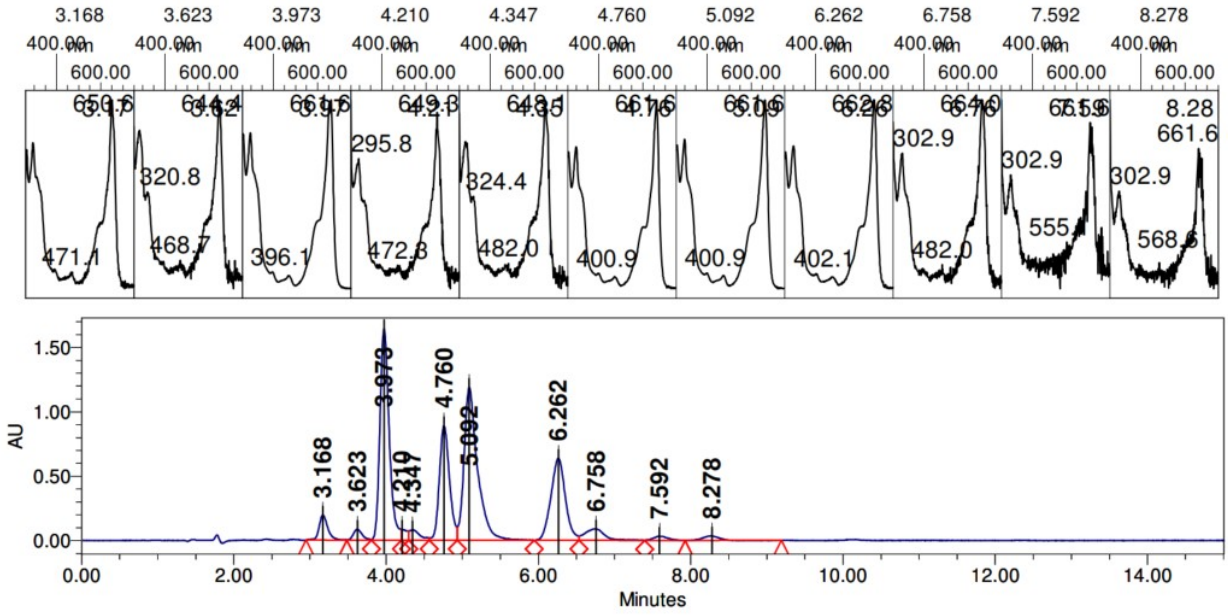

Figure S98: HPLC chromatogram extracted between 600 nm and 700 nm of the 2:1 BBr_3:$B(OPh)_3$ reaction to form BsubNc after 2 hours at reflux. HPLC run conducted with C18 functionalized silica as the stationary phase and 80:20 ACN:DMF (V:V) as the mobile phase.

Industrially Relevant Borate Synthesis

Toluene Process

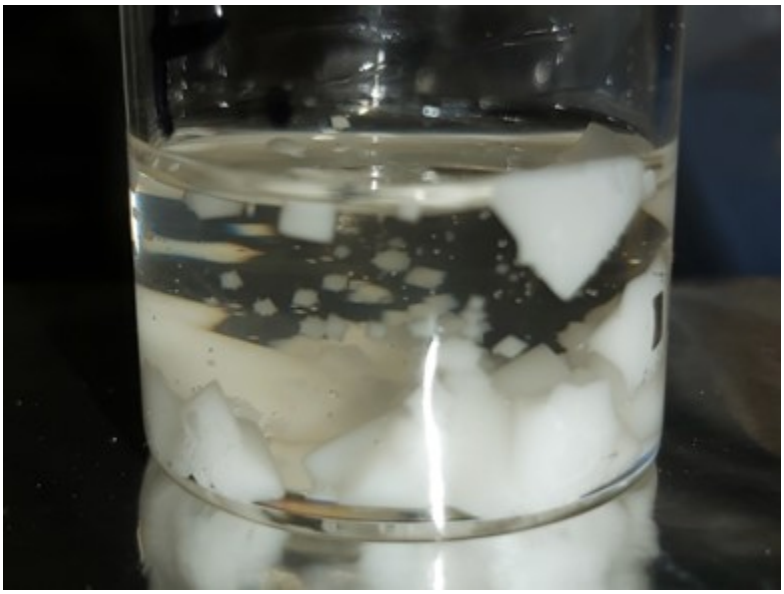

Figure S99: Crystallization of $B(OPh)_3$ from the toluene process.

Figure S100: Triphenyl borate from the toluene process (left) and xylene process a couple weeks after it was made (right).

NMR Spectroscopy

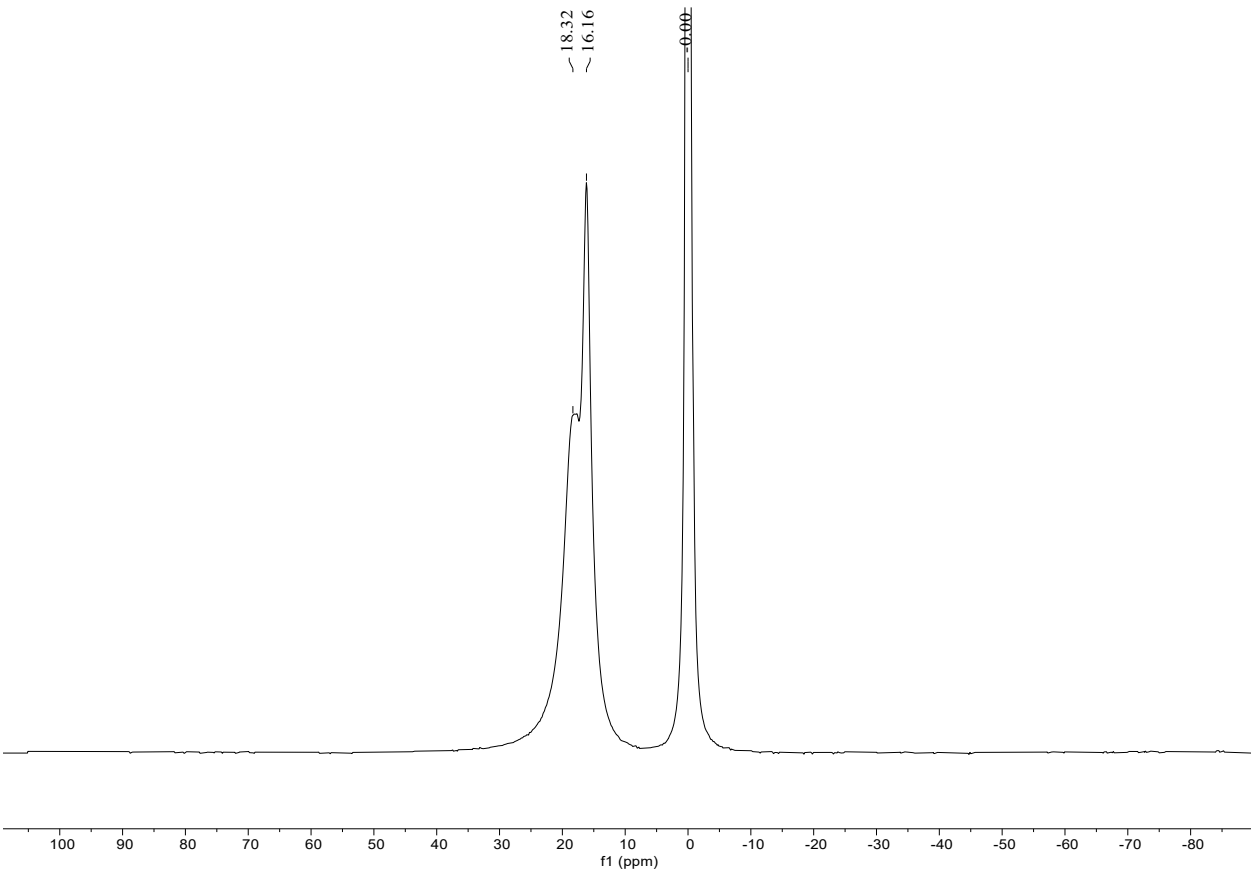

Figure S101: ^{11}B NMR spectrum (400 MHz) of $B(OPh)_3$ from the xylenes process in $CDCl_3$. Referenced to $BF_3{\cdot}OEt_2$ (δ = 0.00 ppm).

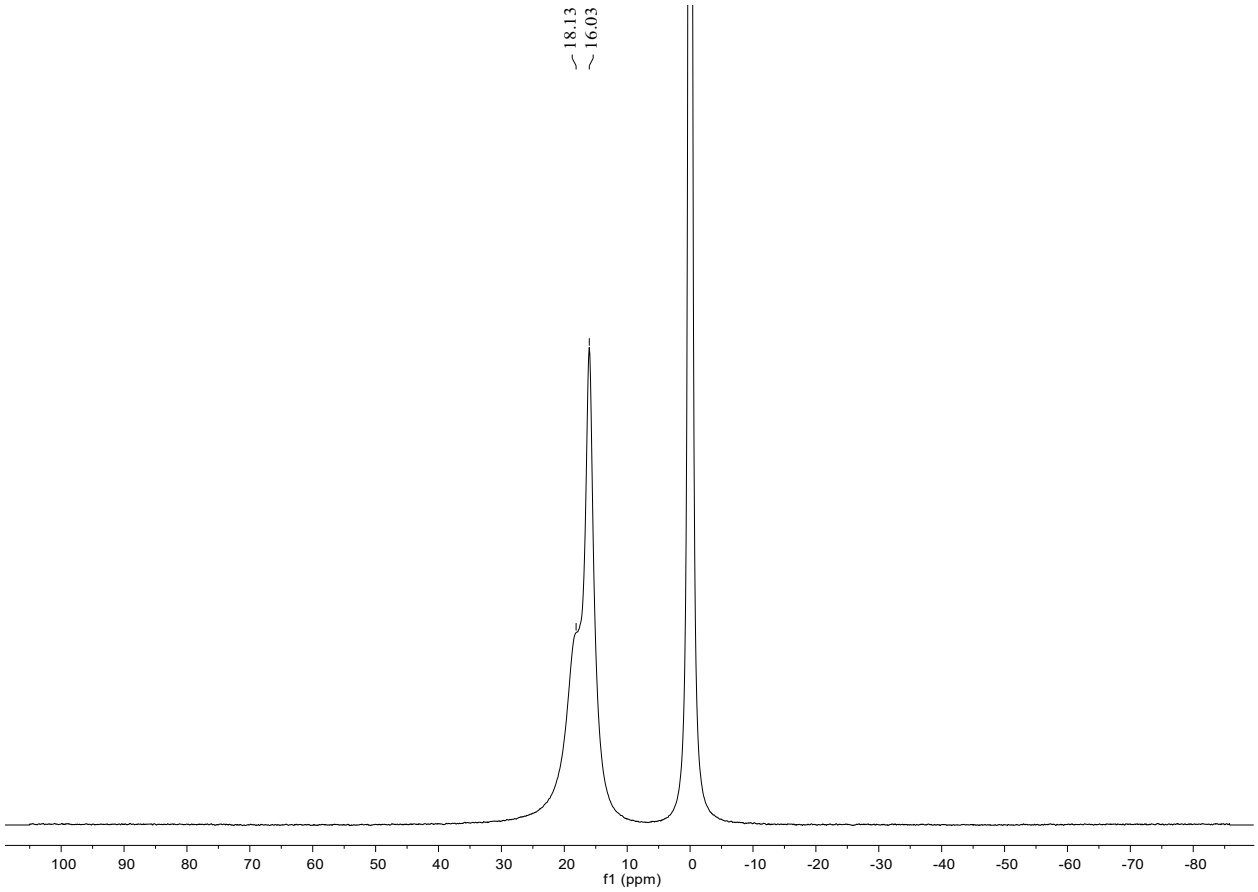

Figure S102: ^{11}B NMR spectrum (400 MHz) of $B(OPh)_3$ from the toluene process in $CDCl_3$. Referenced to $BF_3{\cdot}OEt_2$ (δ = 0.00 ppm).

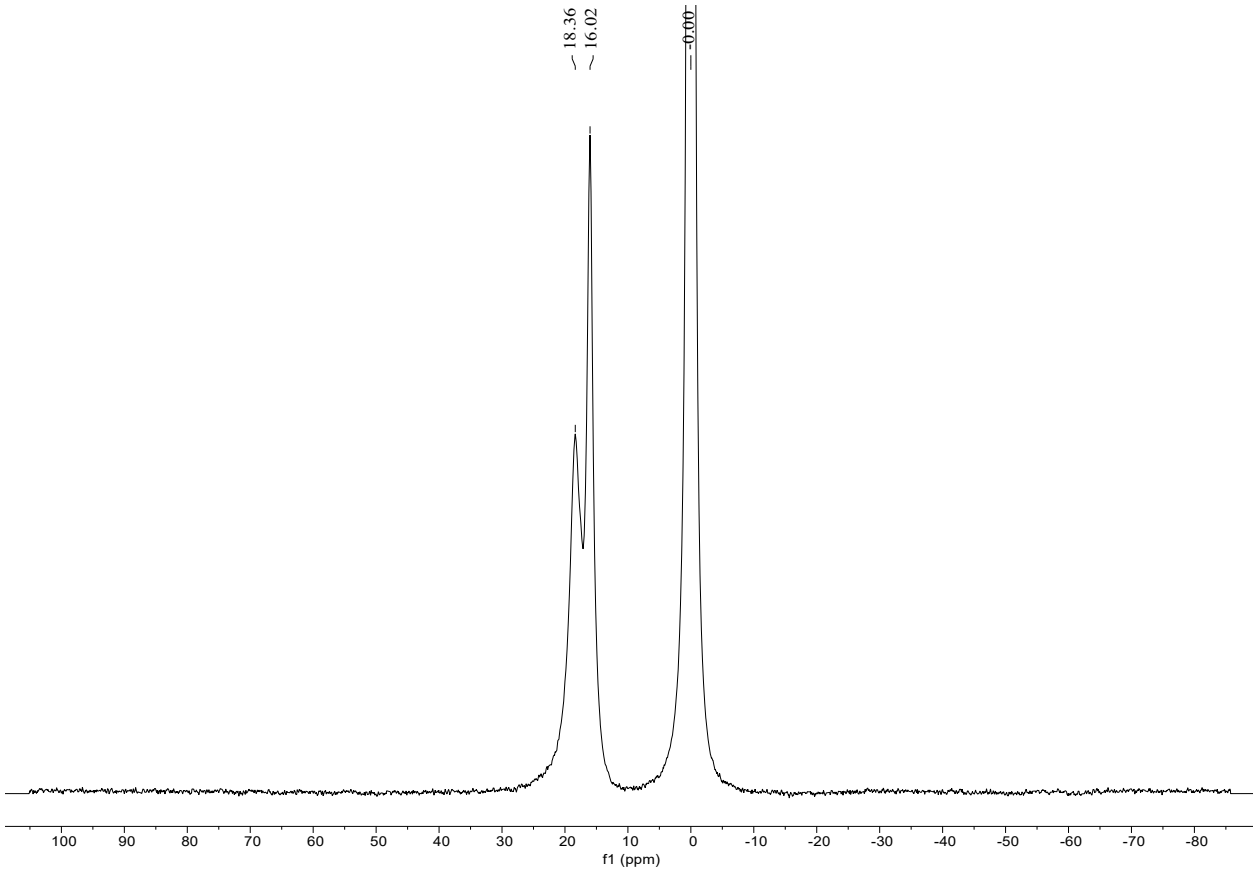

Figure S103: ^{11}B NMR spectrum (400 MHz) of $B(OPh)_3$ from a commercial supplier in $CDCl_3$. Referenced to $BF_3{\cdot}OEt_2$ (δ = 0.00 ppm).

F_5-BsubNc Synthesis Using $B(OC_6F_5)_3$ from the Toluene Process

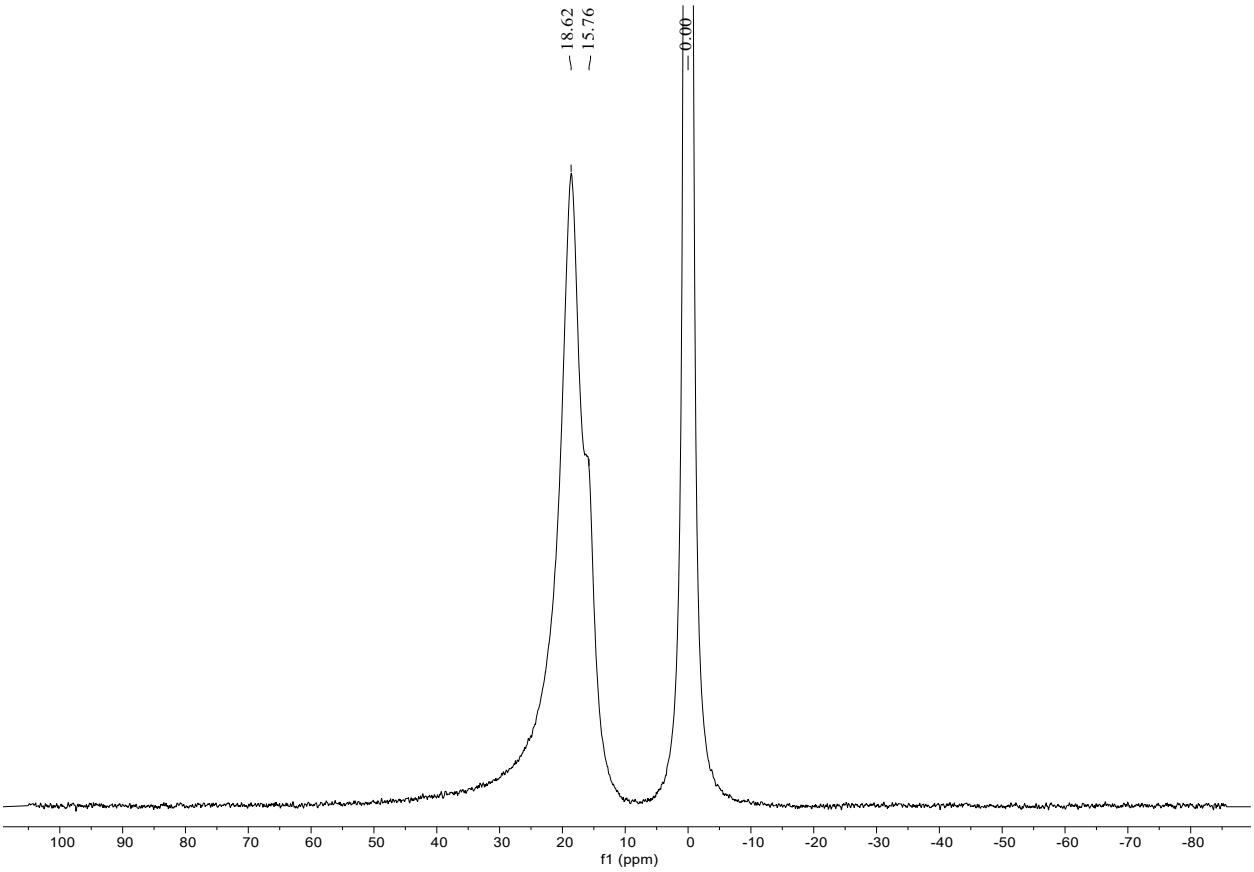

Figure S104: ^{11}B NMR spectrum (400 MHz) of $B(OC_6F_5)_3$ in $CDCl_3$ from the toluene method used for F_5-BsubNc synthesis. Referenced to $BF_3{\cdot}OEt_2$ (δ = 0.00 ppm).

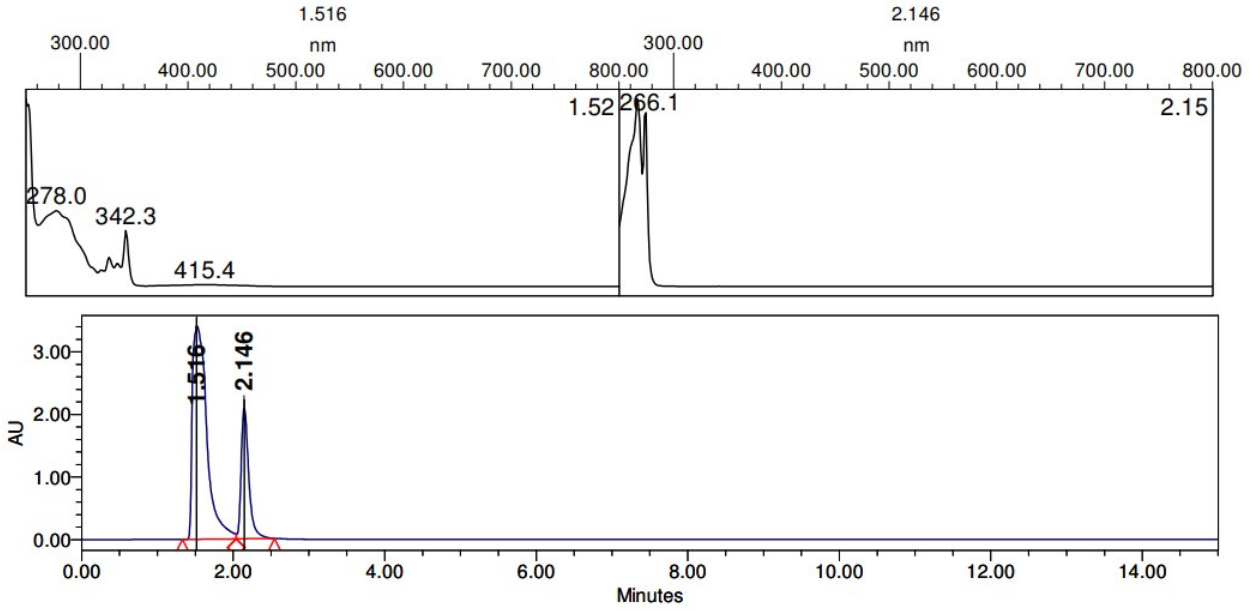

Figure S105: HPLC chromatogram at T=0 h, max plot (260 nm and 750 nm). Conducted with C18 functionalized silica as the stationary phase and 80:20 ACN:DMF (V:V) as the mobile phase.

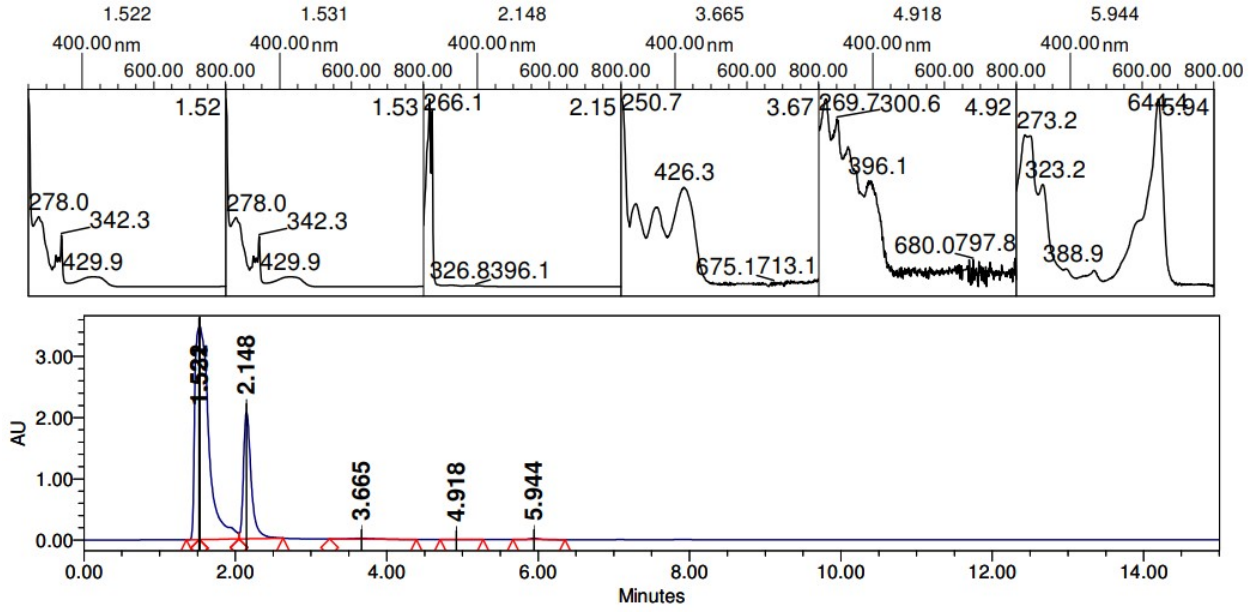

Figure S106: HPLC chromatogram at T=0.5 h, max plot (260 nm and 750 nm). Conducted with C18 functionalized silica as the stationary phase and 80:20 ACN:DMF (V:V) as the mobile phase.

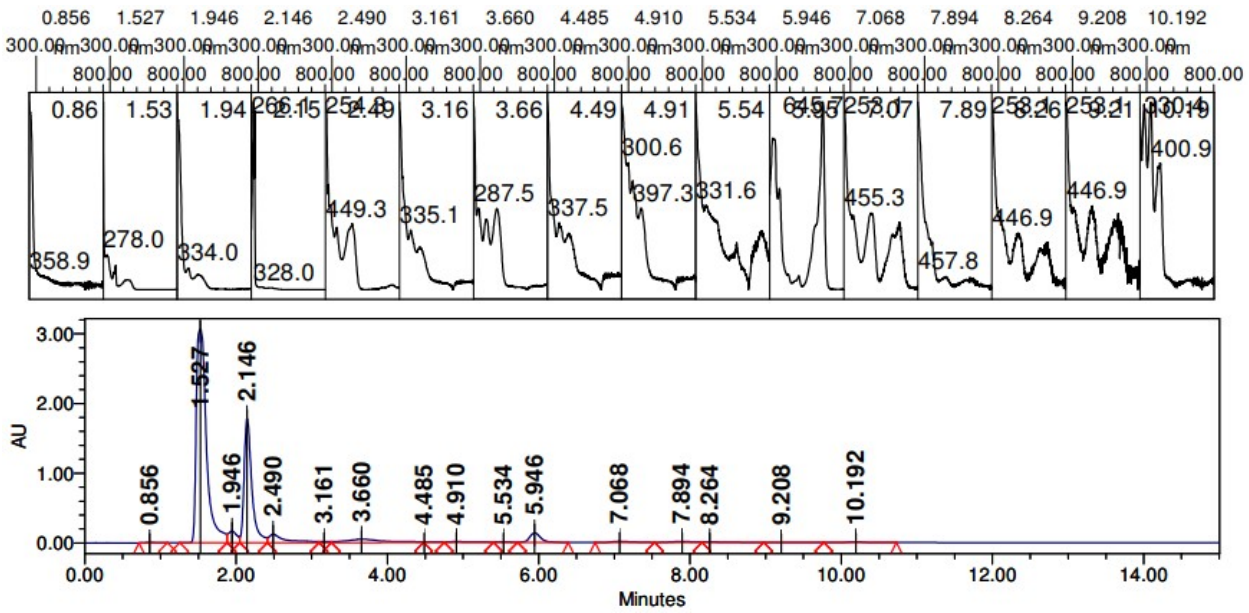

Figure S107: HPLC chromatogram at T=0.75 h, max plot (260 nm and 750 nm). Conducted with C18 functionalized silica as the stationary phase and 80:20 ACN:DMF (V:V) as the mobile phase.

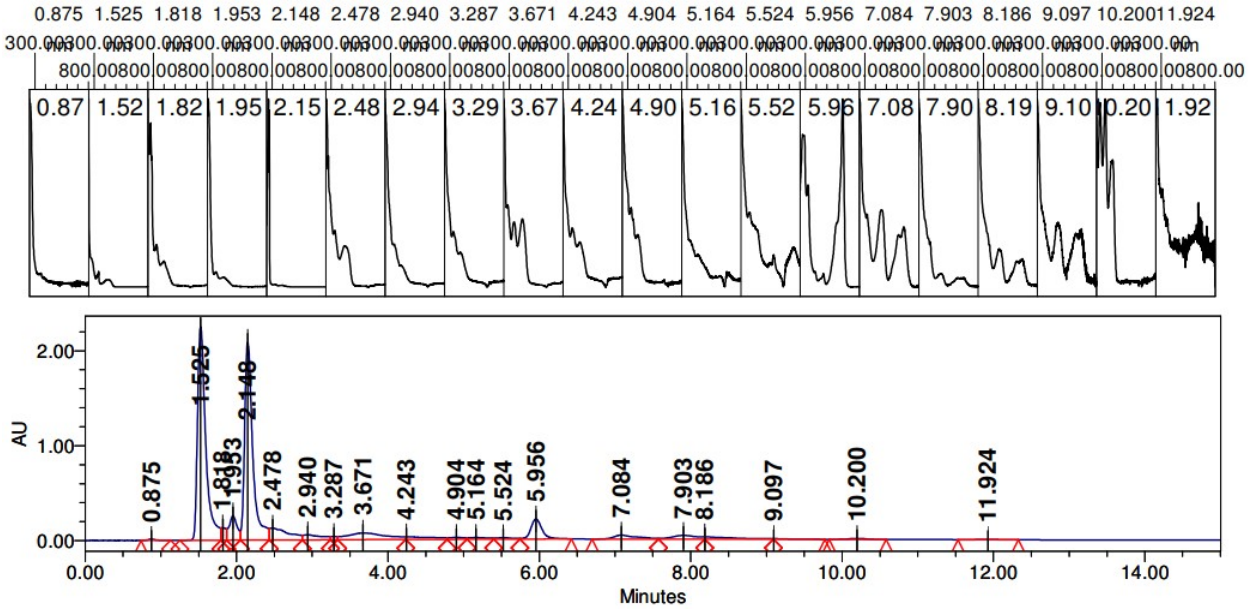

Figure S108: HPLC chromatogram at T=1.0 h, max plot (260 nm and 750 nm). Conducted with C18 functionalized silica as the stationary phase and 80:20 ACN:DMF (V:V) as the mobile phase.

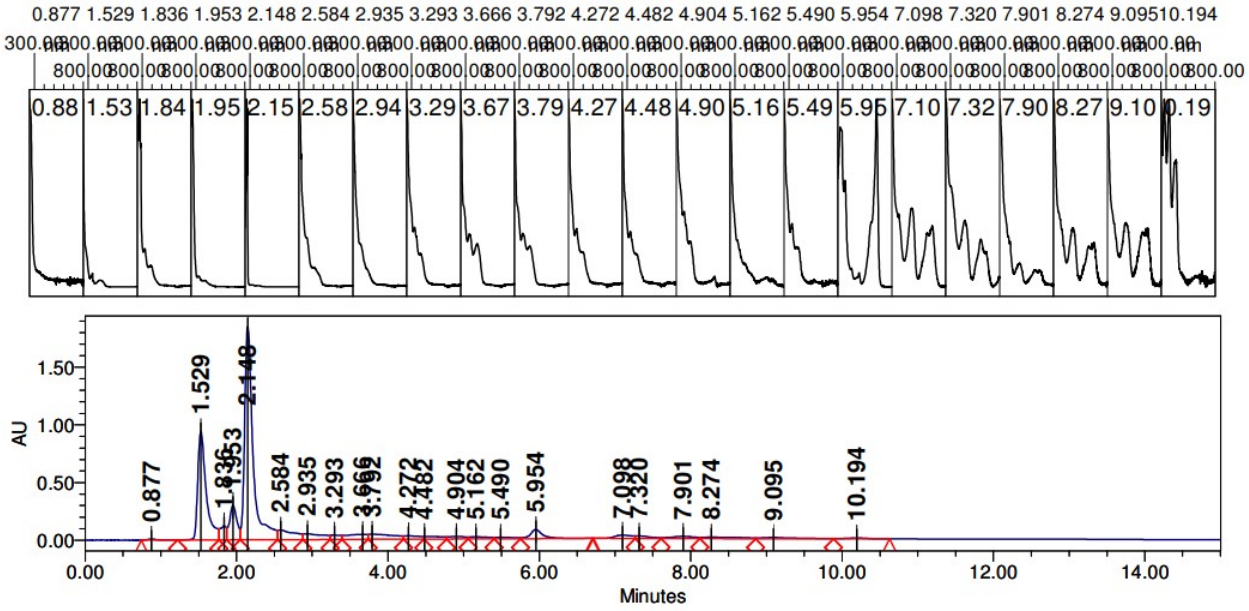

Figure S109: HPLC chromatogram at T=1.25 h, max plot (260 nm and 750 nm). Conducted with C18 functionalized silica as the stationary phase and 80:20 ACN:DMF (V:V) as the mobile phase.

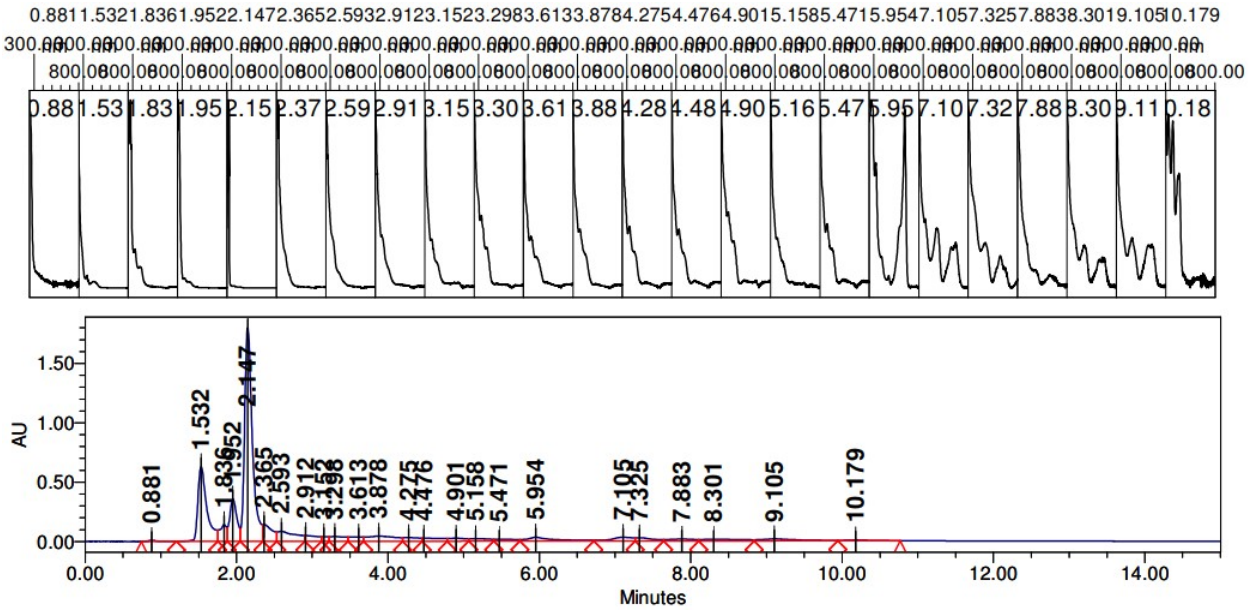

Figure S110: HPLC chromatogram at T=1.5 h, max plot (260 nm and 750 nm). Conducted with C18 functionalized silica as the stationary phase and 80:20 ACN:DMF (V:V) as the mobile phase.

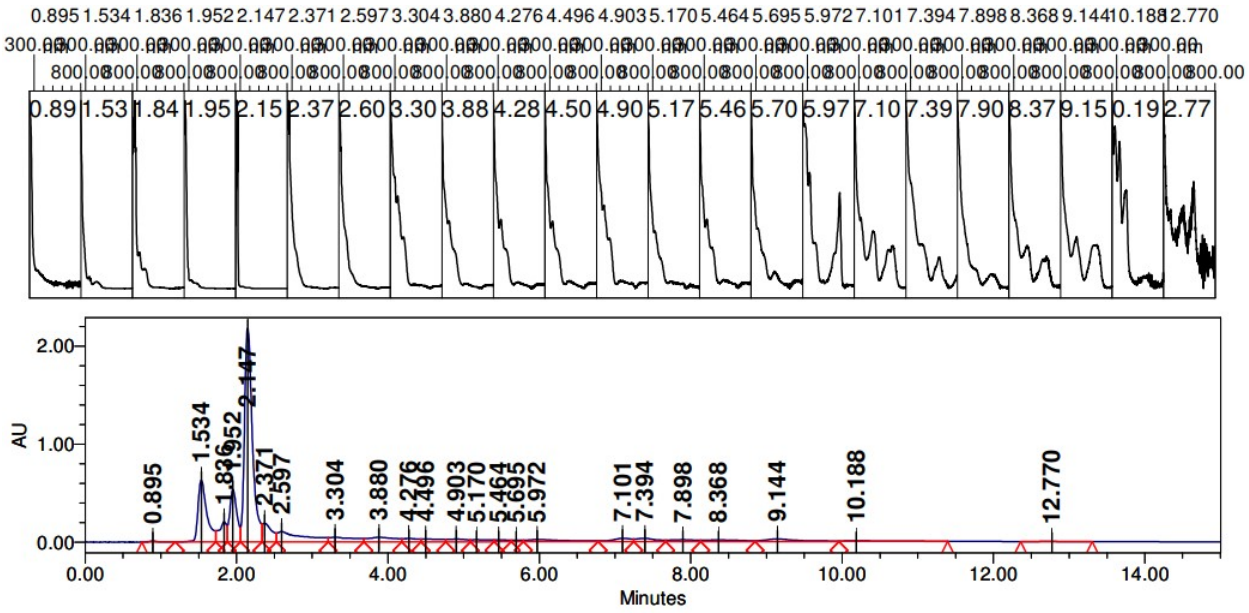

Figure S111: HPLC chromatogram at T=1.75 h, max plot (260 nm and 750 nm). Conducted with C18 functionalized silica as the stationary phase and 80:20 ACN:DMF (V:V) as the mobile phase.

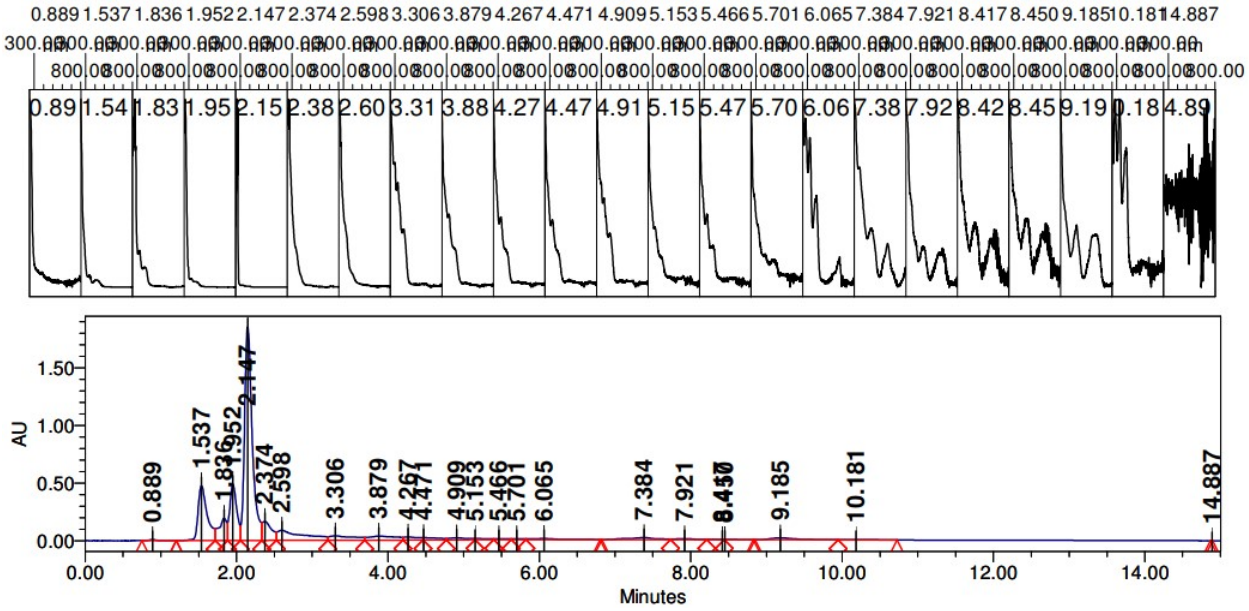

Figure S112: HPLC chromatogram at T=2.0 h, max plot (260 nm and 750 nm). Conducted with C18 functionalized silica as the stationary phase and 80:20 ACN:DMF (V:V) as the mobile phase.

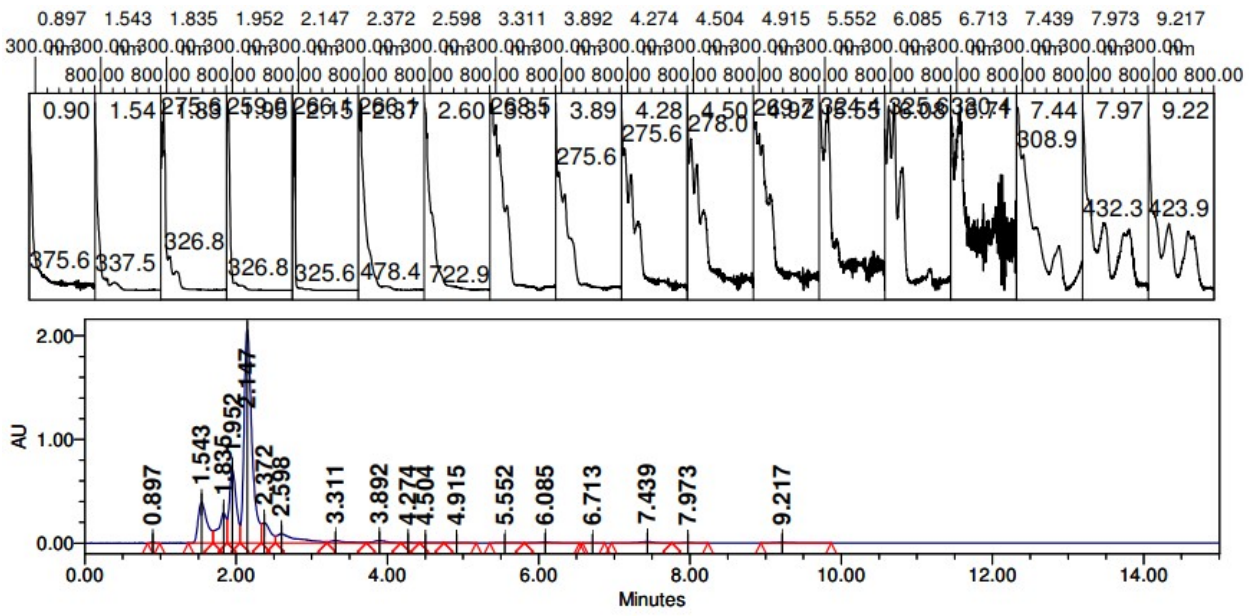

Figure S113: HPLC chromatogram at T=3.0 h, max plot (260 nm and 750 nm). Conducted with C18 functionalized silica as the stationary phase and 80:20 ACN:DMF (V:V) as the mobile phase.

Single Crystal X-Ray Diffraction

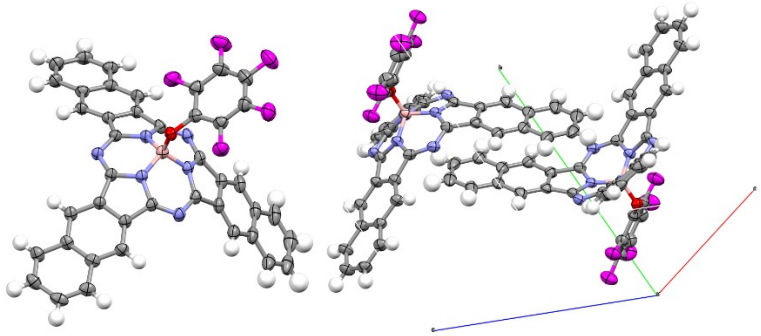

Table S1 Crystal data and structure refinement for F_5-BsubNc (CCDC 2321223).

Identification code	d20154_a_sq
Empirical formula	C42 H18 B F5 N6 O
Formula weight	728.43
Temperature	150(2) K
Wavelength	1.54178 Å
Crystal system	Triclinic
Space group	P-1
Unit cell dimensions	a = 8.2507(3) Å a= 91.155(2)°.
	b = 14.9183(5) Å b= 94.457(2)°.
	c = 16.3974(6) Å g = 92.624(2)°.
Volume	2009.51(12) $Å^3$
Z	2
Density (calculated)	1.204 Mg/m^3
Absorption coefficient	0.762 mm^{-1}
F(000)	740
Crystal size	0.200 x 0.160 x 0.030 mm^3
Theta range for data collection	2.704 to 68.486°.
Index ranges	-9<=h<=9, -16<=k<=17, 0<=l<=19
Reflections collected	78098
Independent reflections	7318 [R(int) = 0.145]
Completeness to theta = 67.679°	99.8 %
Absorption correction	Semi-empirical from equivalents
Max. and min. transmission	0.7530 and 0.3694
Refinement method	Full-matrix least-squares on F^2
Data / restraints / parameters	7318 / 0 / 496
Goodness-of-fit on F^2	1.074
Final R indices [I>2sigma(I)]	R1 = 0.0769, wR2 = 0.2147
R indices (all data)	R1 = 0.0958, wR2 = 0.2292
Extinction coefficient	n/a
Largest diff. peak and hole	0.372 and -0.382 $e.Å^{-3}$

Table S2 Atomic coordinates (x 10^4) and equivalent isotropic displacement parameters ($Å^2$x 10^3) for F_5-BsubNc U(eq) is defined as one third of the trace of the orthogonalized U^{ij} tensor.

x	y	z	U(eq)	
F(1)	5992(3)	2509(2)	862(1)	62(1)
F(2)	3241(3)	2595(2)	-104(1)	78(1)
F(3)	436(3)	1770(2)	310(2)	81(1)
F(4)	430(2)	839(2)	1726(1)	66(1)
F(5)	3154(2)	810(1)	2738(1)	54(1)
O(1)	6033(2)	1611(1)	2336(1)	35(1)
N(1)	7898(3)	2003(1)	3508(1)	32(1)
N(2)	10330(3)	2430(2)	2896(1)	33(1)
N(3)	7803(3)	3022(1)	2433(1)	32(1)
N(4)	5871(3)	4155(2)	2420(2)	37(1)
N(5)	5610(3)	2892(2)	3278(1)	32(1)
N(6)	6042(3)	2138(2)	4538(2)	37(1)
C(1)	7406(3)	1825(2)	4266(2)	32(1)
C(2)	8814(3)	1474(2)	4724(2)	35(1)
C(3)	9009(4)	1120(2)	5487(2)	38(1)
C(4)	10562(4)	859(2)	5784(2)	38(1)
C(5)	10836(4)	441(2)	6554(2)	44(1)
C(6)	12329(4)	188(2)	6827(2)	47(1)
C(7)	13678(4)	338(2)	6356(2)	48(1)
C(8)	13487(4)	733(2)	5615(2)	43(1)
C(9)	11923(3)	996(2)	5301(2)	36(1)
C(10)	11706(3)	1372(2)	4522(2)	37(1)
C(11)	10167(3)	1589(2)	4225(2)	33(1)
C(12)	9543(3)	1986(2)	3468(2)	32(1)
C(13)	9444(3)	2974(2)	2409(2)	34(1)
C(14)	9973(3)	3738(2)	1935(2)	34(1)
C(15)	11465(3)	4011(2)	1685(2)	37(1)
C(16)	11594(4)	4805(2)	1236(2)	39(1)
C(17)	13097(4)	5113(2)	945(2)	45(1)
C(18)	13203(4)	5876(2)	509(2)	50(1)
C(19)	11826(4)	6390(2)	339(2)	48(1)
C(20)	10371(4)	6121(2)	610(2)	43(1)
C(21)	10199(4)	5334(2)	1074(2)	38(1)
C(22)	8688(4)	5057(2)	1364(2)	38(1)
C(23)	8574(3)	4272(2)	1776(2)	35(1)
C(24)	7237(3)	3834(2)	2170(2)	35(1)
C(25)	5162(3)	3720(2)	3019(2)	36(1)
C(26)	4184(3)	4068(2)	3645(2)	40(1)
C(27)	3442(3)	4883(2)	3729(2)	45(1)
C(28)	2743(4)	5076(2)	4463(2)	50(1)

C(29)	1957(4)	5893(2)	4579(3)	60(1)
C(30)	1252(4)	6064(3)	5284(3)	66(1)
C(31)	1319(4)	5456(3)	5923(3)	67(1)
C(32)	2106(4)	4678(3)	5853(2)	59(1)
C(33)	2818(4)	4460(2)	5118(2)	49(1)
C(34)	3588(4)	3640(2)	5028(2)	46(1)
C(35)	4243(3)	3447(2)	4300(2)	38(1)
C(36)	5251(3)	2730(2)	4064(2)	36(1)
C(37)	4655(4)	1679(2)	1843(2)	38(1)
C(38)	4616(4)	2122(2)	1103(2)	47(1)
C(39)	3215(5)	2158(2)	596(2)	53(1)
C(40)	1801(4)	1732(2)	808(2)	55(1)
C(41)	1805(4)	1276(2)	1527(2)	49(1)
C(42)	3187(4)	1260(2)	2032(2)	42(1)
B(1)	6775(4)	2345(2)	2845(2)	33(1)

Table S3 Bond lengths [Å] and angles [°] for F_5-BsubNc

F(1)-C(38)	1.340(4)
F(2)-C(39)	1.333(4)
F(3)-C(40)	1.343(4)
F(4)-C(41)	1.348(4)
F(5)-C(42)	1.351(3)
O(1)-C(37)	1.352(3)
O(1)-B(1)	1.447(4)
N(1)-C(12)	1.365(3)
N(1)-C(1)	1.365(3)
N(1)-B(1)	1.486(4)
N(2)-C(12)	1.349(3)
N(2)-C(13)	1.349(3)
N(3)-C(13)	1.362(4)
N(3)-C(24)	1.383(3)
N(3)-B(1)	1.496(4)
N(4)-C(24)	1.335(4)
N(4)-C(25)	1.343(4)
N(5)-C(36)	1.369(4)
N(5)-C(25)	1.373(3)
N(5)-B(1)	1.499(4)
N(6)-C(1)	1.342(4)
N(6)-C(36)	1.345(4)
C(1)-C(2)	1.457(4)
C(2)-C(3)	1.369(4)
C(2)-C(11)	1.441(4)
C(3)-C(4)	1.409(4)
C(3)-H(3A)	0.9500
C(4)-C(5)	1.428(4)
C(4)-C(9)	1.433(4)
C(5)-C(6)	1.350(5)
C(5)-H(5A)	0.9500
C(6)-C(7)	1.415(5)
C(6)-H(6A)	0.9500
C(7)-C(8)	1.362(4)
C(7)-H(7A)	0.9500
C(8)-C(9)	1.427(4)
C(8)-H(8A)	0.9500
C(9)-C(10)	1.407(4)
C(10)-C(11)	1.379(4)
C(10)-H(10A)	0.9500
C(11)-C(12)	1.454(4)
C(13)-C(14)	1.462(4)
C(14)-C(15)	1.374(4)

C(14)-C(23)	1.443(4)
C(15)-C(16)	1.412(4)
C(15)-H(15A)	0.9500
C(16)-C(17)	1.424(4)
C(16)-C(21)	1.436(4)
C(17)-C(18)	1.360(4)
C(17)-H(17A)	0.9500
C(18)-C(19)	1.413(5)
C(18)-H(18A)	0.9500
C(19)-C(20)	1.358(4)
C(19)-H(19A)	0.9500
C(20)-C(21)	1.420(4)
C(20)-H(20A)	0.9500
C(21)-C(22)	1.415(4)
C(22)-C(23)	1.366(4)
C(22)-H(22A)	0.9500
C(23)-C(24)	1.458(4)
C(25)-C(26)	1.457(4)
C(26)-C(27)	1.396(4)
C(26)-C(35)	1.431(4)
C(27)-C(28)	1.405(5)
C(27)-H(27A)	0.9500
C(28)-C(29)	1.422(5)
C(28)-C(33)	1.428(5)
C(29)-C(30)	1.358(6)
C(29)-H(29A)	0.9500
C(30)-C(31)	1.400(6)
C(30)-H(30A)	0.9500
C(31)-C(32)	1.364(6)
C(31)-H(31A)	0.9500
C(32)-C(33)	1.419(5)
C(32)-H(32A)	0.9500
C(33)-C(34)	1.413(5)
C(34)-C(35)	1.378(4)
C(34)-H(34A)	0.9500
C(35)-C(36)	1.450(4)
C(37)-C(38)	1.393(4)
C(37)-C(42)	1.396(4)
C(38)-C(39)	1.373(5)
C(39)-C(40)	1.376(5)
C(40)-C(41)	1.371(5)
C(41)-C(42)	1.358(5)

C(37)-O(1)-B(1)	123.4(2)
C(12)-N(1)-C(1)	113.5(2)
C(12)-N(1)-B(1)	123.6(2)

C(1)-N(1)-B(1)	122.0(2)
C(12)-N(2)-C(13)	116.8(2)
C(13)-N(3)-C(24)	113.0(2)
C(13)-N(3)-B(1)	123.2(2)
C(24)-N(3)-B(1)	122.9(2)
C(24)-N(4)-C(25)	117.6(2)
C(36)-N(5)-C(25)	112.9(2)
C(36)-N(5)-B(1)	122.3(2)
C(25)-N(5)-B(1)	122.6(2)
C(1)-N(6)-C(36)	116.8(2)
N(6)-C(1)-N(1)	122.9(2)
N(6)-C(1)-C(2)	129.6(3)
N(1)-C(1)-C(2)	105.6(2)
C(3)-C(2)-C(11)	121.2(3)
C(3)-C(2)-C(1)	132.0(3)
C(11)-C(2)-C(1)	106.8(2)
C(2)-C(3)-C(4)	119.1(3)
C(2)-C(3)-H(3A)	120.5
C(4)-C(3)-H(3A)	120.5
C(3)-C(4)-C(5)	122.1(3)
C(3)-C(4)-C(9)	120.1(3)
C(5)-C(4)-C(9)	117.8(3)
C(6)-C(5)-C(4)	121.4(3)
C(6)-C(5)-H(5A)	119.3
C(4)-C(5)-H(5A)	119.3
C(5)-C(6)-C(7)	120.7(3)
C(5)-C(6)-H(6A)	119.6
C(7)-C(6)-H(6A)	119.6
C(8)-C(7)-C(6)	120.4(3)
C(8)-C(7)-H(7A)	119.8
C(6)-C(7)-H(7A)	119.8
C(7)-C(8)-C(9)	120.5(3)
C(7)-C(8)-H(8A)	119.8
C(9)-C(8)-H(8A)	119.8
C(10)-C(9)-C(8)	120.8(3)
C(10)-C(9)-C(4)	120.1(3)
C(8)-C(9)-C(4)	119.1(3)
C(11)-C(10)-C(9)	119.2(3)
C(11)-C(10)-H(10A)	120.4
C(9)-C(10)-H(10A)	120.4
C(10)-C(11)-C(2)	120.2(2)
C(10)-C(11)-C(12)	132.9(3)
C(2)-C(11)-C(12)	106.8(2)
N(2)-C(12)-N(1)	122.4(2)
N(2)-C(12)-C(11)	130.4(3)
N(1)-C(12)-C(11)	105.8(2)

N(2)-C(13)-N(3)	122.6(2)
N(2)-C(13)-C(14)	129.8(3)
N(3)-C(13)-C(14)	106.1(2)
C(15)-C(14)-C(23)	120.8(2)
C(15)-C(14)-C(13)	132.3(3)
C(23)-C(14)-C(13)	106.8(2)
C(14)-C(15)-C(16)	118.9(3)
C(14)-C(15)-H(15A)	120.6
C(16)-C(15)-H(15A)	120.6
C(15)-C(16)-C(17)	121.5(3)
C(15)-C(16)-C(21)	120.3(3)
C(17)-C(16)-C(21)	118.2(3)
C(18)-C(17)-C(16)	121.0(3)
C(18)-C(17)-H(17A)	119.5
C(16)-C(17)-H(17A)	119.5
C(17)-C(18)-C(19)	120.8(3)
C(17)-C(18)-H(18A)	119.6
C(19)-C(18)-H(18A)	119.6
C(20)-C(19)-C(18)	120.0(3)
C(20)-C(19)-H(19A)	120.0
C(18)-C(19)-H(19A)	120.0
C(19)-C(20)-C(21)	121.4(3)
C(19)-C(20)-H(20A)	119.3
C(21)-C(20)-H(20A)	119.3
C(22)-C(21)-C(20)	121.6(3)
C(22)-C(21)-C(16)	119.8(2)
C(20)-C(21)-C(16)	118.6(3)
C(23)-C(22)-C(21)	119.1(3)
C(23)-C(22)-H(22A)	120.5
C(21)-C(22)-H(22A)	120.5
C(22)-C(23)-C(14)	121.1(3)
C(22)-C(23)-C(24)	131.9(3)
C(14)-C(23)-C(24)	106.9(2)
N(4)-C(24)-N(3)	121.8(2)
N(4)-C(24)-C(23)	131.0(2)
N(3)-C(24)-C(23)	105.6(2)
N(4)-C(25)-N(5)	122.9(3)
N(4)-C(25)-C(26)	129.5(3)
N(5)-C(25)-C(26)	105.6(2)
C(27)-C(26)-C(35)	120.4(3)
C(27)-C(26)-C(25)	131.8(3)
C(35)-C(26)-C(25)	107.3(2)
C(26)-C(27)-C(28)	118.7(3)
C(26)-C(27)-H(27A)	120.7
C(28)-C(27)-H(27A)	120.7
C(27)-C(28)-C(29)	121.1(4)

C(27)-C(28)-C(33)	120.8(3)
C(29)-C(28)-C(33)	118.1(3)
C(30)-C(29)-C(28)	120.7(4)
C(30)-C(29)-H(29A)	119.7
C(28)-C(29)-H(29A)	119.7
C(29)-C(30)-C(31)	121.1(4)
C(29)-C(30)-H(30A)	119.5
C(31)-C(30)-H(30A)	119.5
C(32)-C(31)-C(30)	120.5(4)
C(32)-C(31)-H(31A)	119.8
C(30)-C(31)-H(31A)	119.8
C(31)-C(32)-C(33)	120.3(4)
C(31)-C(32)-H(32A)	119.8
C(33)-C(32)-H(32A)	119.8
C(34)-C(33)-C(32)	120.8(4)
C(34)-C(33)-C(28)	119.9(3)
C(32)-C(33)-C(28)	119.3(3)
C(35)-C(34)-C(33)	119.1(3)
C(35)-C(34)-H(34A)	120.5
C(33)-C(34)-H(34A)	120.5
C(34)-C(35)-C(26)	121.2(3)
C(34)-C(35)-C(36)	131.4(3)
C(26)-C(35)-C(36)	106.9(2)
N(6)-C(36)-N(5)	122.7(3)
N(6)-C(36)-C(35)	129.2(3)
N(5)-C(36)-C(35)	106.3(2)
O(1)-C(37)-C(38)	122.9(3)
O(1)-C(37)-C(42)	121.2(2)
C(38)-C(37)-C(42)	115.8(3)
F(1)-C(38)-C(39)	118.5(3)
F(1)-C(38)-C(37)	119.4(3)
C(39)-C(38)-C(37)	122.1(3)
F(2)-C(39)-C(38)	119.8(3)
F(2)-C(39)-C(40)	120.4(3)
C(38)-C(39)-C(40)	119.8(3)
F(3)-C(40)-C(41)	121.0(3)
F(3)-C(40)-C(39)	119.5(3)
C(41)-C(40)-C(39)	119.5(3)
F(4)-C(41)-C(42)	120.1(3)
F(4)-C(41)-C(40)	119.6(3)
C(42)-C(41)-C(40)	120.3(3)
F(5)-C(42)-C(41)	119.0(3)
F(5)-C(42)-C(37)	118.5(3)
C(41)-C(42)-C(37)	122.4(3)
O(1)-B(1)-N(1)	110.6(2)
O(1)-B(1)-N(3)	116.5(2)

N(1)-B(1)-N(3)	104.0(2)
O(1)-B(1)-N(5)	115.2(2)
N(1)-B(1)-N(5)	104.9(2)
N(3)-B(1)-N(5)	104.4(2)

Table S4 Anisotropic displacement parameters ($Å^2$x 10^3) for F_5-BsubNc. The anisotropic displacement factor exponent takes the form: -2□2[h2 a*2U11 + ... + 2 h k a* b* U12]

U^{11}	U^{22}	U^{33}	U^{23}	U^{13}	U^{12}	
F(1)	62(1)	72(1)	51(1)	16(1)	10(1)	-16(1)
F(2)	88(2)	85(2)	57(1)	32(1)	-9(1)	-8(1)
F(3)	63(1)	94(2)	81(2)	18(1)	-26(1)	3(1)
F(4)	44(1)	79(1)	73(1)	8(1)	5(1)	-12(1)
F(5)	57(1)	58(1)	49(1)	18(1)	6(1)	-5(1)
O(1)	34(1)	32(1)	40(1)	3(1)	1(1)	5(1)
N(1)	31(1)	27(1)	37(1)	8(1)	4(1)	0(1)
N(2)	32(1)	31(1)	36(1)	9(1)	6(1)	4(1)
N(3)	32(1)	29(1)	36(1)	10(1)	3(1)	3(1)
N(4)	31(1)	32(1)	48(1)	8(1)	-1(1)	2(1)
N(5)	28(1)	30(1)	40(1)	5(1)	3(1)	-2(1)
N(6)	31(1)	39(1)	43(1)	8(1)	7(1)	-1(1)
C(1)	29(1)	31(1)	38(1)	4(1)	6(1)	-5(1)
C(2)	33(1)	30(1)	42(2)	10(1)	6(1)	-2(1)
C(3)	43(2)	33(1)	38(2)	10(1)	6(1)	-2(1)
C(4)	47(2)	25(1)	40(2)	6(1)	0(1)	-4(1)
C(5)	57(2)	33(2)	41(2)	10(1)	3(1)	-1(1)
C(6)	67(2)	32(2)	40(2)	7(1)	-9(2)	-2(1)
C(7)	50(2)	37(2)	55(2)	10(1)	-11(2)	3(1)
C(8)	41(2)	36(2)	52(2)	11(1)	-2(1)	0(1)
C(9)	37(2)	26(1)	45(2)	9(1)	0(1)	-1(1)
C(10)	34(1)	30(1)	47(2)	10(1)	3(1)	0(1)
C(11)	35(1)	30(1)	36(1)	7(1)	5(1)	1(1)
C(12)	32(1)	26(1)	39(2)	8(1)	7(1)	2(1)
C(13)	36(1)	33(1)	33(1)	7(1)	4(1)	4(1)
C(14)	35(1)	34(1)	34(1)	8(1)	4(1)	2(1)
C(15)	35(2)	40(2)	36(1)	11(1)	2(1)	3(1)
C(16)	41(2)	40(2)	35(2)	10(1)	3(1)	-3(1)
C(17)	39(2)	54(2)	43(2)	15(1)	6(1)	-5(1)
C(18)	48(2)	53(2)	48(2)	16(2)	9(1)	-6(2)
C(19)	63(2)	41(2)	40(2)	13(1)	8(2)	-6(2)
C(20)	51(2)	40(2)	40(2)	11(1)	5(1)	1(1)
C(21)	44(2)	35(2)	34(1)	6(1)	2(1)	-1(1)

C(22)	39(2)	35(1)	40(2)	11(1)	2(1)	5(1)
C(23)	34(1)	36(1)	36(1)	8(1)	2(1)	3(1)
C(24)	32(1)	31(1)	43(2)	8(1)	-3(1)	2(1)
C(25)	28(1)	33(1)	47(2)	7(1)	0(1)	2(1)
C(26)	29(1)	38(2)	52(2)	2(1)	2(1)	0(1)
C(27)	30(1)	38(2)	65(2)	-4(1)	-2(1)	2(1)
C(28)	25(1)	50(2)	74(2)	-14(2)	1(1)	0(1)
C(29)	34(2)	49(2)	95(3)	-18(2)	4(2)	0(1)
C(30)	37(2)	56(2)	104(3)	-38(2)	4(2)	-2(2)
C(31)	33(2)	80(3)	85(3)	-41(2)	5(2)	-9(2)
C(32)	35(2)	76(2)	64(2)	-26(2)	5(2)	-2(2)
C(33)	26(1)	55(2)	65(2)	-15(2)	4(1)	-4(1)
C(34)	32(2)	54(2)	51(2)	-1(2)	6(1)	2(1)
C(35)	25(1)	37(2)	51(2)	3(1)	4(1)	-2(1)
C(36)	28(1)	36(1)	42(2)	4(1)	5(1)	-3(1)
C(37)	40(2)	36(2)	39(2)	1(1)	3(1)	3(1)
C(38)	47(2)	45(2)	50(2)	9(1)	11(1)	-3(1)
C(39)	64(2)	53(2)	40(2)	11(2)	-2(2)	3(2)
C(40)	49(2)	57(2)	57(2)	6(2)	-9(2)	5(2)
C(41)	39(2)	55(2)	54(2)	5(2)	6(1)	0(1)
C(42)	48(2)	39(2)	40(2)	8(1)	7(1)	3(1)
B(1)	31(2)	29(2)	39(2)	9(1)	4(1)	1(1)

Table S5 Hydrogen coordinates (x 10^4) and isotropic displacement parameters ($Å^2$x 10^3) for F_5-BsubNc.

x	y	z	U(eq)	
H(3A)	8110	1050	5813	45
H(5A)	9950	338	6882	52
H(6A)	12475	-93	7340	57
H(7A)	14723	161	6558	57
H(8A)	14402	834	5306	52
H(10A)	12609	1475	4204	44
H(15A)	12394	3671	1813	44
H(17A)	14040	4780	1057	54
H(18A)	14217	6066	316	60
H(19A)	11917	6922	35	58
H(20A)	9449	6467	486	52
H(22A)	7767	5411	1274	45
H(27A)	3410	5300	3298	54
H(29A)	1925	6323	4159	72
H(30A)	704	6605	5343	79
H(31A)	813	5587	6410	80
H(32A)	2178	4279	6298	71
H(34A)	3653	3229	5462	55

Table S6 Torsion angles [°] for F_5-BsubNc.

C(36)-N(6)-C(1)-N(1)	-7.4(4)
C(36)-N(6)-C(1)-C(2)	154.4(3)
C(12)-N(1)-C(1)-N(6)	152.8(3)
B(1)-N(1)-C(1)-N(6)	-16.7(4)
C(12)-N(1)-C(1)-C(2)	-12.7(3)
B(1)-N(1)-C(1)-C(2)	177.8(2)
N(6)-C(1)-C(2)-C(3)	21.7(5)
N(1)-C(1)-C(2)-C(3)	-174.1(3)
N(6)-C(1)-C(2)-C(11)	-156.1(3)
N(1)-C(1)-C(2)-C(11)	8.1(3)
C(11)-C(2)-C(3)-C(4)	-0.4(4)
C(1)-C(2)-C(3)-C(4)	-177.8(3)
C(2)-C(3)-C(4)-C(5)	-176.6(3)
C(2)-C(3)-C(4)-C(9)	2.2(4)
C(3)-C(4)-C(5)-C(6)	179.4(3)
C(9)-C(4)-C(5)-C(6)	0.6(4)
C(4)-C(5)-C(6)-C(7)	0.5(5)
C(5)-C(6)-C(7)-C(8)	-0.6(5)
C(6)-C(7)-C(8)-C(9)	-0.4(5)
C(7)-C(8)-C(9)-C(10)	-177.4(3)
C(7)-C(8)-C(9)-C(4)	1.5(5)
C(3)-C(4)-C(9)-C(10)	-1.5(4)
C(5)-C(4)-C(9)-C(10)	177.4(3)
C(3)-C(4)-C(9)-C(8)	179.6(3)
C(5)-C(4)-C(9)-C(8)	-1.6(4)
C(8)-C(9)-C(10)-C(11)	177.7(3)
C(4)-C(9)-C(10)-C(11)	-1.2(4)
C(9)-C(10)-C(11)-C(2)	3.1(4)
C(9)-C(10)-C(11)-C(12)	179.3(3)
C(3)-C(2)-C(11)-C(10)	-2.4(4)
C(1)-C(2)-C(11)-C(10)	175.7(3)
C(3)-C(2)-C(11)-C(12)	-179.4(3)
C(1)-C(2)-C(11)-C(12)	-1.4(3)
C(13)-N(2)-C(12)-N(1)	6.6(4)
C(13)-N(2)-C(12)-C(11)	-158.4(3)
C(1)-N(1)-C(12)-N(2)	-156.4(3)
B(1)-N(1)-C(12)-N(2)	12.9(4)
C(1)-N(1)-C(12)-C(11)	11.9(3)
B(1)-N(1)-C(12)-C(11)	-178.8(2)
C(10)-C(11)-C(12)-N(2)	-15.5(5)
C(2)-C(11)-C(12)-N(2)	161.1(3)
C(10)-C(11)-C(12)-N(1)	177.6(3)
C(2)-C(11)-C(12)-N(1)	-5.9(3)

C(12)-N(2)-C(13)-N(3)	-5.8(4)
C(12)-N(2)-C(13)-C(14)	157.9(3)
C(24)-N(3)-C(13)-N(2)	154.6(3)
B(1)-N(3)-C(13)-N(2)	-14.5(4)
C(24)-N(3)-C(13)-C(14)	-12.5(3)
B(1)-N(3)-C(13)-C(14)	178.5(3)
N(2)-C(13)-C(14)-C(15)	17.2(5)
N(3)-C(13)-C(14)-C(15)	-177.0(3)
N(2)-C(13)-C(14)-C(23)	-159.4(3)
N(3)-C(13)-C(14)-C(23)	6.5(3)
C(23)-C(14)-C(15)-C(16)	-2.8(4)
C(13)-C(14)-C(15)-C(16)	-178.9(3)
C(14)-C(15)-C(16)-C(17)	-178.7(3)
C(14)-C(15)-C(16)-C(21)	2.5(4)
C(15)-C(16)-C(17)-C(18)	179.6(3)
C(21)-C(16)-C(17)-C(18)	-1.5(5)
C(16)-C(17)-C(18)-C(19)	0.6(5)
C(17)-C(18)-C(19)-C(20)	-0.2(5)
C(18)-C(19)-C(20)-C(21)	0.8(5)
C(19)-C(20)-C(21)-C(22)	179.4(3)
C(19)-C(20)-C(21)-C(16)	-1.7(5)
C(15)-C(16)-C(21)-C(22)	-0.2(4)
C(17)-C(16)-C(21)-C(22)	-179.1(3)
C(15)-C(16)-C(21)-C(20)	-179.1(3)
C(17)-C(16)-C(21)-C(20)	2.1(4)
C(20)-C(21)-C(22)-C(23)	177.0(3)
C(16)-C(21)-C(22)-C(23)	-1.8(4)
C(21)-C(22)-C(23)-C(14)	1.5(4)
C(21)-C(22)-C(23)-C(24)	177.2(3)
C(15)-C(14)-C(23)-C(22)	0.8(5)
C(13)-C(14)-C(23)-C(22)	177.8(3)
C(15)-C(14)-C(23)-C(24)	-175.8(3)
C(13)-C(14)-C(23)-C(24)	1.2(3)
C(25)-N(4)-C(24)-N(3)	8.2(4)
C(25)-N(4)-C(24)-C(23)	-155.6(3)
C(13)-N(3)-C(24)-N(4)	-154.2(3)
B(1)-N(3)-C(24)-N(4)	14.9(4)
C(13)-N(3)-C(24)-C(23)	13.2(3)
B(1)-N(3)-C(24)-C(23)	-177.7(3)
C(22)-C(23)-C(24)-N(4)	-18.6(5)
C(14)-C(23)-C(24)-N(4)	157.5(3)
C(22)-C(23)-C(24)-N(3)	175.6(3)
C(14)-C(23)-C(24)-N(3)	-8.3(3)
C(24)-N(4)-C(25)-N(5)	-11.5(4)
C(24)-N(4)-C(25)-C(26)	150.1(3)
C(36)-N(5)-C(25)-N(4)	155.4(3)

B(1)-N(5)-C(25)-N(4)	-8.3(4)
C(36)-N(5)-C(25)-C(26)	-10.0(3)
B(1)-N(5)-C(25)-C(26)	-173.6(2)
N(4)-C(25)-C(26)-C(27)	13.7(5)
N(5)-C(25)-C(26)-C(27)	177.8(3)
N(4)-C(25)-C(26)-C(35)	-158.2(3)
N(5)-C(25)-C(26)-C(35)	5.8(3)
C(35)-C(26)-C(27)-C(28)	-0.7(4)
C(25)-C(26)-C(27)-C(28)	-171.7(3)
C(26)-C(27)-C(28)-C(29)	-179.4(3)
C(26)-C(27)-C(28)-C(33)	1.3(4)
C(27)-C(28)-C(29)-C(30)	178.4(3)
C(33)-C(28)-C(29)-C(30)	-2.2(5)
C(28)-C(29)-C(30)-C(31)	1.9(5)
C(29)-C(30)-C(31)-C(32)	0.3(5)
C(30)-C(31)-C(32)-C(33)	-2.2(5)
C(31)-C(32)-C(33)-C(34)	-177.8(3)
C(31)-C(32)-C(33)-C(28)	1.8(5)
C(27)-C(28)-C(33)-C(34)	-0.7(4)
C(29)-C(28)-C(33)-C(34)	180.0(3)
C(27)-C(28)-C(33)-C(32)	179.7(3)
C(29)-C(28)-C(33)-C(32)	0.3(4)
C(32)-C(33)-C(34)-C(35)	179.0(3)
C(28)-C(33)-C(34)-C(35)	-0.6(4)
C(33)-C(34)-C(35)-C(26)	1.2(4)
C(33)-C(34)-C(35)-C(36)	171.8(3)
C(27)-C(26)-C(35)-C(34)	-0.6(4)
C(25)-C(26)-C(35)-C(34)	172.5(3)
C(27)-C(26)-C(35)-C(36)	-173.2(3)
C(25)-C(26)-C(35)-C(36)	-0.1(3)
C(1)-N(6)-C(36)-N(5)	11.9(4)
C(1)-N(6)-C(36)-C(35)	-150.9(3)
C(25)-N(5)-C(36)-N(6)	-156.2(3)
B(1)-N(5)-C(36)-N(6)	7.5(4)
C(25)-N(5)-C(36)-C(35)	10.0(3)
B(1)-N(5)-C(36)-C(35)	173.7(2)
C(34)-C(35)-C(36)-N(6)	-12.3(5)
C(26)-C(35)-C(36)-N(6)	159.3(3)
C(34)-C(35)-C(36)-N(5)	-177.2(3)
C(26)-C(35)-C(36)-N(5)	-5.6(3)
B(1)-O(1)-C(37)-C(38)	75.6(4)
B(1)-O(1)-C(37)-C(42)	-108.0(3)
O(1)-C(37)-C(38)-F(1)	-0.6(5)
C(42)-C(37)-C(38)-F(1)	-177.3(3)
O(1)-C(37)-C(38)-C(39)	177.8(3)
C(42)-C(37)-C(38)-C(39)	1.1(5)

F(1)-C(38)-C(39)-F(2)	-2.0(5)
C(37)-C(38)-C(39)-F(2)	179.7(3)
F(1)-C(38)-C(39)-C(40)	177.0(3)
C(37)-C(38)-C(39)-C(40)	-1.4(6)
F(2)-C(39)-C(40)-F(3)	-1.0(6)
C(38)-C(39)-C(40)-F(3)	-180.0(3)
F(2)-C(39)-C(40)-C(41)	179.2(3)
C(38)-C(39)-C(40)-C(41)	0.2(6)
F(3)-C(40)-C(41)-F(4)	1.8(5)
C(39)-C(40)-C(41)-F(4)	-178.4(3)
F(3)-C(40)-C(41)-C(42)	-178.7(3)
C(39)-C(40)-C(41)-C(42)	1.2(6)
F(4)-C(41)-C(42)-F(5)	-0.8(5)
C(40)-C(41)-C(42)-F(5)	179.6(3)
F(4)-C(41)-C(42)-C(37)	178.1(3)
C(40)-C(41)-C(42)-C(37)	-1.4(5)
O(1)-C(37)-C(42)-F(5)	2.5(4)
C(38)-C(37)-C(42)-F(5)	179.2(3)
O(1)-C(37)-C(42)-C(41)	-176.4(3)
C(38)-C(37)-C(42)-C(41)	0.3(5)
C(37)-O(1)-B(1)-N(1)	160.7(2)
C(37)-O(1)-B(1)-N(3)	-80.8(3)
C(37)-O(1)-B(1)-N(5)	41.9(3)
C(12)-N(1)-B(1)-O(1)	97.9(3)
C(1)-N(1)-B(1)-O(1)	-93.7(3)
C(12)-N(1)-B(1)-N(3)	-27.9(3)
C(1)-N(1)-B(1)-N(3)	140.5(2)
C(12)-N(1)-B(1)-N(5)	-137.3(2)
C(1)-N(1)-B(1)-N(5)	31.1(3)
C(13)-N(3)-B(1)-O(1)	-93.4(3)
C(24)-N(3)-B(1)-O(1)	98.6(3)
C(13)-N(3)-B(1)-N(1)	28.6(4)
C(24)-N(3)-B(1)-N(1)	-139.3(3)
C(13)-N(3)-B(1)-N(5)	138.4(3)
C(24)-N(3)-B(1)-N(5)	-29.6(3)
C(36)-N(5)-B(1)-O(1)	95.1(3)
C(25)-N(5)-B(1)-O(1)	-102.7(3)
C(36)-N(5)-B(1)-N(1)	-26.7(3)
C(25)-N(5)-B(1)-N(1)	135.4(2)
C(36)-N(5)-B(1)-N(3)	-135.9(2)
C(25)-N(5)-B(1)-N(3)	26.3(3)

Symmetry transformations used to generate equivalent atoms:

Equations

Beer-Lambert's Law for the Estimation of Reaction Yield from a Crude Product

The Beer-Lambert equation was used to estimate the yield of reaction crudes. First a solution of the crude product was made with known concentration and then the absorbance of the solution was measure by UV-Vis. The concentration of the product of interest can then be estimated using the Beer-Lambert law as follows:

$A = \varepsilon lc$ (Equation S1)

Where; A is the absorbance as measured by UV-Vis, ε is the molar attenuation coefficient of the compound, l is the optical path length, and c is the concentration of the compound.

With an estimated concentration of the product of interest, the mass of the product of interest was estimated using the volume of the solution and the molar mass of the compound as follows:

Mass of the product of interest = concentration x volume x molar mass (Equation S2)

Once the mass of the product of interest was determined, it was compared to the mass used to make the solution to estimate the % mass of the product of interest in the crude. Once the % mass of the product of interest in the crude was known, the total mass of the product of interest in the crude was estimated to then determine the yield.

Fluorescence Quantum Yield

Fluorescence quantum yields (Φ) were calculated using the following formula:

$\Phi = \Phi_R (I / I_R)(OD_R / OD)(n^2 / nR^2)$ (**Equation S3**)

where I is the integrated fluorescence intensity, OD is the absorbance, and n is the refractive index of the solvent. The subscript R denotes oxazine 170, the reference fluorophore we used herein, which has previously been reported to have a fluorescence quantum yield of 0.5793[3] in ethanol at room temperature. The analyses of all ArO-Br_nBsubNcs were acquired in toluene at room temperature.

Estimation of HOMO Energy from the First Oxidation Halfwave Potential

HOMO energies (E_{HOMO}) were estimated from first oxidation halfwave potentials (V_{CV}) using the following equation from D'Andrade *et al.*[4]:

$E_{HOMO} = -(1.4 \pm 0.1)\ qV_{CV} - (4.6 \pm 0.08)$ eV (**Equation S4**)

where q is the electron charge. The electrochemical analyses of all F_5-Cl_nBsubNc samples utilized a 0.1 M Bu_4NClO_4 as the electrolyte solution in nitrogen degassed anhydrous dichloromethane at room temperature with a 100 mV/s scan rate versus Ag/AgCl and decamethylferrocene as an internal standard.

References

1. Christe, K. O.; Dixon, D. A.; McLemore, D.; Wilson, W. W.; Sheehy, J. A.; Boatz, J. A., On a quantitative scale for Lewis acidity and recent progress in polynitrogen chemistry. *J. Fluorine Chem.* **2000,** *101* (2), 151-153.

2. Laurence, C.; Graton, J.; Gal, J.-F., An Overview of Lewis Basicity and Affinity Scales. *J. Chem. Educ.* **2011,** *88* (12), 1651-1657.

3. Rurack, K.; Spieles, M., Fluorescence Quantum Yields of a Series of Red and Near-Infrared Dyes Emitting at 600−1000 nm. *Anal. Chem.* **2011,** *83* (4), 1232-1242.

4. D'Andrade, B. W.; Datta, S.; Forrest, S. R.; Djurovich, P.; Polikarpov, E.; Thompson, M. E., Relationship between the ionization and oxidation potentials of molecular organic semiconductors. *Org. Electron.* **2005,** *6* (1), 11-20.